$\mathcal{H}_\infty$-Optimal Actuator Location

by

Dhanaraja Kasinathan

A thesis
presented to the University of Waterloo
in fulfillment of the
thesis requirement for the degree of
Doctor of Philosophy
in
Applied Mathematics

Waterloo, Ontario, Canada, 2012

I hereby declare that I am the sole author of this thesis. This is a true copy of the thesis, including any required final revisions, as accepted by my examiners.

I understand that my thesis may be made electronically available to the public.

Abstract

There is often freedom in choosing the location of actuators on systems governed by partial differential equations. The actuator locations should be selected in order to optimize the performance criterion of interest. The main focus of this thesis is to consider $\mathcal{H}_\infty$-performance with state-feedback. That is, both the controller and the actuator locations are chosen to minimize the effect of disturbances on the output of a full-information plant.

Optimal $\mathcal{H}_\infty$-disturbance attenuation as a function of actuator location is used as the cost function. It is shown that the corresponding actuator location problem is well-posed. In practice, approximations are used to determine the optimal actuator location. Conditions for the convergence of optimal performance and the corresponding actuator location to the exact performance and location are provided. Examples are provided to illustrate that convergence may fail when these conditions are not satisfied.

Systems of large model order arise in a number of situations; including approximation of partial differential equation models and power systems. The system descriptions are sparse when given in descriptor form but not when converted to standard first-order form. Numerical calculation of $\mathcal{H}_\infty$-attenuation involves iteratively solving large $\mathcal{H}_\infty$-algebraic Riccati equations ($\mathcal{H}_\infty$-AREs) given in the descriptor form. An iterative algorithm that preserves the sparsity of the system description to calculate the solutions of large $\mathcal{H}_\infty$-AREs is proposed. It is shown that the performance of our proposed algorithm is similar to a Schur method in many cases. However, on several examples, our algorithm is both faster and more accurate than other methods.

The calculation of $\mathcal{H}_\infty$-optimal actuator locations is an additional layer of optimization over the calculation of optimal attenuation. An optimization algorithm to calculate $\mathcal{H}_\infty$-optimal actuator locations using a derivative-free method is proposed. The results are illustrated using several examples motivated by partial differential equation models that arise in control of vibration and diffusion.

Acknowledgements

This thesis has been written with the help, support, and advice of many people to whom I am greatly in debt. I would like to thank my supervisor Prof. Kirsten Morris for all her support, patience over these years, enlightening discussions, and for always encouraging me and allowing me to speak my mind. I wish to acknowledge the members of my committee, Prof. John Burns, Prof. Dong Eui Chang, Prof. Hans De Sterck, and Prof. Stephen Vavasis for their interesting comments and suggestions.

I am thankful for the financial support of SHARCNET and AFOSR grant FA9550-10-1-0530. I am extremely grateful for the computing facilities provided by Shared Hierarchical Academic Research Computing Network and Compute/Calcul Canada, without which I'd surely still be waiting for some results. I would like to thank Steven Yang for the parallel computations.

I would also like to extend a special thanks to my good friend (and office-mate) Alex Shum. Thanks for putting up with me all these years and for several lively discussions about math, life in general, teaching, driving lessons and much more. I couldn't have asked for a better officemate. I would like to acknowlegde the support of my group mates Dr. Ahmet Ozkan Ozer, Dr. Matthew Johnston, Amenda Chow, Neda Darivan, Rasha Al Jamal and Robert Huneault.

I appreciate the friendship and support of my friends. I would like to thank Dr. Ravindra Reddy, Dr. Shriprakash Badi, Dr. Mukesh Meshram, Rahul, Venkata Manem, Andree Susanto, Michael Dunphy, Abdulhamed Alsisi and Antonio Sanchez for their friendship, and welcome distractions.

Finally, I wish to thank my wife and best friend Nithya Agatheeswaran for her love, kindness, and support at all times. I would like to thank my family for being a constant source of inspiration throughout my life. Your support has been immeasurable.

Dedication

This is dedicated to the ones I love.

Table of Contents

List of Tables

List of Figures

Chapter 1

Introduction

The location of an actuator has a tremendous impact on the performance of the controlled system; *e.g.,* [40, 117]. In aerospace engineering, the flight wings (Figure 1.1b) can be mounted with piezoelectric actuators (square shaped white patches in Figure 1.1a) at optimal locations to suppress the vibrations [93]. It was shown that the control system performance shows significant improvement and at the same time the energy consumption is minimized when the actuators are placed at optimal locations [6, 109]. On the other hand, placing the actuator near a nodal point (or line) of a structure mode (a point where the corresponding eigenfunction is zero) results in large force requirement to control this mode [109]. Better performance of vibration control of cantilever plate [86], beam [124], inflated torus [68], paraboloidal shell [132] and other flexible structures [60] is observed when actuators are placed at optimal locations. Misplaced actuators can lead to lack of controllability [80]. The amount of energy consumption is a concern in vibration control of smart structures and in process control applications. In chemical processes, an integrated feedback controller design and optimal actuator placement result in achieving the desired performance with the use of minimal control energy [5]. Civil structures such as high rise buildings and suspension bridges are designed to protect against earthquake excitation through the placement of actuators at appropriate heights [1]. In acoustic problems, an arbitrarily placed actuator can actually increase the sound field locally [46]. It is shown in [100] that the achievable noise reduction in a duct (Figure 1.2) varies strongly with

Figure 1.1: Vibration control of flight wings [93, Fig. 1]: Better performance of vibration control is achieved using piezo-electric actuators (square shaped white patches) placed at optimal locations on the surface of wings. An experimental setup [93, Fig. 2] is shown below.

(a) Experimental setup (b) Flight Wings

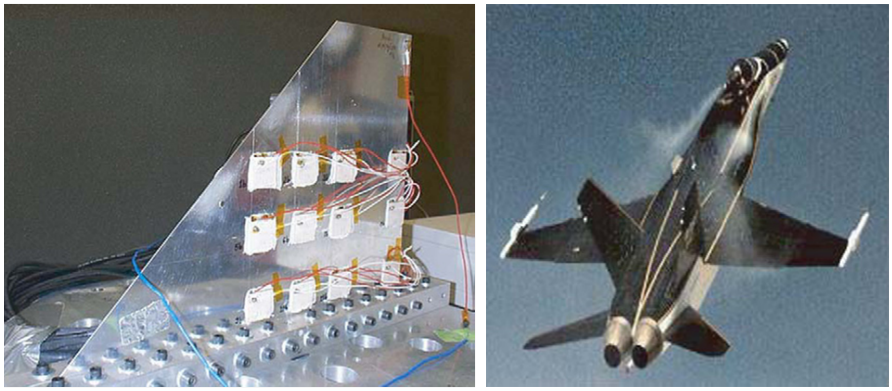

actuator location. The optimal placement of actuators is essential for effective control of structural vibration and acoustic noise [116]. The actuators should therefore be located at positions that optimize certain performance objectives.

In control systems, studies on optimal actuator placement began in the early 1980's [6]. These first studies concentrated on formulating an objective function based on specific performance requirements. Since then, several cost functions for actuator placement have been used; see the survey papers [49, 107, 128]. The location that corresponds to the minimal cost is chosen as the optimal location for placing the actuator.

In systems modeled by partial differential equations, optimal location calculations are performed on approximated problems, although the state space for the full model is infinite-dimensional. Calculations of optimal actuator location using approximations must yield reliable results for the full model. The theory that guarantees optimality of the cost and existence of the optimal actuator location for these models has not been developed in its entirety. In [62], it was shown that using the first n modes to find the actuator location that maximizes the decay rate of the solution to the wave equation yields the worst location

Figure 1.2: Acoustic noise in a duct [96, Fig. 2]: A noise signal is produced by a loudspeaker placed at one end of the duct. An actuator loudspeaker is mounted midway down the duct to control the noise signal.

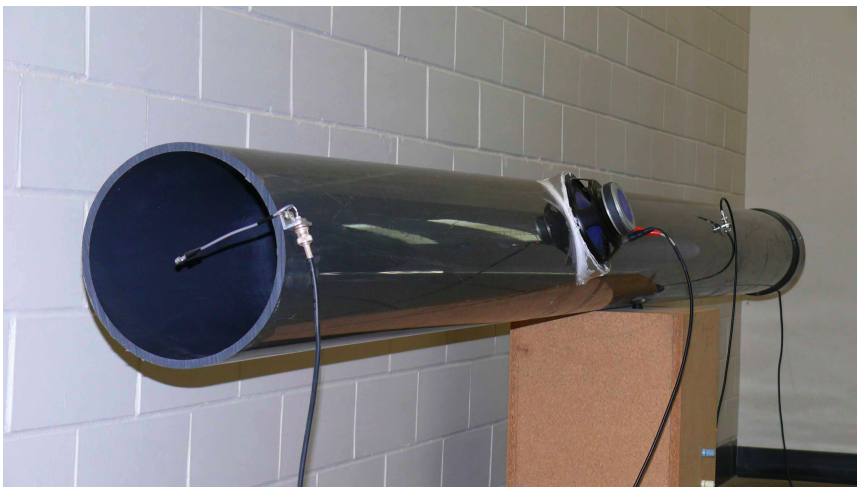

for the $(n+1)$th mode. Conditions that guarantee optimality of the actuator location with a linear quadratic cost are developed in [97].

The aim of this thesis is to develop a mathematical framework for calculating optimal actuator locations with an $\mathcal{H}_\infty$ criterion. Both the controller and the actuator location are chosen to minimize the effect of disturbances on the output of a full-information plant. Optimal disturbance attenuation as a function of actuator location is used as the cost function . First, the problem of using approximations to determine optimal actuator location for $\mathcal{H}_\infty$-control with state feedback is considered. Conditions under which $\mathcal{H}_\infty$-optimal actuator locations calculated using approximations converge to the exact optimal locations for the original model are derived.

Several numerical issues are associated with the calculation of $\mathcal{H}_\infty$-optimal actuator location. Consider first the problem of calculating optimal $\mathcal{H}_\infty$-attenuation at fixed actuator location. Except for a few special classes of systems,*e.g.* [33], calculation of optimal $\mathcal{H}_\infty$-attenuation is accomplished by an iterative bisection method [113, 121, 122]. Multiple solutions of a fixed attenuation problem are required in this bisection method. Each fixed-attenation problem requires solution of a $\mathcal{H}_\infty$-ARE. This $\mathcal{H}_\infty$-ARE is similar to the one

arising in linear quadratic control problem except now the quadratic term is sign-indefinite and this can make solution of the equation more difficult. $\mathcal{H}_\infty$-AREs of large dimensions arise when approximations are used on systems modeled by partial differential equations. Often, for example, when finite element methods are used, the approximating systems are naturally written in the descriptor form. A recursive algorithm [82] to calculate the solution of a $\mathcal{H}_\infty$-ARE is extended to handle large regular descriptor systems. An improvement of the bisection algorithm is suggested to accelerate the calculation of optimal attenuation.

Minimization of optimal $\mathcal{H}_\infty$-attenuation over all actuator locations is an additional layer of optimization. A difficulty with $\mathcal{H}_\infty$-optimal actuator location problem is the lack of gradient information. The directional direct-search method, which is a well-known derivative-free method, is used in an algorithm to optimize the actuator locations based on $\mathcal{H}_\infty$-performance. A distributed parallel implementation of this algorithm is suggested to accelerate the calculations, particularly for large-scale systems.

The outline of this thesis is as follows: In Chapter 2, some background literature on optimal actuator location is reviewed. In Chapter 3, a thorough investigation of linear quadratic optimal actuator location problem is presented. In Chapter 4, a framework for calculating $\mathcal{H}_\infty$-optimal actuator location is developed. Conditions under which the optimal actuator location calculated using approximations yield reliable results are described and illustrated with examples in this chapter. Some numerical methods to calculate $\mathcal{H}_\infty$-control is reviewed in Chapter 5. A recursive algorithm to calculate the solution of a $\mathcal{H}_\infty$-ARE is extended to large descriptor systems in Chapter 5. The extended algorithm is compared against other methods using several examples modeled by partial differential equations and the results are summarized. A fast algorithm to calculate $\mathcal{H}_\infty$-optimal actuator location is developed in Chapter 6. This thesis is concluded in Chapter 7.

Chapter 2

Background on Optimal Actuator Location

In many control systems, the location of actuators can often be chosen. These locations should be selected in order to optimize the performance criterion of interest. Researchers have used a number of performance criteria to find the best possible location for placing the actuator; see *e.g.,* [49, 128]. The most commonly used criteria in the engineering literature are (i) controllability criterion, (ii) linear quadratic control criterion, and (iii) $\mathcal{H}_\infty$ control criterion.

In this chapter, the background material related to the above strategies is reviewed. The application of these criteria to calculate optimal actuator location in the recent literature is described. The advantages and disadvantages of choosing such criteria are discussed. Lastly, other objective functions which have been used are briefly described.

2.1 Problem Statement

Many optimal actuator location problems involve systems modelled by partial differential equations. The state space of such systems is infinite-dimensional. Most often, researchers

in engineering have used an approximation scheme that leads to systems on finite dimensions, $\mathbb{R}^n$. This issue will be addressed in the next chapter. In this section, the optimal actuator location problem is first formulated.

Consider the following linear time-invariant system in $\mathbb{R}^n$,

$$\frac{dz}{dt} = Az(t) + Bu(t), \quad z(0) = z_0 \in \mathbb{R}^n \tag{2.1.1}$$

where $z(\cdot) \in \mathbb{R}^n$ denotes the state of the system, $A \in \mathbb{R}^{n\times n}$ denotes the system dynamics and $u(\cdot) \in \mathbb{R}^m$ is the control applied to the system as a function of time. The effect of control on the state of the system is described by the input matrix $B \in \mathbb{R}^{n\times m}$.

Consider the situation where there are m actuators with locations that could be varied over some compact set (this will be justified later), call it $\Omega \subset \mathbb{R}^a$. Parametrize the actuator locations by r and denote the dependence of the corresponding input matrix with respect to the actuator location by $B(r)$. Note that r is a vector of length m with components in Ω so that r varies over a space denoted by Ω^m. Based on the designer's interest on the choice of a desired performance measure, a suitable cost function $\mu(r)$ that depends on the actuator location is formulated.

Definition 2.1.1. The optimal cost $\hat{\mu}$ over all possible locations is defined as,

$$\hat{\mu} = \inf_{r\in\Omega^m} \mu(r). \tag{2.1.2}$$

Also, if it exists, the location $\hat{r} \in \Omega^m$ that satisfies

$$\hat{r} = \arg \inf_{r\in\Omega^m} \mu(r) \tag{2.1.3}$$

is called the optimal actuator location.

The fundamental issue of showing well-posedness of optimal actuator location problem has not been addressed for many cost functions in the literature. In the rest of this chapter, several formulations of the cost function $\mu(r)$ based on the three most popular strategies used in diverse applications will be discussed.

2.2 Controllability Criterion

The earliest of the three most commonly found strategies involves the use of controllability criterion as a tool for setting up the actuator placement problem; see *e.g.,* [6, 60].

Definition 2.2.1. The dynamical system (2.1.1) or pair $(A, B(r)), r \in \Omega^m$ is said to be *controllable* at the actuator location r if, for any initial state $z(0) = z_0$ and any final state z_f, there exists an input $u(\cdot)$ such that the solution of (2.1.1) satisfies $z(t_f) = z_f$ in a finite time $t_f > 0$. Otherwise, the system or the pair $(A, B(r))$ is said to be *uncontrollable* at the actuator location r.

Definition 2.2.2. The matrix $A \in \mathbb{R}^{n\times n}$ is *Hurwitz*, if $\max_{1\leq i\leq n} \mathrm{Re}(\lambda_i(A)) < 0$, where $\lambda_i(A)$ is the eigenvalue of A.

In placing the actuators it is desirable to minimize the control energy (J_c) required to bring the system from an arbitrary initial state z_0 to some final state z_f in a finite time t_f subjected to (2.1.1). Consider the following minimization problem :

$$\text{Min } J_c = \int_0^{t_f} u^T(t)u(t)dt, \tag{2.2.1}$$

where the superscript T denotes the matrix transpose. The solution to (2.2.1) is

$$u(r;t) = -B^T(r)e^{A^T(t_f-t)}\mathcal{W}_c(r;t_f)^{-1}(e^{At_f}z_0 - z_f),$$

where

$$\mathcal{W}_c(r;t_f) := \int_0^{t_f} e^{At}B(r)B^T(r)e^{A^Tt}dt.$$

See *e.g.,* [102] for details. For systems where A is Hurwitz, the infinite-horizon version of the matrix $\mathcal{W}_c(r;t_f)$ is called the *controllability Gramian*, that is,

$$\mathcal{W}_c(r) = \int_0^{\infty} e^{At}B(r)B^T(r)e^{A^Tt}dt. \tag{2.2.2}$$

The Gramian matrix is calculated by solving the Lyapunov equation,

$$A\mathcal{W}_c(r) + \mathcal{W}_c(r)A + B(r)B^T(r) = 0. \tag{2.2.3}$$

The controllability Gramian provides a measure of controllability of the system depending on the location of the actuator. A small eigenvalue of the controllability Gramian matrix would lead to at least one mode requiring very high control effort. This implies that all the eigenvalues of the controllability Gramian matrix should be as large as possible.

Theorem 2.2.3. (*e.g.,* [102, Thm 2.5]) The pair (A, B) is controllable at r if and only if $\mathcal{W}_c(r; t_f)$ is positive definite for all $t_f > 0$.

It is evident from Theorem 2.2.3 that the Gramian matrix must be non-singular to guarantee controllability of the system.

An objective function for calculating optimal actuator location was formulated in [60] using the Gramian matrix as follows:

$$\max_{r \in \Omega^m} \mu(r) = \left(\sum_{i=1}^{n} \lambda_i \right) \sqrt[n]{\prod_{i=1}^{n} (\lambda_i)}, \tag{2.2.4}$$

where λ_i's are the eigenvalues of $\mathcal{W}_c(r)$ for a given actuator location. The summation term in (2.2.4) is the trace of the Gramian matrix. To ensure that all the eigenvalues of the Gramian are high, the geometric mean of all the eigenvalues is included in the objective function.

Several variants of the above objective function have been proposed in the past decade. A standard deviation term, $1/\sigma(\lambda_i)$, was often included in the performance index (2.2.4) as a product term, see *e.g.,* [68, 116]. In [86], only the trace of the Gramian matrix was used to find the optimal actuator location on flexible structures. The optimal locations of multiple actuators calculated using (2.2.4) suppressed the vibrations in a plate [109].

Controllability Gramian based approach is an open-loop strategy. Calculation of optimal actuator location does not simultaneously provide a controller. For example in [116], the design of optimal control and the optimal actuator location were treated as two separate problems which is cumbersome. An adaptive feedforward controller was designed in [109] after calculating the optimal actuator location. In the rest of this chapter, and thesis, only closed-loop strategies for the calculation of optimal actuator locations with a linear-quadratic or $\mathcal{H}_\infty$-cost will be discussed.

2.3 Linear Quadratic Control Criterion for Linear Systems

Linear quadratic control is a well-known closed-loop strategy for controller design that minimizes energy of both the control signal and the measured signal. The control is calculated by minimizing a quadratic cost function with penalty on both the state of the system and the control input.

Consider the system (2.1.1) on $\mathbb{R}^n$. The quadratic cost functional associated with a particular control $u(\cdot) \in \mathbb{R}^m$ over an infinite-time interval, for a given initial state z_0 is given by

$$J(z_0, u(.)) = \int_0^\infty \langle Cz(t), Cz(t)\rangle + \langle u(t), Ru(t)\rangle dt \tag{2.3.1}$$

subject to (2.1.1), where the matrices $C \in \mathbb{R}^{p\times n}$ and $R(> 0) \in \mathbb{R}^{m\times m}$ are weights for the state and the control input respectively. The linear quadratic control problem is to minimize the cost (2.3.1) over all possible controls or

$$\min_{u\in L_2(0,\infty;\mathbb{R}^m)} J(z_0, u). \tag{2.3.2}$$

The control that achieves this minimum, $u_{opt}(\cdot)$, is often called the *linear quadratic optimal control*.

Definition 2.3.1. The pair (A, B) is *stabilizable* if there exists $K \in \mathbb{R}^{m\times n}$ so that $A - BK$ is Hurwitz.

Definition 2.3.2. The pair (A, C) is *detectable* if there exists $F \in \mathbb{R}^{n\times p}$ so that $A - FC$ is Hurwitz.

Theorem 2.3.3. (*e.g.,* [102, Thm. 5.12, Thm. 5.16]) Let the system given by (2.1.1) be stabilizable and let the pair (A, C) be detectable. Then the infinite-horizon optimization problem (2.3.2) has a minimum for every given initial condition z_0. Furthermore, there exists a symmetric, non-negative matrix, $P \in \mathbb{R}^{n\times n}$, such that

$$\min_{u\in L_2(0,\infty;\mathbb{R}^m)} J(z_0, u) = J(z_0, u_{opt}) = z_0^* P z_0, \tag{2.3.3}$$

where the optimal control $u_{opt}(\cdot)$ is given by

$$u_{opt}(\cdot) = -R^{-1}B^*Pz(\cdot), \tag{2.3.4}$$

and P is the unique nonnegative solution of the algebraic Riccati equation (ARE) given by

$$A^*P + PA - PBR^{-1}B^*P + C^*C = 0. \tag{2.3.5}$$

The corresponding optimal state feedback, $K = -R^{-1}B^*P$ is stabilizing, that is $A - BK$ is Hurwitz.

Numerical methods of calculating solutions to the ARE will be discussed in Section 3.5.

Many researchers have chosen linear quadratic cost criteria to optimize the actuator location, see *e.g.,* [1, 46, 61, 80, 124]. The performance for a particular actuator location r is dependent on the given initial state of the system z_0 and the solution to ARE $P(r)$. That is, the linear quadratic cost at the actuator location r is

$$\min_{u \in L_2(0,\infty;\mathbb{R}^m)} J^r(z_0, u) = J^r(z_0, u_{opt}) = z_0^* P(r) z_0. \tag{2.3.6}$$

Researchers have used a number of techniques in the past to remove this dependency on the initial condition. Considering the worst possible initial condition $\|z_0\| = 1$, an upper bound on the cost (2.3.6) is the induced matrix norm on the solution to LQ-ARE,

$$\max_{\|z_0\|=1} \min_{u \in L_2(0,\infty;\mathbb{R}^m)} J^r(z_0, u) = \max_{\|z_0\|=1} \langle z_0, P(r)z_0 \rangle \;=\; \|P(r)\|. \tag{2.3.7}$$

This objective function

$$\mu(r) := \|P(r)\| \tag{2.3.8}$$

was used for placing actuators on a simply supported beam with a moving mass [124]. If the initial condition is random, with zero mean and unity variance, then the expected cost is trace $[P(r)]$, or $\|P(r)\|_1$ where $\|.\|_1$ indicates the trace norm. In [46], the cost function

$$\mu(r) := \|P(r)\|_1 \tag{2.3.9}$$

was minimized for finding the best locations to place actuators to reduce the interior noise in an acoustic cavity. The trace norm of the solution to (2.3.5) was used in other applications,

see *e.g.,* [1, 80]. Another approach is to average the cost over a set of linearly independent initial states [5]. The effect of a disturbance with fixed frequency content (for instance, a single white noise disturbance) is considered in [98]. This leads to a $\mathcal{H}_2$ control problem and if the spatial distribution of the disturbance is unknown, then the cost function (2.3.8) is used to calculate the optimal actuator location.

Linear quadratic control is a popular choice, since the controller is designed simultaneously with the optimal actuator location. Including the effect of a specific disturbance with fixed frequency content leads to a $\mathcal{H}_2$ control problem and the cost function is similar to a linear quadratic cost [98].

2.4 $\mathcal{H}_\infty$-Control Criterion

Noise in the environment and disturbances will influence the performance of the control system. The disturbance is often unknown. In this section, placing the actuator at a location using an $\mathcal{H}_\infty$-criterion is considered. That is, both the controller and the actuator locations are chosen to minimize the effect of disturbances on the output. A system with the disturbance model is first described. Then, the standard and optimal $\mathcal{H}_\infty$ control problems are stated. Lastly, how this strategy is used to formulate the optimal actuator location problem is discussed.

Consider the following system described on $\mathbb{R}^n$,

$$\begin{aligned} \dot{z}(t) &= Az(t) + Bu(t) + Dv(t),\ z(0) = z_0 \in \mathbb{R}^n \\ y(t) &= Cz(t) + D_{12}u(t), \end{aligned} \tag{2.4.1}$$

where $z(\cdot)$ denotes the state of the system (2.4.1), $v(t) \in \mathbb{R}^q$ is the exogenous input or disturbance, $y(t) \in \mathbb{R}^p$ is the controlled output or cost. Here, $A \in \mathbb{R}^{n\times n}, B \in \mathbb{R}^{n\times m}$. The matrices $C \in \mathbb{R}^{p\times n}$ and $D_{12} \in \mathbb{R}^{p\times m}$ describe the effect of the state and the control input on the output respectively. The usual orthogonality hypotheses $C^T D_{12} = 0$ and $D_{12}^T D_{12} = I$ are assumed in order to simplify the subsequent equations. The full column rank of matrix D_{12} ensures a non-singular map y on the control u. It is assumed that all

states of the system are available for measurement. This system (2.4.1) is a special form of the generalised plant configuration, known as the *full information problem*.

Let $\hat{v}(s)$ and $\hat{y}(s)$ be the Laplace transforms of the exogenous input and the output of the system respectively. The function $G_{yv}(s)$ that describes the ratio of the output $\hat{y}(s)$ over the disturbance $\hat{v}(s)$ is called the *transfer function* of (2.4.1) from disturbance to output. Minimizing the effect of all disturbances on the output is equivalent to minimizing the size of the transfer function G_{yv}. The notation $\mathcal{H}_\infty$ indicates the Hardy space of all functions $G(s)$ which are analytic in the right-half plane $Re(s) > 0$ and for which

$$\sup_{\omega} \lim_{x \downarrow 0} |G(x + j\omega)| < \infty. \tag{2.4.2}$$

The norm of a function in $\mathcal{H}_\infty$ is

$$\|G\|_\infty = \sup_{\omega} \lim_{x \downarrow 0} |G(x + j\omega)|. \tag{2.4.3}$$

More generally, let $|\cdot|$ indicate the maximum singular value of a matrix. The space $\mathcal{H}_\infty(\mathbb{R}^m, \mathbb{R}^p)$ consists of matrix-valued functions $G : \mathbb{C}_0^+ \mapsto \mathcal{L}(\mathbb{R}^m, \mathbb{R}^p)$ that have entries that are analytic in the right-half plane and for which

$$\|G\|_\infty = \sup_{\omega} \lim_{x \downarrow 0} |G(x + j\omega)| < \infty. \tag{2.4.4}$$

This space is sometimes written $M(\mathcal{H}_\infty)$ when no confusion will arise about dimensions. By the Paley-Weiner Theorem, a system with input in $\mathbb{R}^m$ and output in $\mathbb{R}^p$ is L_2-stable if and only if the system transfer function $G \in M(\mathcal{H}_\infty)$. Furthermore, the $\mathcal{H}_\infty$-norm of the transfer function is the L_2-gain of the system, which is the ratio of L_2 norm of output to input. The details of calculating $\mathcal{H}_\infty$ norms are found in many standard texts, see *e.g.,* [102, 133].

Let G be the transfer function of the system (2.4.1):

$$G(s) := C(sI - A)^{-1} \begin{bmatrix} B & D \end{bmatrix} + \begin{bmatrix} D_{12} & 0 \end{bmatrix}. \tag{2.4.5}$$

With state feedback control $u(t) = -Kz(t), K \in \mathbb{R}^{m \times n}$, the closed loop transfer function from disturbance to output is

$$G_{yv}(s) = (C - D_{12}K)\,(sI - (A - BK))^{-1}\,D. \tag{2.4.6}$$

Definition 2.4.1. The controlled system will have input v (disturbance) and output y (measurement). The *fixed attenuation $\mathcal{H}_\infty$ control problem* for attenuation γ of (2.4.1) is to construct a stabilizing controller with transfer function H so that the closed loop system G_{yv} with $\hat{u}(s) = H(s)\hat{z}(s)$ is L_2-stable and satisfies the bound

$$\|G_{yv}\|_\infty \ < \ \gamma. \tag{2.4.7}$$

Even for stabilizable systems, the fixed attenuation problem cannot be solved for every attenuation γ since such a controller may not exist [43]. However, if it is solvable, as in the case of linear quadratic control, the control law can be chosen to be constant state feedback.

Consider the index

$$\rho(u, v; z_0) = \|y\|^2_{L_2(0,\infty;\mathbb{R}^p)} = \int_0^\infty \|Cz(t)\|^2 + \|D_{12}u(t)\|^2 dt \tag{2.4.8}$$

subject to (2.4.1). Consider the performance index

$$J(u, v; z_0) = \rho(u, v; z_0) - \gamma^2 \|v\|^2_{L_2(0,\infty;\mathbb{R}^q)} \tag{2.4.9}$$

subject to (2.4.1) for some $\gamma > 0$. Calculating a controller that achieves the given $\mathcal{H}_\infty$-attenuation bound γ is equivalent to solving the quadratic differential game

$$\max_{v\in\mathbb{R}^q} \min_{u\in\mathbb{R}^m} J(u, v; z_0) \tag{2.4.10}$$

subject to (2.4.1), see [102] for details. The solution to the quadratic differential game (2.4.10) is a saddle point since the optimal control law minimizes the cost function J where as the worst-case disturbance maximizes it, unlike the linear quadratic control problem where the optimal control law is a minimum, see [102] for details.

Theorem 2.4.2. (*e.g.,* [102, Thm 8.8]) Assume that the pair (A, B) is stabilizable and the pair (A, C) is detectable. There exists a stabilizing controller for the full information problem (2.4.1) so that $\|G_{yv}\|_\infty < \gamma$ if and only if there exists a symmetric, non-negative solution denoted by $P \geq 0$, that satisfies the $\mathcal{H}_\infty$-ARE,

$$A^T P + PA + P\left(\frac{1}{\gamma^2} DD^T - BB^T\right) P + C^T C = 0 \tag{2.4.11}$$

such that $A + \left(\frac{1}{\gamma^2} DD^T - BB^T\right) P$ is Hurwitz. If so, one such control is given by,

$$u = -Kz, \text{ where } K := B^T P \tag{2.4.12}$$

and also $A - BB^T P$ is Hurwitz.

With the stabilizing feedback K (2.4.12) the closed loop transfer function G_{yv} achieves a $\mathcal{H}_\infty$ norm less than γ. Hence, the disturbance propagation to output of the plant will always be less than a factor of γ. Except for the quadratic term, the $\mathcal{H}_\infty$-ARE (2.4.11) is similar to the LQ-ARE (2.3.5). A review of existing numerical methods to calculate the solution to $\mathcal{H}_\infty$-ARE (2.4.11) will be presented in Section 5.2. The extension to the more general case where an estimator must be constructed involves solving the dual Riccati equation (*e.g.* [102]). The computational issues are identical to the full-information case.

A question that naturally arises is the existence of a state feedback control that minimizes this attenuation level γ.

Definition 2.4.3. The *optimal $\mathcal{H}_\infty$-control problem* for (2.4.1) with full-information is to find

$$\hat{\gamma} = \inf \gamma \tag{2.4.13}$$

over all γ for which the fixed attenuation problem is solvable. The infimum $\hat{\gamma}$ is called the optimal $\mathcal{H}_\infty$-attenuation.

Optimal $\mathcal{H}_\infty$-attenuation is calculated using a bisection-type algorithm. The numerical issues related with the calculation of optimal attenuation will be dealt with in Chapter 5.

Consider the full-information plant (2.4.1) except now the input matrix is a function of the actuator location r, $B(r)$. The location that minimizes the optimal $\mathcal{H}_\infty$-disturbance attenuation is chosen as the actuator location. The *$\mathcal{H}_\infty$-cost* for a particular actuator location r is $\hat{\gamma}(r)$. The value of $\hat{\gamma}(r)$ provides the best possible attenuation of the worst-case disturbance for the system at the actuator location r. This cost function was used for locating actuators in the vibration control of tensegrity structures [117]. The results in [117] show that the displacement is less with $\mathcal{H}_\infty$ performance than the $\mathcal{H}_2$ performance. Another approach for placing actuators is to use the $\mathcal{H}_\infty$-norm of the closed-loop system;

see [50] for details. This approach is adopted in [123] to place actuators on a plate. An analytical expression to compute the upper bound on the $\mathcal{H}_\infty$-norm of the controlled system was used to optimize the actuator locations in [41, 125]. Using this analytical approach, it was shown in [42] that the resulting optimal actuator location exhibits spatial robustness. Calculation of optimal actuator locations with spatially varying disturbances was addressed in [40]. In [63], the product of a frequency weighting term that represents the design specification and the closed-loop transfer function was used for optimal actuator placement.

The advantages of choosing optimal $\mathcal{H}_\infty$-disturbance attenuation as a closed-loop strategy for actuator placement are threefold; first, the effect of the worst case disturbance on the output of the system is minimal; second, with optimal actuator location, the corresponding optimal state feedback controller is simultaneously designed; third, the stability of the closed loop is guaranteed.

2.5 Other Objective Functions

For space structure systems, a composite objective function that combines the calculation of optimal location, mass of the actuator and the energy dissipated in the system was used in [89]. Other design variables of the actuator such as length, mass, relative thickness, Young's modulus of elasticity, total control force of actuators were simultaneously optimized in [132]. In vibration control of smart tensegrity structures, design variables such as twist angle and location of actuators were optimized in [117]. In the field of acoustics optimization, the influence of mass effect of the actuators was also used to determine the optimal location and shape of the actuators in [90].

Researchers have also used more than one optimization criteria to find the best placement strategy. In vibration control of high-rise buildings structures, multiple objective functions related to different optimization criteria were used, *e.g.,* [118]. In [116], controllability criteria and linear quadratic cost criteria were used to determine the optimal location and optimal controller. In [117], both $\mathcal{H}_\infty$ and $\mathcal{H}_2$ cost criteria were used for actuator placement and their performances were compared.

In this chapter, the three most popular optimization strategies that were used extensively in engineering literature for actuator placement have been discussed. As already noted, one drawback of controllability criterion is that this is an open-loop strategy. Also, when the state space is infinite-dimensional, the system is not exactly controllable (*e.g.,* [37, Thm. 4.1.5]) which complicates the use of such a criterion. In the following chapters, linear quadratic and $\mathcal{H}_\infty$-control criteria for placing actuators on the full partial differential equation model will be discussed.

Chapter 3

Linear Quadratic Optimal Actuator Location

The linear quadratic control criterion for placement of actuators is quite popular among researchers, see *e.g.,* [1, 5, 46, 80]. In control of vibrations, diffusion and many other applications where this problem is studied, the mathematical models are given by partial differential equations; see the review article [79]. The state space for such systems is infinite-dimensional. In practice, approximations are used in controller design and thus in selection of the actuator locations. The optimal cost and the corresponding location computed using the approximated problem may not be the same for the original problem. In fact, the optimal cost and the corresponding location may not even exist for the full partial differential equation. It is necessary to first formulate the optimal actuator location problem with the full partial differential equation and show well-posedness of this problem. Criteria for optimality of linear quadratic actuator locations for the full partial differential equation model was obtained in [97]. In this chapter, the theory of linear quadratic control on infinite dimensions is first described briefly. The well-posedness of the linear quadratic optimal actuator location problem on a Hilbert space is shown next. Then, conditions on an approximation scheme required for convergence of approximating controls to the control for the original model are given. The convergence of optimal actuator locations is proven next. Lastly, numerical methods used in literature to calculate optimal actuator locations

by solving Riccati equations are reviewed.

3.1 Linear Quadratic Control on Infinite-Dimensional Systems

Consider systems described by

$$\frac{dz}{dt} = Az(t) + Bu(t), \quad z(0) = z_0 \in \mathcal{Z}, \tag{3.1.1}$$

where A with domain $\mathbf{D}(A)$ generates a C_0-semigroup $T(t)$ on a Hilbert space $\mathcal{Z}$ and $B \in \mathcal{L}(U, \mathcal{Z})$, where $\mathcal{L}(U, Z)$ indicates bounded linear operators from U to $\mathcal{Z}$; see [37, 83, 108] for details. The input space is a separable Hilbert space denoted by U. Let

$$\mathcal{U} = L_2(0, \infty; U)$$

denote the space of all admissible inputs. The solution of (3.1.1) can be written

$$z(t) = T(t)z_0 + \int_0^t T(t-s)Bu(s)ds. \tag{3.1.2}$$

Example 3.1.1. Consider a metal bar of unit length heated along its length according to

$$\begin{aligned} &\frac{\partial w}{\partial t}(x,t) = \frac{\partial^2 w}{\partial x^2}(x,t) + b(x)u(t), \quad w(x,0) = w_0(x), \\ &\frac{\partial w}{\partial x}(0,t) = 0 = \frac{\partial w}{\partial x}(1,t), \end{aligned} \tag{3.1.3}$$

where $w(x,t)$ represents the temperature at position x and time t with Neumann boundary conditions, $w_0(x)$ is the initial temperature profile, $u(t)$ is the heat source, and $b(x)$ denotes the variation of addition of heat along the bar. The parabolic system (3.1.3) can be rewritten in the abstract form (3.1.1) by choosing $\mathcal{Z} = L_2(0,1)$ as the state space and $z(t) = \{w(x,t), 0 \le x \le 1\}$ as the state. Then (3.1.3) resembles (3.1.1) if the operators A and B on $\mathcal{Z}$ are given as follows:

$$Ah = \frac{d^2h}{dx^2} \text{ with } \mathbf{D}(A) = \left\{ h \in \mathcal{H}^2(0,1) \mid \frac{dh}{dx}(0) = 0 = \frac{dh}{dx}(1) \right\}, \; Bu = b(x)u, \tag{3.1.4}$$

where the function $w_0(\cdot) \in L_2(0,1)$ is the initial state z_0. The solution to (3.1.3) is given by

$$w(x,t) = \int_0^1 g(t,x,y)w_0(y)\ dy + \int_0^t \int_0^1 g(t-s,x,y)b(y)u(s)\ dyds, \tag{3.1.5}$$

where $g(t,x,y)$ represents the Green's function

$$g(t,x,y) = 1 + \sum_{n=1}^{\infty} 2e^{-n^2\pi^2 t}\cos(n\pi x)\cos(n\pi y). \tag{3.1.6}$$

The solution (3.1.5) can also be represented in the abstract form (3.1.2).

In finite dimensions $T(t)$ is the matrix exponential e^{At} and the equation (3.1.2) is the familiar variation of constants formula. The well-known semigroup theory, *e.g.,* [37, 83, 108], is the generalization of e^{At} to unbounded operators A on abstract spaces and clarifies the concept of solutions (3.1.2) on these spaces. Control problems that arise from partial differential equations and delay differential equations (*e.g.* [37]) can be formulated mathematically as ordinary differential equations on an infinite-dimensional abstract linear vector space. These two special classes of infinite-dimensional systems motivate the usefulness of developing a theory for linear infinite-dimensional systems.

Definition 3.1.2. A C_0-semigroup, $T(t)$, on $\mathcal{Z}$ is *exponentially stable*, if there exists positive constants, M and α such that

$$\|T(t)\| \leq Me^{-\alpha t}, \tag{3.1.7}$$

where $\|\cdot\|$ is the operator norm on $\mathcal{L}(\mathcal{Z},\mathcal{Z})$.

Consider the abstract formulation (3.1.1) on the Hilbert space $\mathcal{Z}$. The linear-quadratic controller design objective is to find a control $u(\cdot)$ that minimizes the cost functional

$$J(z_0,u(\cdot)) = \int_0^{\infty} \langle Cz(t), Cz(t)\rangle + \langle u(t), Ru(t)\rangle\ dt, \tag{3.1.8}$$

where $R \in \mathcal{L}(U,U)$ is a self-adjoint positive definite operator weighting the control, $C \in \mathcal{L}(\mathcal{Z},Y)$ weights the state, and $z(\cdot)$ is determined by (3.1.2). This problem is very similar to the one described in Section 2.3 except now the state space is infinite dimensional.

Definition 3.1.3. The system (A, B) is said to be *stabilizable* if there exists $K \in \mathcal{L}(\mathcal{Z}, U)$ such that $A - BK$ generates an exponentially stable semigroup.

Definition 3.1.4. The pair (A, C) is said to be *detectable* if there exists $F \in \mathcal{L}(Y, \mathcal{Z})$ such that $A - FC$ generates an exponentially stable semigroup.

Theorem 3.1.5. (*e.g.,* [37, Thm 6.2.4, 6.2.7]) If the system (3.1.1) is stabilizable and (A, C) is detectable, then the cost (3.1.8) has a minimum for every $z_0 \in \mathcal{Z}$. Furthermore, there exists a self-adjoint non-negative operator $\Pi \in \mathcal{L}(\mathcal{Z})$ such that

$$\min_{u \in L_2(0,\infty;U)} J(u, z_0) = \langle z_0, \Pi z_0 \rangle. \tag{3.1.9}$$

The operator Π is the unique non-negative solution to the Riccati operator equation,

$$\langle Az_1, \Pi z_2 \rangle + \langle \Pi z_1, Az_2 \rangle + \langle Cz_1, Cz_2 \rangle - \langle B^*\Pi z_1, R^{-1}B^*\Pi z_2 \rangle = 0, \tag{3.1.10}$$

for all $z_1, z_2 \in \mathbf{D}(A)$. Defining, $K = R^{-1}B^*\Pi$, the corresponding optimal control is $u(t) = -Kz(t)$ and $A - BK$ generates an exponentially stable semigroup.

Thus, as in finite-dimensions, the linear quadratic optimal control is given by a state feedback. In the next section, the formulation of the LQ cost function for placing actuators on systems described on an infinite-dimensional state space will be described.

3.2 Well-posedness of LQ-Optimal Actuator Location Problem

Consider the situation of placing m actuators and parametrize the input operator B by the actuator location r, $B(r)$. For each r, there is a linear quadratic optimal control problem (3.1.8) which is indicated by $J_r(u, z_0)$ with corresponding optimal cost $\langle \Pi(r)z_0, z_0 \rangle$. A scalar cost that depends only on the actuator location is needed. In this section, well-posedness of the optimal actuator location problem on $\mathcal{Z}$ under different assumptions on the initial condition is proven.

First, the actuator location is chosen to minimize the response to the worst initial condition, and the objective function to be minimized by the best actuator location is given by,

$$\max_{z_0 \in \mathcal{Z}, \|z_0\|=1} \min_{u \in L_2(0,\infty;U)} J_r(u, z_0) = \|\Pi(r)\|. \tag{3.2.1}$$

The performance for a particular r is $\mu(r) = \|\Pi(r)\|$ and the optimal performance is

$$\hat{\mu} = \inf_{r \in \Omega^m} \|\Pi(r)\|. \tag{3.2.2}$$

The following result shows that the optimal cost is continuous with respect to the actuator location, provided that $B(r)$ is a family of input operators that are compact and continuous with respect to actuator location.

Theorem 3.2.1. [97, Thm. 2.6] Let $B(r) \in \mathcal{L}(U, \mathcal{Z})$ be a family of compact input operators such that for any $r_0 \in \Omega^m$

$$\lim_{r \to r_0} \|B(r) - B(r_0)\| = 0.$$

If $(A, B(r))$ is stabilizable for all $r \in \Omega^m$ and (A, C) is detectable, then the Riccati operators $\Pi(r)$ are continuous functions of r in the operator norm as follows:

$$\lim_{r \to r_0} \|\Pi(r) - \Pi(r_0)\| = 0,$$

and there exists an optimal actuator location $\hat{r}$ such that

$$\|\Pi(\hat{r})\| = \inf_{r \in \Omega^m} \|\Pi(r)\| = \hat{\mu}.$$

The above theorem provides the conditions that are required for the existence of an optimal actuator location.

Some technical definitions are necessary before discussing the second case.

Definition 3.2.2. [130] Let H_1 and H_2 be Hilbert spaces. An operator $S \in \mathcal{L}(H_1, H_2)$ is said to be *Hilbert-Schmidt* if

$$\sum_{n \in \mathbb{N}} \|Se_n\|^2 < +\infty$$

for some orthonormal basis $\{e_n\}_{n \in \mathbb{N}}$.

Every Hilbert-Schmidt operator is compact (*e.g.,* [130, Thm. 6.10]). If S is a compact operator, then the non-zero eigenvalues of $|S| = (S^*S)^{\frac{1}{2}}$ are called the *singular values* of S. An alternative characterization of Hilbert-Schmidt operator is the following : an operator S is Hilbert-Schmidt if and only if

$$\sum_{n\in\mathbb{N}}(\sigma_n(S))^2 < +\infty,$$

where $\sigma_n(S)$ is the nth singular value of the operator $S \in \mathcal{L}(H_1, H_2)$.

Definition 3.2.3. If the singular values of an operator $S \in \mathcal{L}(H_1, H_2)$ are summable, then it is said to be a *nuclear operator*:

$$\sum_{n\in\mathbb{N}}\sigma_n(S) < +\infty.$$

Clearly, every nuclear operator is Hilbert-Schmidt since

$$\sum_{n\in\mathbb{N}}(\sigma_n(S))^2 \leq \left(\sum_{n\in\mathbb{N}}\sigma_n(S)\right)^2.$$

If the initial condition is random, with zero mean and unity variance, then the expected cost is trace $[\Pi(r)]$, or since Π is self-adjoint and non-negative on $\mathcal{L}(\mathcal{Z}, \mathcal{Z})$, $\|\Pi(r)\|_1$, where $\|.\|_1$ indicates the nuclear norm:

$$\|\Pi(r)\|_1 = \text{ trace } [\Pi(r)] = \sum_{n\in\mathbb{N}}\sigma_n(\Pi(r)).$$

See [130] for details. The performance for a particular actuator location r is

$$\mu(r) = \|\Pi(r)\|_1 \tag{3.2.3}$$

and the optimal performance is

$$\hat{\mu} = \inf_{r\in\Omega^m} \|\Pi(r)\|_1. \tag{3.2.4}$$

The difficulty with using the nuclear norm of Π as an objective function is that the operator Π does not always have a finite nuclear norm and it may not even be a compact operator, as the following examples show. It will be shown that compactness and nuclearity of Π are required to show well-posedness of optimal actuator location problem and thus, convergence of LQ optimal actuator location. The notation $*$ denotes the adjoint of an operator.

Example 3.2.4. [37] Consider (3.1.1)-(3.1.8) with any A, B, C such that $A^* = -A$ and $C = B^*$. Then $\Pi = I$ is a solution to the ARE

$$A^*\Pi + \Pi A - \Pi B B^* \Pi + C^* C = 0. \tag{3.2.5}$$

The identity operator is not compact on any infinite-dimensional Hilbert space.

Example 3.2.5. This example from [97] is a generalization of [30, Example 1]. Let $\mathcal{Z} = \mathbb{R} \times \mathcal{X}$, where $\mathcal{X}$ is any infinite-dimensional Hilbert space and define the operators A, B, C on $\mathcal{Z}$ by

$$A = \begin{bmatrix} -1 & 0 \\ 0 & -I \end{bmatrix}, B = \begin{bmatrix} 1 \\ 0 \end{bmatrix}, C = \begin{bmatrix} \sqrt{3} & 0 \\ 0 & \sqrt{2}M \end{bmatrix}$$

where M is a bounded operator on $\mathcal{X}$. By direct computation it follows that

$$\Pi = \begin{bmatrix} 1 & 0 \\ 0 & M^2 \end{bmatrix}$$

is the solution to (3.2.5). This operator is not compact if M is not a compact operator; for instance $M = I$. Also, if M is a compact operator, but not a Hilbert-Schmidt operator, then Π is a compact operator, but not nuclear. This example is particularly interesting because A generates an exponentially stable semigroup.

Theorem 3.2.6. [97, Thm. 2.9] Assume that the pair (A, B) is stabilizable and the pair (A, C) is detectable and that B and C are compact operators. Then Π is a compact operator.

If the input space U and output space Y are both finite-dimensional then Π is a nuclear operator [36, Thm. 3.3]. Thus, Π has a finite nuclear norm. This implies that the nuclear norm of the optimal cost is a continuous function of the actuator location.

Theorem 3.2.7. [97, Thm. 2.10] Let $B(r) \in \mathcal{L}(U, \mathcal{Z}), r \in \Omega^m$, be a family of input operators such that for any $r_0 \in \Omega^m$

$$\lim_{r \to r_0} \|B(r) - B(r_0)\| = 0.$$

Assume that $(A, B(r))$ are all stabilizable and that (A, C) is detectable, where $C \in \mathcal{L}(Z, Y)$. If U and Y are finite-dimensional, then the corresponding Riccati operators $\Pi(r)$ are continuous functions of r in the nuclear norm:

$$\lim_{r \to r_0} \|\Pi(r) - \Pi(r_0)\|_1 = 0,$$

and there exists an optimal actuator location $\hat{r}$ such that

$$\|\Pi(\hat{r})\|_1 = \inf_{r \in \Omega^m} \|\Pi(r)\|_1 = \hat{\mu}.$$

Thus, the LQ optimal actuator location problem is well-posed with two different treatments of the initial condition.

3.3 Approximating Solutions

The Riccati operator equation (3.1.10) can rarely be solved exactly. In practice, the control is calculated using an approximation Π^N to Π. Most numerical schemes for approximating systems governed by partial differential equations developed during the last fifty years have focused on providing convergent and efficient simulations. However, many papers have also appeared describing conditions under which approximating controls converge to the control for the original infinite-dimensional system, see *e.g.,* [12, 52, 83, 64] for details. In this section, conditions on the approximation scheme under which the finite-dimensional approximation Π^N converges to Π in some sense are given.

Let $\{\mathcal{Z}^N\}$ be a family of finite dimensional subspaces of $\mathcal{Z}$, and let P^N be the orthogonal projection of $\mathcal{Z}$ onto $\mathcal{Z}^N$. The space $\mathcal{Z}^N$ is equipped with the norm inherited from $\mathcal{Z}$. Consider a sequence of operators $A^N \in \mathcal{L}(\mathcal{Z}^N)$ that generate a C_0 semigroup $T^N(t)$, $B^N \in \mathcal{L}(U, \mathcal{Z}^N)$. This leads to a sequence of approximations

$$\frac{dz}{dt} = A^N z(t) + B^N u(t), \quad z(0) = z_0^N = P^N z_0, \tag{3.3.1}$$

with cost functional,

$$J^N(u(\cdot), z_0) = \int_0^\infty \langle C^N z(t), C^N z(t)\rangle + \langle u(t), Ru(t)\rangle \, dt \tag{3.3.2}$$

where $C^N = C \mid_{\mathcal{Z}^N}$. If (A^N, B^N) is stabilizable and (A^N, C^N) is detectable, then the cost functional has the minimum cost $\langle P^N z_0, \Pi^N P^N z_0\rangle$, where Π^N is the unique non-negative solution to the algebraic Riccati equation,

$$(A^N)^*\Pi^N + \Pi^N A^N - \Pi^N B^N R^{-1}(B^N)^*\Pi^N + (C^N)^* C^N = 0 \tag{3.3.3}$$

on the finite-dimensional space $\mathcal{Z}^N$.

The feedback control $K^N = R^{-1}(B^N)^*\Pi^N$ is used to control the original system (3.1.1). Assumptions that guarantee that Π^N converges to Π in some sense are required in order for the use of finite-dimensional approximations in designing a controller for the original infinite-dimensional system to be valid. The following set of assumptions on the approximation scheme is standard in approximation of controllers for partial differential equations.

(A1) Convergence of semigroup and its adjoint: For each $z \in \mathcal{Z}$

(i) $\|T^N(t)P^N z - T(t)z\| \to 0$;
(ii) $\|(T^N)^*(t)P^N z - T^*(t)z\| \to 0$;

uniformly in t on bounded intervals.

(A2) Uniform exponential stabilizability and detectability:
(i) The family of pairs (A^N, B^N) is uniformly exponentially stabilizable; there exists a uniformly bounded sequence of operators $K^N \in \mathcal{L}(Z^N, U)$ such that

$$\|e^{(A^N - B^N K^N)t} P^N z\| \le M_1 e^{-\omega_1 t}\|z\| \tag{3.3.4}$$

for some positive constants $M_1 \ge 1$ and ω_1.
(ii) The family of pairs (A^N, C^N) is uniformly exponentially detectable; there exists a uniformly bounded sequence of operators $F^N \in \mathcal{L}(Y, Z^N)$ such that

$$\|e^{(A^N - F^N C^N)t} P^N z\| \le M_2 e^{-\omega_2 t}\|z\| \tag{3.3.5}$$

for some positive constants $M_2 \ge 1$ and ω_2.

(A3) Convergence of operators B, C and their adjoints: For each $z \in \mathcal{Z}, u \in U, y \in Y$,

$$\text{(i) } \|B^N u - Bu\| \to 0 \text{ and } \|(B^N)^* P^N z - B^* z\| \to 0; \tag{3.3.6}$$

$$\text{(ii) } \|C^N P^N z - Cz\| \to 0 \text{ and } \|(C^N)^* y - C^* y\| \to 0; \tag{3.3.7}$$

Note that the Trotter-Kato Theorem [108, Chap. 3, Thm. 4.2] is an important equivalent statement of (A1)(i), which is required for convergence of initial conditions. The assumption (A1)(ii) is required for the strong convergence of the approximating feedback operator. A counter-example may be found in [29]. Assumption (A1) implies that $P^N z \to z$ for all $z \in \mathcal{Z}$.

Many approximation schemes, such as modal approximation, linear splines for the diffusion problem and cubic splines for damped beam vibrations are uniformly stabilizable (detectable), provided that the original system is stabilizable (detectable) [96], [99, Thm. 5.2, Thm. 5.3].

Theorem 3.3.1. [12, Thm. 6.9],[64, Thm 2.1, Cor 2.2] Assume that (A1)-(A3) are satisfied and that (A, B) is stabilizable and (A, C) is detectable. Then for each N, the finite dimensional ARE (3.3.3) has a unique non-negative solution Π^N with $\sup \|\Pi^N\| < \infty$. There exists constants $M_3 \geq 1, \omega_3 > 0$, independent of N, such that,

$$\|e^{\left(A^N - B^N R^{-1} (B^N)^* \Pi^N\right) t}\| \leq M_3 e^{-\omega_3 t}. \tag{3.3.8}$$

Furthermore, for all $z \in \mathcal{Z}$,

$$\lim_{N \to \infty} \|\Pi^N P^N z - \Pi z\| = 0, \tag{3.3.9}$$

and

$$\lim_{N \to \infty} \|K^N P^N z - Kz\| = 0. \tag{3.3.10}$$

The above result provides sufficient conditions for strong convergence of the approximating Riccati operators. For large N performance arbitrarily close to the optimal is obtained with K^N. However, it was shown in [97, Example 3.2] that the strong convergence of the Riccati operators is not sufficient to ensure that the optimal cost and a

corresponding sequence of optimal actuator locations converge. Since the cost is the norm (or trace norm) of the Riccati operator, uniform convergence (or trace norm convergence) of the operators is required. That is,

$$\lim_{N\to\infty} \|\Pi^N P^N - \Pi\| = 0 \text{ (or } \lim_{N\to\infty} \|\Pi^N P^N - \Pi\|_1 = 0) \tag{3.3.11}$$

is needed in order to use approximations in determining optimal actuator location.

Conditions for uniform convergence of the Riccati operators are provided below. Conditions stronger than those used in Theorem 3.3.1 are needed.

Theorem 3.3.2. [97, Thm 3.3] Let assumptions (A1)-(A3) be satisfied. If B and C are both compact operators, with $\lim_{N\to\infty} \|B^N - P^N B\| = 0$ then the minimal non-negative solution Π^N to (3.3.3) converges uniformly to the non-negative solution Π to (3.1.10).

The following theorem shows that if U and Y are finite-dimensional, then any approximation scheme that satisfies (A1)-(A3) will lead to uniform convergence of Riccati operators in nuclear norm.

Theorem 3.3.3. [97, Thm. 3.8] Assume that (A, B) is stabilizable and (A, C) is detectable, and that U and Y are finite-dimensional. Let (A^N, B^N, C^N) be a sequence of approximations to (A, B, C) that satisfy assumptions (A1)-(A2). Then

$$\lim_{N\to\infty} \|\Pi^N P^N - \Pi\|_1 = 0 \tag{3.3.12}$$

Thus, assumptions on the approximation scheme that are required to establish uniform convergence of Riccati operators have been described. Convergence of a sequence of LQ optimal actuator locations for the approximations to the correct location for the full partial differential equation model is described in the next section.

3.4 Convergence of LQ-Optimal Actuator Locations

Thus, the objective functions (3.2.1) and (3.2.3) for calculating the LQ-optimal actuator locations are posed on the infinite-dimensional state space. But, the operator Riccati equation (3.1.10) can only be solved by an approximation scheme that satisfies the assumptions

(A1)-(A3). For the sequence of approximating problems $(A^N, B^N(r), C^N)$ define analogously to J_r, $\mu(r)$, and $\hat{\mu}$, the cost-functional $J_r^N(u, z_0)$, the cost for a particular location $\mu^N(r)$ and the optimal cost $\hat{\mu}^N$. Theorems 3.2.1 and 3.2.7 apply to these finite-dimensional problems. Since the operators $B^N(r)$ and C^N have finite rank, the performance measure $\mu^N(r)$ is continuous with respect to actuator location r and the optimal performance $\hat{\mu}^N$ is well-defined in both cases. Conditions under which approximations yield reliable results for the calculation of LQ optimal actuator location are given in this section.

The following result shows that if Π^N converges to Π in operator norm at each actuator location, then the sequence of optimal performance and corresponding optimal locations for the approximations converge to the exact performance and corresponding optimal location.

Theorem 3.4.1. [97, Thm. 3.5] Assume that the input operators $B(r)$ are compact and such that for any $r_0 \in \Omega^m$

$$\lim_{r \to r_0} \|B(r) - B(r_0)\| = 0.$$

Assume also that (A1)-(A3) are satisfied for each $(A^N, B^N(r), C^N)$ where $B^N = P^N B$ and that for each r

$$\lim_{n \to \infty} \|\Pi^N(r) - \Pi(r)\| = 0.$$

Letting $\hat{r}$ be an optimal actuator location for $(A, B(r), C)$ with optimal cost $\hat{\mu}$ and defining similarly $\hat{r}^N, \hat{\mu}^N$, it follows that:

$$\hat{\mu} = \lim_{N \to \infty} \hat{\mu}^N, \tag{3.4.1}$$

and also there exists a subsequence $\{\hat{r}^M\}$ of $\{\hat{r}^N\}$ such that

$$\hat{\mu} = \lim_{M \to \infty} \|\Pi(\hat{r}^M)\|. \tag{3.4.2}$$

The following result shows that if U and Y are finite-dimensional, then again any approximation scheme that satisfies (A1)-(A3) will lead to a convergent sequence of actuator locations that are optimal in the nuclear norm.

Theorem 3.4.2. [97, Thm. 3.9] Assume a family of control systems $(A, B(r), C)$ with finite-dimensional input space U and finite-dimensional output space Y such that

1. $(A, B(r))$ are stabilizable and (A, C) is detectable;

2. for any $r_0 \in \Omega^m$, $\lim_{r \to r_0} \|B(r) - B(r_0)\| = 0$.

Choose some approximation scheme such that assumptions (A1)-(A3) are satisfied for each $(A, B(r), C)$ with $B^N(r) = P^N B(r), C^N = C|_{\mathcal{Z}^N}$. Letting $\hat{r}$ be an optimal actuator location for $(A, B(r), C)$ with optimal cost $\hat{\mu}$ and defining similarly $\hat{r}^N, \hat{\mu}^N$, it follows that:

$$\hat{\mu} = \lim_{N \to \infty} \hat{\mu}^N, \tag{3.4.3}$$

and also there exists a subsequence $\{\hat{r}^M\}$ of $\{\hat{r}^N\}$ such that

$$\hat{\mu} = \lim_{M \to \infty} \|\Pi(\hat{r}^M)\|_1. \tag{3.4.4}$$

Thus, the approximations yield reliable results. A brief summary of numerical calculation of LQ-optimal actuator location is presented next.

3.5 Computation of LQ-Optimal Actuator Locations

Once the problem is formulated and a suitable approximation scheme found, there remain several numerical issues associated with the calculation of LQ-optimal actuator locations. Often approximating partial differential equations leads to systems of large model order (3.3.1). Hence, calculating the LQ-cost functions (3.2.1), (3.2.3) require efficient numerical methods for solving large LQ-AREs. First, a short description of the existing methods for solving AREs is reviewed. Then, a survey of solving large LQ-AREs is presented. Finally, some methods used to solve the resulting optimization problem are mentioned.

Solving Algebraic Riccati Equation

The algebraic Riccati equation,

$$A^*P + PA - PBR^{-1}B^*P + C^*C = 0, \tag{3.5.1}$$

is nonlinear, but amenable to solution by methods which rely heavily on linear algebra and the theory of matrices [81]. The existing methods of solving (3.5.1) are broadly classified into two main categories: Hamiltonian methods and iterative methods.

The Hamiltonian methods are basically eigenvector decomposition techniques. The associated Hamiltonian matrix for (3.5.1), denoted by $H \in \mathbb{R}^{2n\times 2n}$ is,

$$H := \begin{bmatrix} A & BR^{-1}B^* \\ -C^*C & -A^* \end{bmatrix}. \tag{3.5.2}$$

Let H be diagonalizable and have the eigendecomposition:

$$V^{-1}HV = \begin{pmatrix} -\overline{\Lambda} & 0 \\ 0 & \Lambda \end{pmatrix},$$

where $\Lambda = \text{diag}(\lambda_1, \ldots, \lambda_n)$ and $\lambda_1, \ldots, \lambda_n$ are the n eigenvalues of H with positive real parts. Let V be partitioned conformably:

$$V = \begin{bmatrix} V_{11} & V_{12} \\ V_{21} & V_{22} \end{bmatrix}$$

such that $\begin{pmatrix} V_{11} \\ V_{12} \end{pmatrix}$ is the matrix of eigenvectors corresponding to the stable eigenvalues. In [114], LQ-AREs were solved by computing the stable invariant eigenspace of the associated Hamiltonian matrix (3.5.2), that is $P = V_{21}V_{11}^{-1}$ is the unique stabilizing solution of (3.5.1). It is also called the eigenvector method in literature. The method is numerically unstable when the space spanned by the eigenvectors of (3.5.2) is not full, that is, when (3.5.2) is not diagonalizable. The numerical difficulties of the eigenvector method may be reduced if H is transformed to an ordered real Schur form rather than using its eigendecomposition. Let U^THU be an ordered real Schur matrix:

$$U^THU = \begin{pmatrix} T_{11} & T_{12} \\ 0 & T_{22} \end{pmatrix},$$

where the eigenvalues of H with negative real parts are stacked in T_{11} and positive real parts are stacked in T_{22}. Let

$$U = \begin{pmatrix} U_{11} & U_{12} \\ U_{21} & U_{22} \end{pmatrix}$$

be a conformable partition of U. Then, the matrix $P = U_{21}U_{11}^{-1}$ is the unique stabilizing solution of (3.5.1). Such a technique was suggested in [84] where the eigenvector calculation is replaced with the calculation of Schur vectors U. The Schur algorithm can be numerically unstable if the matrices involved in the computation are poorly scaled. This difficulty can be overcome by proper scaling [75]. Thus for all practical purposes, the Schur method when combined with an appropriate scaling, is numerically stable. This method may not be suitable for large systems due to limitations on the calculation of eigenvectors for large non-symmetric matrices. A structure preserving method for computing the stable invariant subspace of the matrix pencils $H - \lambda I$, was suggested in [16]. An iterative projection onto the block Krylov subspace by computing the orthonormal basis was proposed in [66, 67]. A general framework to define new low-rank approximations obtained from stable invariant subspaces of the Hamiltonian matrix associated with large-scale systems was introduced in [3]. In [119], the matrix sign function of the corresponding Hamiltonian (3.5.2),

$$sgn(H) = T \begin{bmatrix} -I & 0 \\ 0 & I \end{bmatrix} T^{-1}$$

where $T \in \mathbb{R}^{2n \times 2n}$, was computed using a scaled Newton iteration (see for instance [31, 39, 94]). Then, this method computes the stable invariant subspace using projectors $(I - sgn(H))$ calculated with this sign function. A library of parallel routines was developed for solving LQ problems involving systems of dimensions up to $\mathcal{O}(10^4)$ in [21]. The algorithms involve computing the sign-function of the corresponding Hamiltonian matrices which provides projectors onto certain subspaces of the matrix.

Two common iterative methods are Chandrasekhar [69] and Newton-Kleinman iterations [78]. In Chandrasekhar iterations, the Riccati equation is not itself solved directly. A system of 2 differential equations

$$\dot{K}(t) = -B^T L^T(t) L(t), \qquad K(0) = 0, \tag{3.5.3}$$

$$\dot{L}(t) = L(t)(A - BK(t)), \qquad L(0) = C, \tag{3.5.4}$$

is solved for $K \in \mathbb{R}^{m \times n}, L \in \mathbb{R}^{p \times n}$ [32, 69]. Chandrasekhar systems have been used by many researchers, for *e.g.,* [11, 25, 26, 28, 104, 120]. This technique is attractive due to its significant savings in storage when the number of controls m and number of observations

p is less than the number of the states n. This situation occurs in the approximation of partial differential equations. The feedback operator is obtained as $\lim_{t\to-\infty} K(t)$ and the convergence can be very slow [11]. A strategy for approximating long-time behaviour of (3.5.4) was used in [25, 26]. If this approach is used alone, a very accurate algorithm must be used [120]. This can lead to very large computation times for large system and/or a stiff system.

The Newton-Kleinman iteration proposed in [78], has been a favourite technique among researchers, for *e.g.,* [10, 18, 39, 47, 103].This technique involves the following iterative scheme,

$$\begin{aligned} A_n^T\Pi_n + \Pi_n A_n + C^T C + K_n^T R K_n = 0, \\ K_{n+1} := R^{-1}B^T\Pi_n, \\ A_{n+1} := A - BK_{n+1}. \end{aligned} \tag{3.5.5}$$

The first equation in (3.5.5) is a Lyapunov equation which is linear in nature and easier to solve than the ARE (3.5.1). This iterative method (3.5.5) produces a sequence of symmetric matrices that converges to the solution of the Riccati equation. The local quadratic convergence of $\lim\limits_{n\to\infty} \Pi_n = \Pi$ was shown with an initial stabilizing matrix Π_0 in [78]. Following the standard Newton-Kleinman iterative scheme (3.5.5), an exact line-search method to improve the convergence of Riccati solutions was suggested in [14]. The solution of Lyapunov equations obtained by computing the matrix sign function was suggested in [18]. The solutions to the linear quadratic optimal control problem for infinite-dimensional systems was calculated using this method [55].

Instead of the standard Newton-Kleinman form (3.5.5), a modified Newton-Kleinman iteration was first suggested in [11]:

$$(A - BK_i)^T X_i + X_i(A - BK_i) = -D_i^T D_i, \quad i = 1, 2, \ldots, \tag{3.5.6}$$

where $X_i = \Pi_{i-1} - \Pi_i$, $K_{i+1} = K_i - R^{-1}B^T X_i$ and $D_i = K_i - K_{i-1}$. The resulting Lyapunov equation is solved for X_i. In [11], the partial solution obtained by solving Chandrasekhar equations is used as a stabilizing initial feedback for (3.5.6). Following (3.5.6), a Cholesky-ADI algorithm (*e.g.,* [88, 111]) was used in [103, 104] that exploits features such as sparsity,

symmetry and the fact that the number of inputs and outputs are small when compared to the order of the system in many applications. If an inexact Newton-Kleinman method is applied to calculate the solution of the resulting Lyapunov equation in (3.5.6), then the residuals accumulate at the end of each iteration making this implementation unstable; see [47, Section 7] for details.

Optimization Techniques

For the LQ cost criteria, the cost function is a norm on the solution of the ARE. Despite being the minimal non-negative solution, $\|\Pi(r)\|$ is non-convex with respect to the actuator location r. The computation of optimal actuator locations (2.1.2) is an additional layer of optimization. The location that corresponds to the minimal cost $\hat{\mu}$ is chosen as the optimal actuator location. A number of approaches have been used in literature to minimize the cost function over all possible actuator locations.

Genetic algorithm, a heuristic based global search, is a favorite approach among engineers; see for *e.g.,* [1, 68, 80, 109]. Its most attractive feature is that it does not need derivatives or any auxiliary information about the function to be optimized. This makes its application relatively easy. Such an algorithm may fail to find the best location and is typically slow, e.g., [38]. Other heuristic procedures include simulated annealing [63], tabu search [77] and guided neighbourhood search [118]. Standard search algorithms like sequential quadratic programming [7], interior point methods [40] and gradient based optimization [46] have also been employed.

The non-convex LQ optimal actuator location problem was converted into a convex problem by reformulating it as a discrete optimization on $\mathbb{R}^N$ with N discrete set of possible actuator locations in [51]. Once the problem is written in the convex form, it was further relaxed and solved using a linear $0-1$ mixed program. It was shown that a gradient based optimization algorithm is much faster and is more accurate than genetic algorithm in determining the global solution to this reformulated convex problem in [38].

In this chapter, the LQ optimal actuator location problem for systems modeled by partial differential equations has been studied. Conditions that guarantee reliable solutions for

the calculation of LQ optimal actuator location using approximations have been described. Computation of LQ optimal actuator location has been discussed.

Chapter 4

$\mathcal{H}_\infty$-Optimal Actuator Locations : Theoretical Framework

Noise in the environment and disturbances have a significant impact on the performance of the controlled system. In fact, the effect of disturbance can nullify the control authority of an actuator at a location which is considered optimal using some other performance criterion [42]. In this chapter and the rest of this thesis, optimal actuator locations using $\mathcal{H}_\infty$-performance with state feedback is considered. That is both, the controller and the actuator locations are chosen to minimize the effect of disturbances on the output.

A theoretical framework for calculating $\mathcal{H}_\infty$-optimal actuator locations is developed in this chapter. First, the $\mathcal{H}_\infty$ control problem on an infinite-dimensional state space is described. Next, continuity of $\mathcal{H}_\infty$-performance with respect to actuator locations and hence, existence of $\mathcal{H}_\infty$-optimal actuator locations are proved. Approximations to systems modeled by partial differential equations are used in $\mathcal{H}_\infty$ controller design and thus in selection of the actuator location. The issues associated with the use of approximations in determining optimal actuator locations have not been extensively investigated. An approximation theory that shows convergence of $\mathcal{H}_\infty$ cost for fixed actuator locations [65] is described next. This leads to the main result: conditions under which $\mathcal{H}_\infty$-optimal actuator locations calculated using approximations converge to the exact optimal locations. An example is provided to illustrate that convergence may fail when these conditions are

not satisfied.

4.1 $\mathcal{H}_\infty$-Control of Infinite-Dimensional Systems

Consider the system described on a Hilbert space $\mathcal{Z}$ by

$$\frac{dz}{dt} = Az(t) + Bu(t) + Dv(t), \quad t \geq 0 \;\; z(0) = z_0 \in \mathcal{Z} \tag{4.1.1}$$

where A with $\mathbf{D}(A)$ generates a C_0-semigroup $S(t)$ on $\mathcal{Z}$. Here, $B \in \mathcal{L}(U, \mathcal{Z}), D \in \mathcal{L}(W, \mathcal{Z})$. It is assumed that U and W are separable Hilbert spaces. The signal $u(\cdot) \in L_2(0, \infty; U)$ is the control input and $v(\cdot) \in L_2(0, \infty; W)$ is the exogenous disturbance. Write $\mathcal{U} = L_2(0, \infty; U)$ and $\mathcal{W} = L_2(0, \infty; W)$ to denote the space of all admissible controls and disturbances respectively. For a separable Hilbert space Y, for $C \in \mathcal{L}(\mathcal{Z}, Y)$, $R \in \mathcal{L}(U, U)$, where R is coercive, define the cost

$$y(t) = \begin{bmatrix} Cz(t) \\ R^{\frac{1}{2}} u(t) \end{bmatrix}, \tag{4.1.2}$$

and the index

$$\rho(u, v; z_0) = \|y\|^2_{L_2(0,\infty;Y)} = \int_0^\infty \|Cz(t)\|^2 + \|R^{\frac{1}{2}} u(t)\|^2 dt. \tag{4.1.3}$$

Systems of the form (4.1.1)-(4.1.2) will often be abbreviated $(A, [B \;\; D], C)$. The system (4.1.1)-(4.1.2) is a special form of the generalised plant configuration, known as *the full information problem.*

The definition for fixed attenuation $\mathcal{H}_\infty$ control problem for (4.1.1) - (4.1.2) is similar to finite-dimensional systems (Definition 2.4.1) except now the system is infinite-dimensional.

Definition 4.1.1. If there is a $\delta > 0$ such that for each disturbance $v \in \mathcal{W}$, there exists a control $u \in \mathcal{U}$ with

$$\rho(u, v; 0) \leq (\gamma^2 - \delta) \parallel v \parallel^2_{\mathcal{W}}, \tag{4.1.4}$$

then the system (4.1.1) with (4.1.2) is said to be *stabilizable with attenuation* γ.

As in the finite-dimensional case, if the problem (4.1.1)-(4.1.2) is stabilizable with attenuation γ then this attenuation can be achieved with state feedback.

Definition 4.1.2. The state feedback $K \in \mathcal{L}(\mathcal{Z}, U)$ is said to be γ - *admissible* if it is stabilizing and the linear feedback $u(t) = -Kz(t)$ is such that the attenuation bound (4.1.4) is achieved.

Theorem 4.1.3. [23, 76] Assume that (A, B) is stabilizable and (A, C) is detectable. For $\gamma > 0$ the following are equivalent:
(1) there exists a γ-admissible state feedback;
(2) the system is stabilizable with attenuation γ;
(3) there exists a non-negative, self-adjoint operator Σ on $\mathcal{Z}$ satisfying the $\mathcal{H}_\infty$-Riccati operator equation,

$$(A^*\Sigma + \Sigma A - \Sigma B R^{-1} B^*\Sigma + \frac{1}{\gamma^2}\Sigma D D^*\Sigma + C^*C)z = 0 \tag{4.1.5}$$

for all $z \in \mathbf{D}(A)$, and $A - BR^{-1}B^*\Sigma + \frac{1}{\gamma^2}DD^*\Sigma$ generates an exponentially stable semigroup on $\mathcal{Z}$. Moreover, in this case a γ-admissible state feedback is given by $K = R^{-1}B^*\Sigma$.

A question that naturally arises is the existence of a state feedback $K \in \mathcal{L}(\mathcal{Z}, U)$ that minimizes this attenuation level γ.

Definition 4.1.4. The *optimal $\mathcal{H}_\infty$-control problem* for (4.1.1)-(4.1.2) is to calculate

$$\hat{\gamma} = \inf \gamma \tag{4.1.6}$$

over all $K \in \mathcal{L}(\mathcal{Z}, U)$ such that the system (4.1.1)-(4.1.2) is stabilizable with attenuation γ. The infimum $\hat{\gamma}$ is called the optimal $\mathcal{H}_\infty$-disturbance attenuation.

4.2 Well-posedness of $\mathcal{H}_\infty$-Optimal Actuator Location on a Hilbert Space

Consider the situation of placing m actuators and parametrize the input operator with respect to the actuator location by $B(r)$. The location that minimizes the optimal $\mathcal{H}_\infty$-disturbance attenuation is chosen as the actuator location.

Definition 4.2.1. The *optimal $\mathcal{H}_\infty$-cost* μ over all possible locations is defined as,

$$\mu = \inf_{r \in \Omega^m} \hat{\gamma}(r) \tag{4.2.1}$$

Also, if it exists, the location $\hat{r} \in \Omega^m$ that satisfies,

$$\hat{r} = \arg \inf_{r \in \Omega^m} \hat{\gamma}(r) \tag{4.2.2}$$

is the *$\mathcal{H}_\infty$-optimal actuator location.*

The value $\hat{\gamma}(r)$ provides the best possible attenuation of the disturbance that has the worst effect on the output.

Continuity of the $\mathcal{H}_\infty$-performance $\hat{\gamma}(r)$ with respect to actuator location will be proved under the following assumptions:

(C1) The family of input operators $B(r) \in \mathcal{L}(U, \mathcal{Z})$, $r \in \Omega^m$ are continuous functions of r in the operator norm, that is for any $r_0 \in \Omega^m$,

$$\lim_{r \to r_0} \| B(r) - B(r_0) \| = 0. \tag{4.2.3}$$

(C2) The family of pairs $(A, B(r))$, $r \in \Omega^m$, are stabilizable and the pair (A, C) is detectable.

(C3) The input operators $B(r)$ and the disturbance operator D are compact. Also, Ω^m is compact.

Assumption (C2) implies that the operator Riccati equation for linear quadratic control of the system at some location $r_0 \in \Omega^m$,

$$\langle Az_1, \Pi(r_0)z_2 \rangle + \langle \Pi(r_0)z_1, Az_2 \rangle + \langle Cz_1, Cz_2 \rangle - \langle B^*(r_0)\Pi(r_0)z_1, R^{-1}B^*(r_0)\Pi(r_0)z_2 \rangle = 0, \tag{4.2.4}$$

has the unique non-negative, self-adjoint solution $\Pi(r_0)$ for all $z_1, z_2 \in \mathbf{D}(A)$ (Theorem 3.1.5). Let $S_0(t)$ be the exponentially stable semigroup generated by $A - B(r_0)R^{-1}B^*(r_0)\Pi(r_0)$.

For any given disturbance $v \in \mathcal{W}$, define $L(r_0) \in \mathcal{L}(\mathcal{W}, \mathcal{L}_2(0,\infty;\mathcal{Z}))$ by

$$(L(r_0)v)(t) = \int_t^\infty S_0^*(\tau - t)\Pi(r_0)Dv(\tau)d\tau. \tag{4.2.5}$$

Define $z_{r_0}(\cdot)$ as the state of the system $(A, [B(r_0)\ D], C)$. Before presenting the continuity result and its proof a technical lemma is stated below. The details may be found in [23] or [76, Thm. 4.4].

Lemma 4.2.2. Assume that the assumption (C2) holds for the system at some location $r_0 \in \Omega^m$. Then for every $v \in \mathcal{W}$, $z_0 \in \mathcal{Z}$,

$$u_{r_0}(t) = -R^{-1}B^*(r_0)[\Pi(r_0)z_{r_0}(t) + (L(r_0)v)(t)] \tag{4.2.6}$$

minimizes $\rho_{r_0}(u, v; z_0)$ over $u \in \mathcal{U}$ subject to (4.1.1)-(4.1.2) at the location r_0.

Proof. For $v \in \mathcal{W}$ and $z_0 \in \mathcal{Z}$, the index at the location r_0 is

$$\rho_{r_0}(u, v; z_0) = \int_0^\infty \langle Cz_{r_0}(t), Cz_{r_0}(t)\rangle + \langle u(t), Ru(t)\rangle\ dt. \tag{4.2.7}$$

where $z_{r_0}(\cdot)$ is the state of the system $(A, [B(r_0)\ D], C)$. For this system, substituting (4.2.4) and (4.2.5) and rearranging, the equation (4.2.7) becomes

$$\begin{aligned}\rho_{r_0}(u, v; z_0) &= \langle z_0, \Pi(r_0)z_0\rangle + 2\langle z_0, (L(r_0)v)(0)\rangle \\ &+ \int_0^\infty 2\langle Dv(t), (L(r_0)v)(t)\rangle dt - \int_0^\infty \|R^{-1}B^*(r_0)(L(r_0)v)(t)\|^2 dt \\ &+ \int_0^\infty \|u(t) + R^{-1}B^*(r_0)\Pi(r_0)z_{r_0}(t) + R^{-1}B^*(r_0)(L(r)v)(t)\|^2 dt.\end{aligned}$$

The details may be found in [23] or [76, Thm. 4.4]. Clearly, the control (4.2.6) minimizes $\rho_{r_0}(u, v; z_0)$ over $u \in \mathcal{U}$ subject to (4.1.1)-(4.1.2) at the location r_0. □

Theorem 4.2.3. Let $(A, [B(r)\ D], C)$ be a family of systems such that assumptions (C1)-(C3) are satisfied. Assume that the system at r_0 is stabilizable with attenuation $\gamma(r_0)$ and $K(r_0) \in \mathcal{L}(\mathcal{Z}, U)$ is $\gamma(r_0)$-admissible. There is $\delta > 0$ such that for all $\|r - r_0\| < \delta$ the systems $(A, [B(r)\ D], C)$ are stabilizable with attenuation $\gamma(r_0)$. Furthermore, a sequence of state feedback operators $K(r) \in \mathcal{L}(\mathcal{Z}, U)$ can be chosen that are $\gamma(r_0)$-admissible at r and also $K(r)$ is continuous at r_0.

Proof. This is based on the approach in [65, Thm. 2.5]. Consider a sequence $\{r\}$ that converges to a point r_0. The proof has several parts. First, it is shown that the system at r is stabilizable with attenuation $\gamma(r_0)$ and a sequence of state feedback operators $K(r) \in \mathcal{L}(\mathcal{Z}, U)$ can be chosen that are $\gamma(r_0)$-admissible at r. Then, it is proven that the $\mathcal{H}_\infty$-Riccati operator at r converges strongly to r_0 and finally, it is shown that the sequence of state feedback operators $K(r)$ is continuous at r_0.

Since the problem at r_0 is stabilizable with attenuation $\gamma(r_0)$, it follows from Theorem 4.1.3 that the $\mathcal{H}_\infty$-Riccati operator equation (4.1.5) for the system at r_0 has a self-adjoint non-negative solution $\Sigma(r_0)$ on $\mathcal{Z}$. It can be written [23, 76]

$$\Sigma(r_0)z = \Pi(r_0)z + \int_0^\infty S_0^*(t)\Pi(r_0)Dv_{r_0}(t)dt, \tag{4.2.8}$$

where $v_{r_0} \in \mathcal{W}$ is the unique solution of

$$Q(r_0)v_{r_0}(\cdot) - D^*\Pi(r_0)S_0(\cdot)z = 0 \tag{4.2.9}$$

where

$$Q(r_0) = \gamma^2(r_0)I - D^*L(r_0) - L^*(r_0)D + L^*(r_0)B(r_0)B^*(r_0)L(r_0) \tag{4.2.10}$$

is both self-adjoint and coercive. The optimal control $u_{r_0} \in \mathcal{U}$ is of feedback form:

$$u_{r_0}(t) = -R^{-1}B^*(r_0)\Sigma(r_0)z(t). \tag{4.2.11}$$

Choose $K = R^{-1}B^*(r_0)\Sigma(r_0)$ so that $A - B(r_0)K$ generates an exponentially stable semigroup $S_{K,r_0}(t)$ with bound $Me^{-\alpha t}$, where $\alpha > 0$. Let δ be such that $A - B(r)K$ generates an exponentially stable semigroup with bound $Me^{-\frac{\alpha}{2}t}$ for all $\|B(r) - B(r_0)\| < \delta$. There is $\epsilon > 0$ such that for all $\|r - r_0\| < \epsilon$, $\|B(r) - B(r_0)\| < \delta$. Thus, there is a sequence of uniformly exponentially stabilizable systems $(A, B(r))$. It follows from Theorem 3.1.5 that at each $r \in \Omega^m$, the LQR Riccati equation has a non-negative, self-adjoint solution $\Pi(r)$ and $A - B(r)R^{-1}B^*(r)\Pi(r)$ generates an exponentially stable semigroup $S_r(t)$. The sequence $(A, B(r))$ with $r \to r_0$ satisfies the assumptions of Theorem 3.2.1 and hence

$$\lim_{r \to r_0} \|\Pi(r) - \Pi(r_0)\| = 0.$$

Furthermore, the semigroups $S_r(t)$ are uniformly exponentially stable: there exists $M \geq 1$, $\alpha > 0$ such that $\|S_r(t)\| \leq Me^{-\alpha t}$. Defining $\tilde{K}(r_0) := R^{-1}B^*(r_0)\Pi(r_0)$ and $\tilde{K}(r) := R^{-1}B^*(r)\Pi(r)$ it follows that $\|\tilde{K}(r) - \tilde{K}(r_0)\| \to 0$ as $r \to r_0$. Since $B(r)\tilde{K}(r)$ converges in norm to $B(r_0)\tilde{K}(r_0)$, the adjoint operators also converge and so

$$S_r(t)z \to S_0(t)z, \quad S_r^*(t)z \to S_0^*(t)z \tag{4.2.12}$$

for all $z \in \mathcal{Z}$, uniformly on bounded intervals of time. Since D is a compact operator, $\|S_r^*(t)\Pi(r)D - S_0^*(t)\Pi(r_0)D\| \to 0$ converges uniformly on bounded intervals of time. For $\tau > 0$ and $p \in [1, \infty)$,

$$\begin{aligned}
&\int_0^\infty \|S_r^*(t)\Pi(r)D - S_0^*(t)\Pi(r_0)D\|^p dt \\
&\quad \leq \int_0^\tau \|S_r^*(t)\Pi(r)D - S_0^*(t)\Pi(r_0)D\|^p dt \\
&\quad\quad + \int_\tau^\infty \left(\|S_r^*(t)\|^p \|\Pi(r)\|^p + \|S_0^*(t)\|^p \|\Pi(r_0)\|^p\right) \|D\|^p dt.
\end{aligned}$$

For all $p \in [1, \infty)$, it follows from (4.2.12) and uniform exponential stability of $S_r(t)$ that

$$\int_0^\infty \|S_r^*(t)\Pi(r)D - S_0^*(t)\Pi(r_0)D\|^p dt \to 0 \tag{4.2.13}$$

as $r \to r_0$. Define the linear operator $L(r)$ on $\mathcal{W}$ for the problem at r that corresponds to (4.2.5). It follows that

$$\| \left((L(r) - L(r_0))v\right)(t)\|^2 \leq \left(\int_0^\infty \|(S_r^*(t)\Pi(r) - S_0^*(t)\Pi(r_0))D\| dt\right)^2 \|v\|_{\mathcal{W}}^2 \tag{4.2.14}$$

for any $v \in \mathcal{W}$. It follows from (4.2.13) that

$$\lim_{r \to r_0} \|L(r) - L(r_0)\| = 0. \tag{4.2.15}$$

From Lemma 4.2.2,

$$u_r(t) = -R^{-1}B^*(r)[\Pi(r)z_r(t) + (L(r)v)(t)] \tag{4.2.16}$$

minimizes $\rho_r(u, v; z_0)$ over $u \in \mathcal{U}$ subject to (4.1.1)-(4.1.2) at the location r, where $z_r(\cdot)$ is the state of (4.1.1)-(4.1.2) at r . Then, with initial condition $z_0 = 0$,

$$z_r(t) = \int_0^t S_r(t-s)\left(-B(r)R^{-1}B^*(r)(L(r)v)(s) + Dv(s)\right) ds, \tag{4.2.17}$$

$$z_{r_0}(t) = \int_0^t S_0(t-s)\left(-B(r_0)R^{-1}B^*(r_0)(L(r_0)v)(s) + Dv(s)\right) ds. \tag{4.2.18}$$

Since $B(r), B(r_0)$ and D are compact, it follows that

$$\| z_r - z_{r_0} \|^2_{L_2(0,\infty;\mathcal{Z})} \;\leq\; \epsilon_1^2 \| v \|^2_{\mathcal{W}}, \quad \| u_r - u_{r_0} \|^2_{\mathcal{U}} \;\leq\; \epsilon_2^2 \| v \|^2_{\mathcal{W}},$$

where $\epsilon_1, \epsilon_2 \to 0$ as $r \to r_0$. Since $C \in \mathcal{L}(\mathcal{Z}, Y)$ and R is coercive it follows that

$$| \rho_r(u_r, v; 0) - \rho_{r_0}(u_{r_0}, v; 0) | \;\leq\; \epsilon^2 \| v \|^2_{\mathcal{W}}, \tag{4.2.19}$$

where $\epsilon \to 0$ as $r \to r_0$. Since the system at r_0 is stabilizable with attenuation $\gamma(r_0)$ there is $\delta_1 > 0$ so that

$$\rho_{r_0}(u_{r_0}, v; 0) \;\leq\; (\gamma^2(r_0) - \delta_1)\|v\|^2_{\mathcal{W}}. \tag{4.2.20}$$

Choosing ϵ sufficiently small, there is δ so that for all $\|r - r_0\| < \delta$, the system at r has attenuation $\gamma(r)$ where

$$\gamma(r) \;\leq\; \gamma(r_0). \tag{4.2.21}$$

It follows from Theorem 4.1.3 that there exists a state feedback $K(r) = R^{-1}B^*(r)\Sigma(r)$ which is $\gamma(r_0)$-admissible at r, where $\Sigma(r)$ is the self-adjoint non-negative solution (4.2.8) to the $\mathcal{H}_\infty$-Riccati operator equation (4.1.5) for the system at r. The disturbance $v_r(\cdot) \in \mathcal{W}$ is the unique solution of (4.2.9) at r. Define the linear operator $Q(r) \in \mathcal{W}$ for the problem at r with attenuation $\gamma(r_0)$ that corresponds to (4.2.10). Clearly,

$$\|Q(r) - Q(r_0)\| \to 0 \tag{4.2.22}$$

as $r \to r_0$. Also, (4.2.13) implies that

$$\int_0^\infty \|D^*\Pi(r)S_r(t) - D^*\Pi(r_0)S_{r_0}(t)\|^2 dt \to 0 \tag{4.2.23}$$

as $r \to r_0$. Therefore, the solution to (4.2.9) at r satisfies

$$\|v_r\|_{\mathcal{W}} \leq M_1 \|z\|_{\mathcal{Z}}, \tag{4.2.24}$$

for some constant M_1. Note that

$$Q(r_0)(v_r - v_{r_0}) = (Q(r_0) - Q(r))v_r + (D^*\Pi(r)S_r(t) - D^*\Pi(r_0)S_{r_0}(t))z. \tag{4.2.25}$$

It follows from (4.2.22)-(4.2.24) that v_r converges strongly to v_{r_0} in $\mathcal{W}$ as $r \to r_0$. It now follows from (4.2.8) and (4.2.13) that

$$\|\Sigma(r)z - \Sigma(r_0)z\| \to 0 \tag{4.2.26}$$

as $r \to r_0$.

Thus,

$$\begin{aligned}\|K(r) - K(r_0)\| &= \|R^{-1}B^*(r)\Sigma(r) - R^{-1}B^*(r_0)\Sigma(r_0)\| \\ &\leq \|R^{-1}\|\|(\Sigma(r) - \Sigma(r_0))B(r)\| + \|R^{-1}\|\|\Sigma(r_0)\|\|B(r) - B(r_0)\|.\end{aligned}$$

Since $B(r)$ is compact and $\Sigma(r)$ converges strongly to $\Sigma(r_0)$, it follows from (C1) that $K(r)$ converges uniformly to $K(r_0)$. □

Theorem 4.2.4. Consider a family of control systems $(A, [B(r)\ D], C)$ such that the assumptions (C1) - (C3) are satisfied. Then

$$\lim_{r \to r_0} \hat{\gamma}(r) = \hat{\gamma}(r_0), \tag{4.2.27}$$

where $\hat{\gamma}(r_0)$ is the optimal disturbance attenuation at r_0 and there exists an optimal actuator location $\hat{r}$ such that

$$\hat{\gamma}(\hat{r}) = \inf_{r \in \Omega^m} \hat{\gamma}(r) = \mu.$$

Proof. A similar argument may be found in [65, Thm. 2.8]. Consider any sequence $\{r_n\}$ that converges to r_0. Theorem 4.2.3 implies

$$\limsup_{n \to \infty}\ \hat{\gamma}(r_n) \leq \hat{\gamma}(r_0). \tag{4.2.28}$$

Because of (4.2.28), it is sufficient to show that

$$\liminf_{n\to\infty} \hat{\gamma}(r_n) \geq \hat{\gamma}(r_0). \tag{4.2.29}$$

Assume that this statement is false. Then there is an $\delta > 0$ such that for all n there is $p > n$ with $\hat{\gamma}(r_p) \leq \hat{\gamma}(r_0) - \delta$. In this way a subsequence $\{r_p\}$ of the sequence $\{r_n\}$ is constructed with $\hat{\gamma}(r_p) \leq \hat{\gamma}(r_0) - \delta$. Thus, the system at r_p is stabilizable with attenuation $\hat{\gamma}(r_0) - \frac{\delta}{2}$ and

$$\rho_{r_p}(u_{r_p}, v; 0) \leq \left(\hat{\gamma}(r_0) - \frac{\delta}{2}\right)^2 \|v\|^2_{\mathcal{W}} \tag{4.2.30}$$

where $v \in \mathcal{W}$, $u_{r_p}(t)$ is defined by (4.2.16) at the location r_p. Moreover, from (4.2.19)

$$|\rho_{r_p}(u_{r_p}, v; 0) - \rho_{r_0}(u_{r_0}, v; 0)| \ \leq \ \epsilon^2 \ \|v\|^2_{\mathcal{W}}, \tag{4.2.31}$$

where $\epsilon \to 0$ as $r_p \to r_0$ and $u_{r_0}(t)$ is given by (4.2.6). Therefore, the problem at r_0 is stabilizable with attenuation $\hat{\gamma}(r_0) - \frac{\delta}{2}$. This contradicts the optimality of $\hat{\gamma}(r_0)$ and thus (4.2.29) holds. Hence (4.2.27) holds. This shows that $\hat{\gamma}(r)$ is a continuous function of r on Ω^m. Since Ω^m is compact, an optimal actuator location exists. □

4.3 Approximating Solutions

In practice, the operator equation (4.1.5) cannot be solved and the control is calculated using an approximation. Let $\mathcal{Z}^N$ be a family of finite-dimensional subspaces of $\mathcal{Z}$ and P^N the orthogonal projection of $\mathcal{Z}$ onto $\mathcal{Z}^N$. The space $\mathcal{Z}^N$ is equipped with the norm inherited from $\mathcal{Z}$. Consider a sequence of operators $A^N \in \mathcal{L}(\mathcal{Z}^N, \mathcal{Z}^N)$, $B^N \in \mathcal{L}(U, \mathcal{Z}^N)$, $D^N \in \mathcal{L}(W, \mathcal{Z}^N)$, and $C^N = C|_{\mathcal{Z}^N}$. The same assumptions (A1)-(A3) (Section 3.3) on the approximation scheme as for the linear quadratic control problem are used except (A3), is replaced by the following assumption that includes convergence of D^N.

(A3') Convergence of operators B, C and D: The approximating sequence of input and disturbance operators converge in norm

$$\lim_{N\to\infty} \|B^N - B\| = 0, \ \lim_{N\to\infty} \|D^N - D\| = 0, \tag{4.3.1}$$

and for each $z \in \mathcal{Z}, y \in Y$,

$$\|C^N P^N z - Cz\| \to 0 \text{ and } \|(C^N)^* y - C^* y\| \to 0.$$

Since the approximating spaces $\mathcal{Z}^N$ are finite-dimensional, B^N and D^N are finite-rank operators. Thus (4.3.1) holds only if the operators B and D are compact [130]. The assumption (A3') is automatically satisfied if the definitions $B^N = P^N B, D^N = P^N D$ and $C^N = C|_{\mathcal{Z}^N}$ are used.

Theorem 4.3.1. Assume that (A, B) is stabilizable and (A, C) is detectable, and (A1)-(A2) and (A3') hold. If the original system is stabilizable with attenuation γ, then so are the approximating systems for sufficiently large N. For such N, the Riccati equation

$$(A^N)^*\Sigma^N + \Sigma^N A^N - \Sigma^N B^N R^{-1}(B^N)^*\Sigma^N + \frac{1}{\gamma^2}\Sigma^N D^N (D^N)^*\Sigma^N + (C^N)^* C^N = 0 \quad (4.3.2)$$

has a non-negative, self-adjoint solution Σ^N and $\Sigma^N P^N z \to \Sigma z$ strongly in $\mathcal{Z}$ as $N \to \infty$. Moreover, $K^N = R^{-1}(B^N)^*\Sigma^N$ converges to $K = R^{-1}B^*\Sigma$ in norm. For N sufficiently large, K^N is γ-admissible for the original system.

Proof. This follows from [65, Thm. 2.5, Cor. 2.6] with the extension of $B^N = P^N B$ and $D^N = P^N D$ to more general approximations. □

This implies that the corresponding finite-dimensional controls converge to that obtained with the infinite-dimensional solution and yield a performance which is arbitrarily close to the original model for the given fixed attenuation. Let $\{\hat{\gamma}^N\}$ indicate the optimal disturbance attenuation for the approximating problems.

Theorem 4.3.2. Assume that (A1)-(A2), (A3') hold, (A, B) is stabilizable, and (A, C) is detectable. Then

$$\lim_{N\to\infty} \hat{\gamma}^N = \hat{\gamma}. \quad (4.3.3)$$

Proof. This follows from Theorem 4.3.1 and [65, Thm. 2.8] with the extension of $B^N = P^N B$ and $D^N = P^N D$ to more general approximations. □

This implies that the optimal $\mathcal{H}_\infty$-disturbance attenuation of the approximating systems converge to the correct value of the original model for fixed actuator locations. In the next section, convergence of $\mathcal{H}_\infty$-optimal actuator locations is proven.

4.4 Convergence of $\mathcal{H}_\infty$-optimal actuator locations

For the sequence of approximating problems $(A^N, [B^N(r)\ D^N], C^N)$ parameterized by the actuator location define, analogously to $\hat{\gamma}(r)$ and μ, $\hat{\gamma}^N(r)$ and μ^N. Theorems 4.2.3 and 4.2.4 apply to these finite-dimensional problems. Since the operators $B^N(r)$ and D^N have finite rank, the $\mathcal{H}_\infty$-performance $\hat{\gamma}^N(r)$ is continuous with respect to r and the optimal performance μ^N is well-defined. The optimal cost and the corresponding actuator locations for the approximating problems converge to the exact cost and optimal actuator locations.

Any approximation method satisfying assumptions (A1)-(A2) and (A3') will not only guarantee convergence of optimal attenuation for fixed actuator locations but also will lead to a convergent sequence of $\mathcal{H}_\infty$-optimal actuator locations.

Theorem 4.4.1. Let $(A, [B(r)\ D], C)$ be a family of control systems depending on actuator location such that assumptions (C1) - (C3) are satisfied. Choose some approximation scheme such that assumptions (A1) - (A2) are satisfied for each $(A^N, [B^N(r)\ D^N], C^N)$ where $B^N = P^N B, D^N = P^N D, C^N = C|_{\mathcal{Z}^N}$. Letting $\hat{r}$ be an optimal actuator location for $(A, [B(r)\ D], C)$ with optimal cost μ and defining similarly $\hat{r}^N$, μ^N, it follows that

$$\mu = \lim_{N\to\infty} \mu^N,$$

and there exists a subsequence $\{\hat{r}^M\}$ of $\{\hat{r}^N\}$ such that

$$\mu = \lim_{M\to\infty} \hat{\gamma}(\hat{r}^M).$$

Proof. A similar proof for the convergence of linear quadratic optimal actuator locations

may be found in [97].

$$\begin{aligned}\mu^N &= \inf_{r\in\Omega^m} \hat{\gamma}^N(r) \\ &\leq \hat{\gamma}^N(\hat{r}) \\ &= \hat{\gamma}^N(\hat{r}) - \hat{\gamma}(\hat{r}) + \hat{\gamma}(\hat{r}) \\ &= \hat{\gamma}^N(\hat{r}) - \hat{\gamma}(\hat{r}) + \mu.\end{aligned}$$

Since $\lim_{N\to\infty} \hat{\gamma}^N(\hat{r}) = \hat{\gamma}(\hat{r})$ (Theorem 4.3.2),

$$\limsup \mu^N \leq \mu. \tag{4.4.1}$$

It remains only to show that

$$\liminf \mu^N \geq \mu. \tag{4.4.2}$$

To this end, choose a subsequence $\mu^M \to \liminf \mu^N$, with corresponding actuator locations $\hat{r}^M$. Since $\{\hat{r}^M\} \subset \Omega^m$, it has a convergent subsequence, also denoted by $\hat{r}^M$, with limit $\underline{r}$. Now,

$$\begin{aligned}\|B^M(\hat{r}^M) - B(\underline{r})\| &= \|P^M B(\hat{r}^M) - B(\underline{r})\| \\ &\leq \|P^M B(\hat{r}^M) - P^M B(\underline{r})\| + \|P^M B(\underline{r}) - B(\underline{r})\| \\ &\leq \|P^M\|\|B(\hat{r}^M) - B(\underline{r})\| + \|P^M B(\underline{r}) - B(\underline{r})\|.\end{aligned}$$

Thus, $\| B^M(\hat{r}^M) - B(\underline{r}) \| \to 0$. By assumption (A2)(i), there is a uniformly bounded sequence $K^M_{\underline{r}} \in \mathcal{L}(\mathcal{Z}, U)$ such that $A^M - B^M(\underline{r})K^M_{\underline{r}}$ generate semigroups bounded by $M_1 e^{-\omega_1 t}$ for some $M_1 \geq 1, \omega_1 > 0$. For some $\epsilon < \frac{\omega_1}{M_1\|K^M_{\underline{r}}\|}$, choose N large enough such that $\| B^M(\hat{r}^M) - B^M(\underline{r}) \| < \epsilon$ for $M > N$. Then for all $M > N$, $A^M - B^M(\hat{r}^M)K^M_{\underline{r}}$ generates an exponentially stable C_0-semigroup with bound $M_1 e^{\left(-\omega_1 + \epsilon M_1 \|K^M_{\underline{r}}\|\right)}$. Applying then Theorem 4.3.2 to the sequence $(A^M, [B^M(\hat{r}^M)\ D^M], C^M)$, it follows that $\hat{\gamma}^M(\hat{r}^M) \to \hat{\gamma}(\underline{r})$. Thus,

$$\begin{aligned}\liminf \mu^N &= \lim_{M\to\infty} \mu^M \\ &= \lim_{M\to\infty} \hat{\gamma}^M(\hat{r}^M) \\ &= \hat{\gamma}(\underline{r}) \\ &\geq \mu.\end{aligned} \tag{4.4.3}$$

Thus, $\liminf \mu^N \geq \mu$ and so $\lim \mu^N = \mu$ as required.

Since $\mu = \lim \mu^N = \liminf \mu^N$, (4.4.3) implies that

$$\begin{aligned} \mu &= \liminf \mu^N \\ &= \hat{\gamma}(\underline{r}) \\ &= \lim_{M \to \infty} \hat{\gamma}(\hat{r}^M). \end{aligned} \tag{4.4.4}$$

where the latter equality follows from continuity of $\mathcal{H}_\infty$ performance with respect to actuator location (Theorem 4.2.4). Thus, as was to be shown, a sequence of approximating actuator locations yield performance arbitrarily close to optimal. □

This result shows that the problem of calculating an optimal actuator location for $\mathcal{H}_\infty$-cost using approximation yields reliable results. The following example illustrates this result.

Example 4.4.2. Consider a simply supported Euler-Bernoulli beam and let $w(x,t)$ denote the deflection of the beam from its rigid body motion at time t and position x. The deflection is controlled by applying a force $u(t)$ around the point r with width ϵ. The exogenous disturbance $v(t)$ induces a distributed load $d(x)v(t)$ where $d(x) \in \mathbf{C}(0,1)$. If the variables are normalized and a viscous damping with parameter ξ is included, the following partial differential equation is obtained

$$\frac{\partial^2 w}{\partial t^2} + \xi \frac{\partial w}{\partial t} + \frac{\partial^4 w}{\partial x^4} = b_r(x)u(t) + d(x)v(t), \quad t \geq 0, 0 < x < 1, \tag{4.4.5}$$

$$b_r(x) = \begin{cases} \frac{1}{\epsilon}, & |r - x| < \frac{\epsilon}{2} \\ 0, & |r - x| \geq \frac{\epsilon}{2}. \end{cases}$$

The boundary conditions are

$$w(0,t) = 0, \quad w''(0,t) = 0, \quad w(1,t) = 0, \quad w''(1,t) = 0. \tag{4.4.6}$$

where $'$ denotes a derivative with respect to space. In the computer simulations, the parameters were set to $\xi = 0.1, \epsilon = 0.001$. Let

$$H_2(0,1) = \{w \in C^1(0,1) \mid w'(x) \text{ is absolutely continuous and } w''(x) \in L_2(0,1)\}, \tag{4.4.7}$$

Figure 4.1: Convergence of $\mathcal{H}_\infty$-performance and corresponding optimal actuator location for different approximations of the viscously damped beam with $C = I, R = 1, d = b_{0.7}$. The optimal $\mathcal{H}_\infty$ cost μ^N and the corresponding actuator location $\hat{r}^N$ are shown with respect to different approximation size (number of eigenmodes N)

(a) Optimal $\mathcal{H}_\infty$-cost

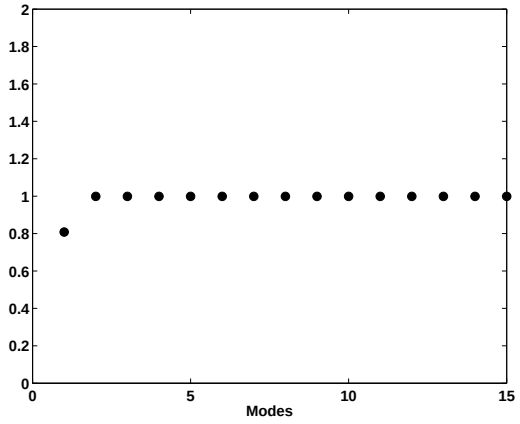

(b) Optimal actuator location

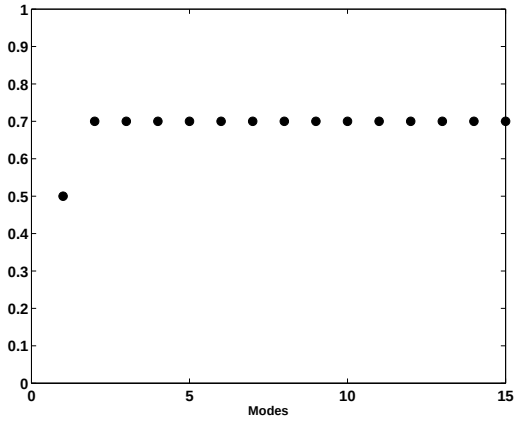

$$H_s(0,1) = \{w \in H_2(0,1), w(0) = 0, w(1) = 0\}, \tag{4.4.8}$$

and define the state space $\mathcal{Z} = H_s(0,1) \times L_2(0,1)$ with state $z(t) = (w(\cdot,t), \frac{\partial}{\partial t}w(\cdot,t))$. A state space formulation of the above partial differential equation problem is

$$\frac{d}{dt}z(t) = Az(t) + B(r)u(t) + Dv(t), \tag{4.4.9}$$

where

$$A = \begin{bmatrix} 0 & I \\ -\frac{d^4}{dx^4} & -\xi I \end{bmatrix}, B(r) = \begin{bmatrix} 0 \\ b_r(\cdot) \end{bmatrix}, D = \begin{bmatrix} 0 \\ d(\cdot) \end{bmatrix}, \tag{4.4.10}$$

with domain

$$\mathbf{D}(A) = \{(\phi, \psi) \in H_s(0,1) \times H_s(0,1) \text{ with } \phi'' \in H_s(0,1)\}.$$

It is well-known that A with domain $\mathbf{D}(A)$ generates an exponentially stable semigroup on $\mathcal{Z}$ [37]. Since there is only one control, choose control weight $R = 1$. An obvious choice

of measurement is $C = I$. Consider the disturbance $d = b_{0.7}$ centered at $r = 0.7$ with width $\epsilon = 0.001$. Since only one pair of actuator and disturbance is used, both $B(r)$ and D are finite-rank operators, and hence compact. Therefore, the corresponding $\mathcal{H}_\infty$-control with full-information problem satisfies the assumptions of Theorem 4.2.4. Hence, the cost $\hat{\gamma}(r)$ depends continuously on the actuator location and there exists an optimal actuator location. Since a closed form solution to the partial differential equation problem is not available, the optimal actuator location must be calculated using an approximation. Let $\phi_i(x)$ indicate the eigenfunctions of $\frac{\partial^4 w}{\partial x^4}$ with boundary conditions (4.4.6). For any positive integer N, define Z^N to be the span of $\phi_i, i = 1...N$. Choose $\mathcal{Z}^N = Z^N \times Z^N$ and define P^N to be the projection onto $\mathcal{Z}^N$. Define A^N to be the Galerkin approximation to A, $B^N := P^N B$ and $D^N := P^N D$. This approximation scheme satisfies all the assumptions of Theorem 4.4.1 [99] and hence, convergence of the approximating optimal performance and the actuator locations is obtained. This is illustrated in Figures 4.1a and 4.1b.

If D is not a compact operator then neither the optimal cost nor the corresponding actuator locations for approximating problem may converge. Even optimal attenuation for fixed actuator locations may not converge as shown in the following example.

Example 4.4.3. Consider the same example as before, except that now, the effect of worst disturbance on the entire state is minimized and $D = I$ is chosen in (4.4.9). Now D is not a compact operator. As shown in Figures 4.2a and 4.2b, neither optimal cost nor the optimal actuator location converges. In fact, the optimal attenuation does not converge even at a fixed actuator location, say for example at $r = 0.5$, as the approximation size increases. This is illustrated in Figure 4.3.

In the case of linear-quadratic optimal control, the actuator location is chosen to minimize $\|\Pi\|$ or trace Π where Π is the solution to the LQ algebraic Riccati equation. Compactness of the measurement operator C is required to guarantee optimality of LQ-optimal actuator locations; see [97] for details. This is because uniform convergence of the LQ Riccati operators is required to prove convergence of LQ-optimal actuator locations (Theorem 3.4.1). However, in the case of $\mathcal{H}_\infty$-performance strong convergence of $\mathcal{H}_\infty$-Riccati operator is enough to ensure convergence of $\mathcal{H}_\infty$-optimal actuator locations.

Figure 4.2: Neither $\mathcal{H}_\infty$-performance nor corresponding optimal actuator location converge for different approximations of the viscously damped beam with $C = I, R = 1, D = I$

(a) Optimal $\mathcal{H}_\infty$-cost

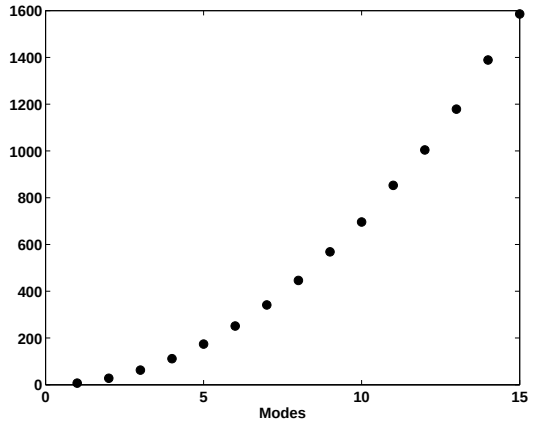

(b) Optimal actuator location

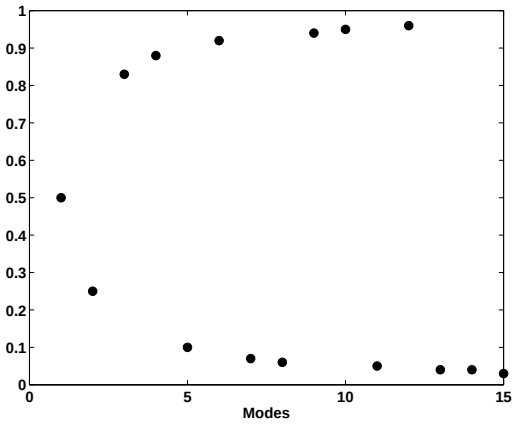

Figure 4.3: Performance $\hat{\gamma}$ at actuator location $r = 0.5$ for different approximations of the viscously damped beam with $C = I, R = 1, D = I$

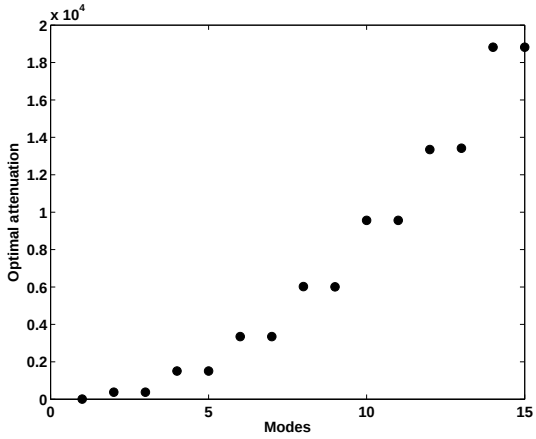

A theoretical framework for calculating optimal actuator locations using $\mathcal{H}_\infty$ criterion for the full partial differential equation model has been described in this chapter.

Conditions that guarantee reliable calculation of $\mathcal{H}_\infty$-optimal actuator location using approximations have been obtained.

Chapter 5

Numerical Calculation of $\mathcal{H}_\infty$-Control for Large-Scale Systems

Systems of large model order arise in a number of situations; including approximation of partial differential equation models. There is not a generally accepted algorithm that is suitable for solving large $\mathcal{H}_\infty$-algebraic Riccati equations. Furthermore, when finite-elements are used, the approximation is naturally written in a regular descriptor form. Many other important applications, such as electrical power systems and computer communication systems, lead to large-scale systems in descriptor form. In this form, the associated matrices are typically sparse and symmetric. The naive way of handling such systems is to explicitly convert the descriptor form into the standard form. From a theoretical point of view, this strategy solves the problem. On the other hand, from a numerical perspective this approach destroys the sparsity of the problem and thus creates computational difficulties for large-scale applications. It is desirable to preserve the sparse structure of the given descriptor form by avoiding explicit conversion into standard form.

In this chapter, a number of algorithms for computing a controller that achieves a given $\mathcal{H}_\infty$-attenuation are discussed. These algorithms are also used for the calculation of optimal $\mathcal{H}_\infty$-attenuation and a controller whose performance is close to the optimal. An extension of a game-theoretic iterative algorithm [82] to solve the $\mathcal{H}_\infty$-AREs for large regular descriptor systems is presented. A parallel implementation of the extended algorithm

is briefly described. The proposed method is compared to other methods using several examples arising in control of systems modeled by partial differential equations.

5.1 $\mathcal{H}_\infty$-Control for Descriptor Systems on $\mathbb{R}^n$

Consider the generalized linear system on $\mathbb{R}^n$

$$E\dot{z} = Az + Bu + Dv, \quad z(0) = z_0 \in \mathbb{R}^n, \tag{5.1.1}$$

$$y = Cz + D_{12}u, \tag{5.1.2}$$

where the matrices A, B, C, D, D_{12} are as described in Section 2.4. It is assumed that the mass matrix $E \in \mathbb{R}^{n\times n}$ is non-singular, that is (5.1.1) is a *regular descriptor system*. Approximating partial differential equations with finite element methods yield large descriptor systems where a mass matrix E is included in the description.

Definition 5.1.1. [54] The set of all matrices of the form $A - \lambda E$ with $\lambda \in \mathbb{C}$ is said to be a *matrix pencil*. The *eigenvalues* of the pencil are elements of the set $\lambda(A, E)$ defined by

$$\lambda(A, E) = \{z \in \mathbb{C} | \ \det\,(A - zE) = 0\}.$$

Definition 5.1.2. The matrix pair (A, E) is *Hurwitz*, if $\max_{1\le i\le n} \mathrm{Re}(\lambda_i) < 0$, where $\lambda_i \in \lambda(A, E), i = 1, \ldots, n$ are the eigenvalues of the pencil $A - \lambda E$.

Definition 5.1.3. [94] Let (E, A, B) be a matrix triple as in (5.1.1). Then the descriptor system (5.1.1) is *stabilizable* if there exists $K \in \mathbb{R}^{m\times n}$ such that the matrix pair $(A-BK, E)$ is Hurwitz.

Definition 5.1.4. [94] Let (E, A, C) be a matrix triple as in (5.1.1)-(5.1.2). Then the descriptor system (5.1.1)-(5.1.2) is *detectable* if there exists $F \in \mathbb{R}^{n\times p}$ such that the matrix pair $(A - FC, E)$ is Hurwitz.

Definition 5.1.5. Let λ be an eigenvalue of the matrix pencil (A, E). Then, the mode λ is said to be *controllable (observable)* for the matrix triple (E, A, B) ((E, A, C)) if $z^T B \neq 0$ ($Cz \neq 0$) for all left (right) generalized eigenvectors of the matrix pair (A, E) associated with λ, that is $z^T A = \lambda z^T E$ ($Az = \lambda Ez$) and $0 \neq z \in \mathbb{R}^n$. Otherwise, the mode λ is said to be uncontrollable (unobservable).

Since E is non-singular the above definitions are equivalent to those for standard systems (AE^{-1}, B, CE^{-1}), see *e.g.* [102].

The definitions for fixed-attenuation $\mathcal{H}_\infty$-control problem and optimal $\mathcal{H}_\infty$ control problem for (5.1.1)-(5.1.2) are similar to the standard systems (Definitions 2.4.1 and 2.4.3) except now G_{yv} is calculated without converting descriptor form into standard form. The following theorem is a straight-forward generalization of the result for standard systems (Theorem 2.4.2) to regular descriptor systems.

Theorem 5.1.6. Assume that the matrix triple (E, A, B) is stabilizable and (E, A, C) is detectable. For some given attenuation $\gamma > 0$, the fixed-attenuation $\mathcal{H}_\infty$-control problem for (5.1.1)-(5.1.2) is solvable if and only if there exists a symmetric, non-negative solution denoted by $P \geq 0$, that satisfies the $\mathcal{H}_\infty$-ARE

$$A^T PE + E^T PA - E^T P(BB^T - \frac{1}{\gamma^2} DD^T)PE + C^T C = 0, \tag{5.1.3}$$

such that the pair $(A + (\frac{1}{\gamma^2} DD^T - BB^T)PE, E)$ is Hurwitz. If so, one such control is

$$u = -Kz, \text{ where } K := B^T PE, \tag{5.1.4}$$

and also the pair $(A - BK, E)$ is Hurwitz.

Proof. Let $x = Ez$. The descriptor system (5.1.1)-(5.1.2) is converted into the standard state space form

$$\dot{x} = AE^{-1}x + Bu + Dv, \ x(0) := x_0 = Ez_0 \tag{5.1.5}$$

$$y = CE^{-1}x + D_{12}u. \tag{5.1.6}$$

Solving the $\mathcal{H}_\infty$-control problem for the descriptor system (5.1.1)-(5.1.2) is equivalent to solving it for the standard system (5.1.5)-(5.1.6). It follows from Theorem 2.4.2 that there exists a stabilizing controller for (5.1.5)-(5.1.6) if and only if there exists a symmetric, non-negative solution $P \geq 0$, that satisfies

$$(AE^{-1})^T P + P(AE^{-1}) - P(BB^T - \frac{1}{\gamma^2} DD^T)P + (CE^{-1})^T (CE^{-1}) = 0, \tag{5.1.7}$$

such that the matrix $AE^{-1} + (\frac{1}{\gamma^2}DD^T - BB^T)P$ is Hurwitz and one such control is $u = -Kx$, where $K := B^TP$, and also the matrix $AE^{-1} - BK$ is Hurwitz. The result follows for the descriptor system (5.1.1)-(5.1.2) when both the sides of equation (5.1.7) is multiplied by E^T on the left and E on the right. □

Except for a few special classes of systems, *e.g.* [33], calculation of optimal $\mathcal{H}_\infty$-attenuation is accomplished by an iterative bisection method [113, 121, 122]. As γ approaches $\hat{\gamma}$, the calculation of an accurate solution to the $\mathcal{H}_\infty$-ARE often becomes difficult; see Section 5.4 for details.

5.2 Review of Existing Numerical Methods

In this section, some numerical methods to calculate $\mathcal{H}_\infty$-controllers for both fixed and optimal attenuation are reviewed.

Invariant subspace of Hamiltonian

This approach for solving $\mathcal{H}_\infty$-Riccati equations is identical to a popular approach for solving LQ-AREs (see Section 3.5). The associated Hamiltonian matrix for the standard system (2.4.1) for $\gamma > 0$ denoted by $H \in \mathbb{R}^{2n\times 2n}$ is

$$H := \begin{bmatrix} A & \tilde{B}R^{-1}\tilde{B}^T \\ -C^TC & -A^T \end{bmatrix}, \tag{5.2.1}$$

where

$$\tilde{B} := \begin{bmatrix} D & B \end{bmatrix} \quad R := \begin{bmatrix} -\gamma^2 I_q & 0 \\ 0 & I_m \end{bmatrix}. \tag{5.2.2}$$

It is assumed that the pair (A, B) is stabilizable and the Hamiltonian matrix H does not have eigenvalues on the imaginary axis. These assumptions guarantee one-to-one correspondence between the stable invariant subspaces of H and the solutions to ARE (2.4.11) [81]. Therefore, these assumptions are required for the accurate calculation of a unique solution to (2.4.11).

An algorithm for solving the Riccati equations by computing the stable invariant subspace spanned by Schur vectors (see Section 3.5) of the associated Hamiltonian matrix H was proposed in [84]. However, the Schur algorithm can be numerically unstable if the matrices involved in the computation are poorly scaled. This difficulty can be overcome by proper scaling [75]. The Schur method when combined with an appropriate scaling, is numerically stable.

This method was extended to descriptor systems (5.1.1)-(5.1.2) in [8], where the solution of (5.1.3) is calculated by computing the stable invariant subspace spanned by Schur vectors of the extended Hamiltonian matrix pencil $H - \lambda J, \lambda \in \mathbb{C}, H, J \in \mathbb{R}^{(2n+m+q)\times(2n+m+q)}$, where

$$H := \begin{bmatrix} A & 0 & \tilde{B} \\ -C^TC & -A^T & 0 \\ 0 & \tilde{B}^T & R \end{bmatrix}, J := \begin{bmatrix} E & 0 & 0 \\ 0 & E^T & 0 \\ 0 & 0 & 0 \end{bmatrix}. \tag{5.2.3}$$

This method as implemented in [22, 35] is good for small and medium scale linear quadratic control problems but not suitable for most large-scale systems due to the difficulties involved in calculating Schur vectors for large matrices.

The matrix sign function method introduced in [119] (see Section 3.5) can also be used to solve AREs with a sign indefinite quadratic term. In this method, the matrix sign function of the corresponding Hamiltonian (5.2.1) is first computed iteratively using a scaled Newton iteration (see [31, 39, 94]). The sign function provides projectors onto the stable invariant subspace of the corresponding Hamiltonian. The solution to $\mathcal{H}_\infty$-ARE (2.4.11) is calculated using these projectors.

The size of the matrices involved in these methods are twice the order n of the system. The Schur method requires $240n^3$ floating point operations (flops) of which $25(2n^3)$ flops are required to reduce a $2n \times 2n$ Hamiltonian matrix to its real Schur form and the rest accounts for the computation of eigenvalues and solving a linear equation of order n.

The optimal $\mathcal{H}_\infty$ attenuation is calculated using a bisection algorithm where a $\mathcal{H}_\infty$-ARE is solved for a fixed attenuation at every iteration using the above method. As γ approaches the optimal attenuation, the eigenvalues of the corresponding Hamiltonian tend to the imaginary axis. The rounding errors made while calculating eigenvalues may destroy

the uniqueness of the stable invariant subspace causing the Riccati solver to fail (Example 5.6.2). In such case, the accuracy of the solution P to $\mathcal{H}_\infty$-ARE (5.1.3) is determined by calculating the normalized residual norm given by

$$NRN(P) = \frac{\|A^TPE + E^TPA - E^TP(BB^T - \frac{1}{\gamma^2}DD^T)PE + C^TC\|_F}{\|C^TC\|_F}. \tag{5.2.4}$$

where $\|.\|_F$ is the Frobenius norm. Both Schur and matrix sign function methods rely on calculating the stable-invariant subspaces. Problems can arise for cases when the Hamiltonian has eigenvalues near the imaginary axis (Example 5.6.1). This occurs for some lightly damped second-order systems (Example 5.6.4).

An iterative method for the calculation of optimal attenuation of a general linear system given in the standard state space form was suggested in [17]. This method uses an embedding of the Hamiltonian matrices and avoids calculating explicit solutions to Riccati equations. This methodology involves a structure-preserving method for extracting the stable subspace of the embedded Hamiltonian, which is very expensive to calculate for large matrices ($1280n^3$ flops [16]). Additionally, the symplectic QR and CS decomposition techniques employed in this method require $8n^3$ flops each. Thus, the overall complexity of this algorithm is quite high. An algorithm to calculate the CS decomposition used in [17, lemma 4.2] is neither described in this paper nor in the references. This iterative method was later extended to descriptor systems in [91] but the $\mathcal{H}_\infty$-optimal controller formulas for descriptor systems are not given. Therefore, this method was not tested on the examples below.

Convex method

A convex approach to calculate optimal $\mathcal{H}_\infty$-attenuation for the standard systems without using bisection, was proposed in [112]. The descriptor system given by (5.1.1)-(5.1.2) should be converted to the standard form (2.4.1) before applying this method. The set of all stabilizing controllers that guarantee a fixed attenuation is defined as a convex set on a suitable parameter space. Additional assumptions such as full-rank of a certain matrix, restriction on the dimension of the disturbance with respect to rank of the outputdesc

matrix C and order of the system n are required to reformulate the calculation of optimal attenuation as a convex problem. See [112, Thm. 3.4] for details.

Figure 5.1: Variation of μ_M as the order increases. Optimizer : $\mu^*(= 0.01) << \mu_M$

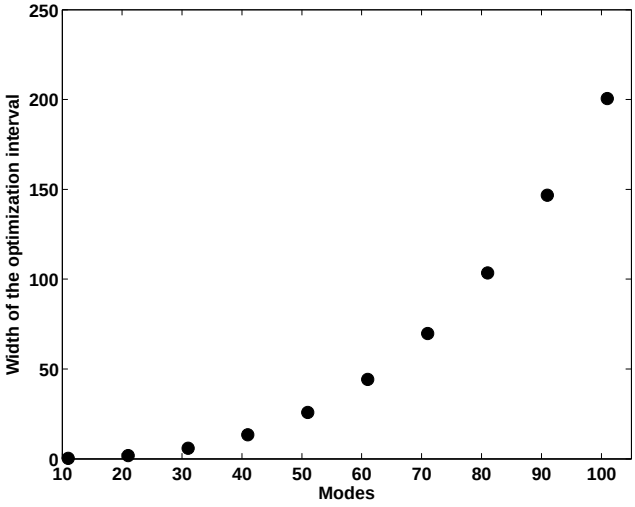

Once the problem is reformulated, many standard routines may be used. A possibility is to use the best approximation for the convex set following Kelley's cutting plane technique [92]. In this globally convergent technique, a convex problem is solved at each iteration. If the solution does not belong to this convex set, then a separating hyperplane between that point and the convex set is calculated. This technique shows exceedingly poor convergence [92, 126]. Cutting plane techniques require calculation of eigenvalues and eigenvectors which is expensive for large-scale systems.

A key hypothesis of this method is that the perturbations v should be rich in the sense that

$$\dim\,(v) \geq n - \ \text{rank}\,(C).$$

However, the assumptions in this algorithm are not generally satisfied by control problems where the model is a partial differential equation since the number of states is typically much larger than the number of disturbances.

Also, the complexity of the calculations is quite high. For large approximation order, re-writing optimal $\mathcal{H}_\infty$-attenuation as a convex problem on a suitable parameter space results in $\mathcal{O}(n^2)$ unknowns. At each iteration, the calculation of separating hyperplane requires $59n^3$ flops. Since the number of unknown variables are $n(n+1)/2$, the overall complexity of solving the convex problem at each iteration is $\mathcal{O}(n^6)$ flops. Consider the eigenvalue approximation of heat diffusion problem on a one-dimensional rod of unit length with an actuator placed at the centre, a disturbance collocated with the actuator and the observation $C = \sqrt{1000}I$. Larger the numerical value of

$$\mu_M = \min\{\mu > 0 : \det(V^*V - \mu\mathcal{R})\},$$

where

$$V := (D^*D)^{-1}D^* \begin{bmatrix} A & -B \end{bmatrix}, \mathcal{R} := \begin{bmatrix} C^TC & 0 \\ 0 & D_{12}^TD_{12} \end{bmatrix},$$

larger is the number of iterations required to achieve the best approximation to the convex set using cutting-plane method and hence, this technique is slower. The width of the optimization interval $[0, \mu_M]$ explodes with the order of the approximation, see Figure 5.1. The optimal attenuation for this problem is $\hat{\gamma} = \frac{1}{\mu^*} = 9.9$. However, the value of μ_M was much greater than the optimizer $\mu^* = 0.01$, even for systems of moderate size. Therefore, the number of iterations required to find the best approximation for the convex set grew exponentially with respect to the order of the system. Thus, it is difficult to extend this method to problems of large model order.

Non-linear optimization

In [27], a public domain package for $\mathcal{H}_\infty$-optimization, HIFOO, is introduced. The acronym HIFOO stands for $\mathcal{H}_\infty$ Fixed-Order Optimization. This method treats the $\mathcal{H}_\infty$-norm of the closed-loop system as a non-linear function with respect to the controller coefficients, which are the vector components of state feedback K. This non-linear optimization-based method neither solves Riccati equations nor Riccati inequalities. HIFOO does not have any restrictions on plant nor controller such as nullity or full-rank conditions.

Figure 5.2: Closed-loop attenuation achieved with the controller obtained from HIFOO for $\gamma = 10$ for different orders of approximation of (4.4.5)

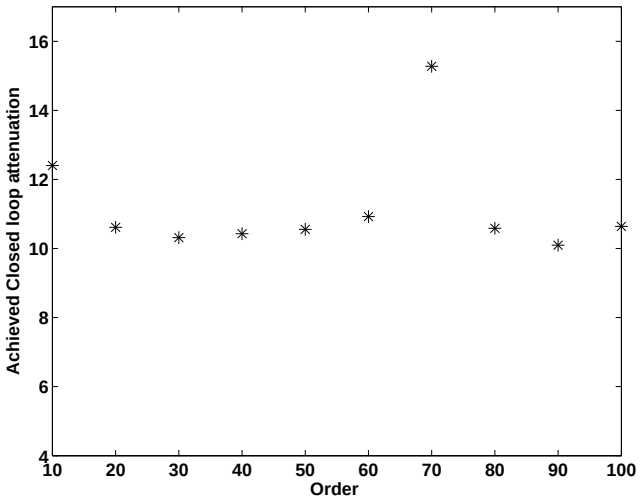

HIFOO uses two phases: stabilization and performance optimization. In the stabilization phase, HIFOO uses a quasi-Newton method (BFGS) to minimize the largest real part of eigenvalues of the closed loop system matrix. In the performance optimization phase, a local minimizer of the $\mathcal{H}_\infty$-norm of the closed loop system matrix is found using line-search methods, see [95, Appendix] for details. In both these stages, HIFOO uses a hybrid algorithm for nonsmooth, nonconvex optimization (HANSO) based on the following techniques: a quasi-Newton algorithm (BFGS) that provides a fast way to approximate a local minimizer and other optimization techniques to verify the local optimality for the best point found by BFGS. The complexity of using HIFOO is $2L \times (93n^3 + K \times \frac{28}{3}n^3))$ where K denotes the number of iterations required for the convergence of BFGS algorithm and L denotes the number of iterations required to achieve optimality.

Several benchmark examples were chosen from [85] and optimal $\mathcal{H}_\infty$-controllers of low-order were designed using HIFOO; see *e.g.,* [58, 59] for details. Systems were either in standard state space form or converted to standard state space form and the order of the systems used was no greater than 240. In each phase, BFGS optimization algorithm is used

extensively. HIFOO method is initiated with random starting points. Due to the inherent randomness in both phases and the fact that HIFOO solves a non-convex optimization problem, it may find a non-local minimum. If the calculated controller does not satisfy the required performance, then it is recommended to invoke HIFOO again with the obtained controller as an initial guess. For the fixed attenuation $\gamma = 10$, HIFOO is used to calculate the $\mathcal{H}_\infty$-controller on a simply supported beam model with viscous damping, see Example 4.4.2 for details. The HIFOO method failed to calculate the required controller even when it was invoked repeatedly. Figure 5.2 shows that the attenuation of the closed-loop system calculated with controllers for different modes did not converge to the required performance. This is because HIFOO randomizes all the controller coefficients. However, if the controller coefficients are constrained as

$$u(t) = \begin{bmatrix} \text{ones}(m,n) & \text{zeros}(m,q) \end{bmatrix} \begin{bmatrix} z(t) \\ v(t) \end{bmatrix}, \tag{5.2.5}$$

where ones imply that these coefficients can be randomized and zeros imply that these coefficients cannot be randomized and forced to be 0's, then the performance of HIFOO was satisfactory. In all our simulations, HIFOO method was used to synthesis a constant state-feedback control, where the order of the required controller was fixed as 0, and the constraint (5.2.5) was used while invoking this method.

HIFOO is primarily designed to synthesize output feedback controllers when the order of the controller is fixed to be less than that of the open-loop plant. It is also capable of calculating the optimal $\mathcal{H}_2$-controller with order fixed to be less than the given plant. Also, HIFOO can be used to design fixed-order controllers for the optimization of complex stability radius, stability margin and robust stability margin. The ability to handle multiple plants with mixed $\mathcal{H}_\infty$ and $\mathcal{H}_2$ optimization problems was added in HIFOO 3.0; see *e.g.,* [9, 57] for details.

Game theoretic iterative method

A recursive algorithm that reduces a $\mathcal{H}_\infty$-ARE to a series of LQ-AREs was proposed in [82]. This algorithm is motivated by the following game theoretic strategy. For $\gamma = 1$, consider

the quadratic differential game (2.4.10) for the standard system subject to (2.4.1). It is well-known that the optimal control law and the worst-case disturbance (a saddle point of (2.4.10)) are $u_{optimal} = -B^T P z$ and $v_{worst} = D^T P z$ where $P \geq 0$ is the unique stabilizing solution to (2.4.11); see *e.g.,* [102, 134] for details.

Define, $F : \mathbb{R}^{n\times n} \mapsto \mathbb{R}^{n\times n}$,

$$F(P) = PA + A^T P - P(BB^T - DD^T)P + C^T C. \tag{5.2.6}$$

In this algorithm, the game theory index (2.4.10) is reduced to a series of linear quadratic optimal control problems by guessing the disturbance (not the optimal but a strategy) at every iteration. Starting with $v_0 := 0$, suppose at the k-th iteration a trial control law is given by $u_k = -B^T P_k z$, where P_k is the solution sequence to LQ-AREs, then update the disturbance to be $v_k := D^T P_k z$ in both (2.4.1) and (2.4.10). The index (2.4.10) is reduced to a LQ control problem $J(u, v_k, z_0)$. Provided certain solvability conditions (discussed below) are satisfied, the resulting ARE

$$0 = P_{k+1}(A + DD^T P_k) + (A + DD^T P_k)^T P_{k+1} - P_{k+1} BB^T P_{k+1} + (C^T C - P_k DD^T P_k). \tag{5.2.7}$$

is solved and the control law $u_{k+1} = -B^T P_{k+1} z$ is calculated. The disturbance is again updated ($v_{k+1} := D^T P_{k+1} z$) and the process repeated. With every iteration, $P_k \to P$, the control law approaches the best (optimal) control, and the disturbance approaches the worst-disturbance; See [82, Section VI] for details.

Define $Z_k := P_{k+1} - P_k$ or use $P_{k+1} = P_k + Z_k$, then (5.2.7) reduces to

$$0 = Z_k A_k + A_k^T Z_k - Z_k BB^T Z_k + F(P_k) \tag{5.2.8}$$

where $A_k := A + DD^T P_k - BB^T P_k$. Thus, solving (5.2.7) for P_{k+1} is equivalent to solving (5.2.8) for Z_k and updating P_{k+1} as $P_k + Z_k$. Necessary and sufficient conditions for the existence of Z_k are:

(A_k, B) is stabilizable and $(F(P_k), A_k)$ has no unobservable modes on the imaginary axis. (5.2.9)

The solution sequence $\{P_k\}$ is unique, monotonic, non-decreasing and converges to the positive semi-definite stabilizing solution of (2.4.11) [82, Section III]. It was proved in [82] that this algorithm has global convergence and the local convergence rate is quadratic. Therefore, this algorithm has the same convergence rate as the Newton-Kleinman algorithm.

The examples presented in [82] were in the standard state space form and the order of the systems used was no greater than 100. A numerical method to solve the sequence of intermediate LQ-AREs (5.2.8) is not specified in [82]. This set of intermediate LQ-AREs can be solved by a number of methods, for example [31], [78], [84]. However, an inexact Newton-Kleinman method [47] cannot be used to solve this sequence of LQ-AREs. At every iteration the solution to a $\mathcal{H}_\infty$-ARE is computed by solving for the increment $P_{k+1} - P_k$ in (5.2.8). This idea resembles the modified Newton-Kleinman iteration scheme (3.5.6) [11, 104]. Results in [47, Section 7] show that application of inexact N-K on (3.5.6) is unstable. Similarly, if the sequence (5.2.8) is not solved accurately, then the residuals add up cumulatively and this algorithm becomes unstable (see Section 5.6.1 and [82, Appendix:Example 2]). Therefore, it is critical to calculate the solutions of intermediate LQ-AREs accurately. If a Newton-Kleinman method is used to solve the intermediate AREs (5.2.8), then a stabilizing feedback must be chosen at every intermediate step. A numerical method to calculate this stabilizing feedback is not given in [82]. Also, a numerical method to verify stabilizability of a matrix pair (5.2.9) in this algorithm is not discussed in [82].

Complexity of the algorithm depends on the complexity of calculating the solutions to the intermediate sequence of linear quadratic problems. If a Kleinman algorithm is used to solve the intermediate LQ-AREs then this method reduces a sign-indefinite ARE to a sequence of negative semi-definite AREs which are further reduced to solving a series of Lyapunov equations; the complexity of solving Lyapunov equations is $32n^3$ and hence, the overall complexity is $\mathcal{O}(n^3)$ which depends on the number of outer iterations required to achieve certain pre-specified tolerance, the number of Kleinman iterations and the number of Lyapunov iterations.

5.3 Numerical Solution of Large Descriptor $\mathcal{H}_\infty$-Riccati Equations

The optimal $\mathcal{H}_\infty$-attenuation is calculated accurately with this method, which can be a problem for methods which rely on calculating the invariant subspace of the Hamiltonian [8, 31, 84, 119]; see Section 5.6.2 for details. Therefore, the game theoretic iterative method was chosen to be extended to descriptor form and to systems of large model order.

In this section, an extension of the iterative method to large descriptor systems is given. Our implementation exploits system properties such as sparsity and symmetry. An improved bisection algorithm is described to calculate $\mathcal{H}_\infty$-optimal attenuation. A parallel implementation of this extension is also described.

The notation $\sigma_{\max}(Y)$ denotes the maximum singular value of a matrix Y.

The following technical result is a straightforward generalization of Lemma 1 in [82] for descriptor systems to avoid the inversion of the mass matrix E.

Lemma 5.3.1. For the given descriptor system (5.1.1)-(5.1.2), define $\tilde{F} : \mathbb{R}^{n\times n} \mapsto \mathbb{R}^{n\times n}$ as

$$\tilde{F}(P) = E^T PA + A^T PE - E^T P(BB^T - \frac{1}{\gamma^2} DD^T)PE + C^T C. \tag{5.3.1}$$

For $P = P^T, Z = Z^T \in \mathbb{R}^{n\times n}$ then defining $\tilde{A} := A + (\frac{1}{\gamma^2} DD^T - BB^T)PE$

$$\tilde{F}(P+Z) = \tilde{F}(P) + E^T Z\tilde{A} + \tilde{A}^T ZE - E^T Z(BB^T - \frac{1}{\gamma^2} DD^T)ZE, \tag{5.3.2}$$

and if also

$$0 = E^T Z\tilde{A} + \tilde{A}^T ZE - E^T ZBB^T ZE + \tilde{F}(P) \tag{5.3.3}$$

then

$$\tilde{F}(P+Z) = \frac{1}{\gamma^2} E^T ZDD^T ZE, \tag{5.3.4}$$

and

$$\sigma_{\max}[\tilde{F}(P+Z)] = \sigma_{\max}(\frac{1}{\gamma} D^T ZE)^2. \tag{5.3.5}$$

Proof. Using algebraic manipulations, (5.3.2) follows easily. Equations (5.3.4) and (5.3.5) are simple consequences of (5.3.2) and (5.3.3). □

The main result of [82], which immediately extends to descriptor systems, is formally stated in the next theorem.

Theorem 5.3.2. Assume that the matrix triple (E, A, B) is stabilizable and the matrix triple (E, A, C) has no unobservable modes on the imaginary axis and $\tilde{F} : \mathbb{R}^{n\times n} \mapsto \mathbb{R}^{n\times n}$ is defined as in (5.3.1). Suppose there exists a stabilizing solution $P \geq 0$ for (5.1.3). Then

1. the matrix series $\{Z_k\}$ and $\{P_k\}$ are defined for all $k \geq 0$ recursively as follows:

$$P_0 = 0 \tag{5.3.6}$$

$$A_k = A + \frac{1}{\gamma^2} DD^T P_k E - BB^T P_k E. \tag{5.3.7}$$

Letting $Z_k \geq 0$ be the unique stabilizing solution of

$$0 = E^T Z_k A_k + A^T Z_k E - E^T Z_k BB^T Z_k E + \tilde{F}(P_k), \tag{5.3.8}$$

define

$$P_{k+1} = P_k + Z_k. \tag{5.3.9}$$

2. the matrix series $\{Z_k\}$ and $\{P_k\}$ have the following properties: For every $k \geq 0$
   (a) $(E, A + \frac{1}{\gamma^2} DD^T P_k E, B)$ is stabilizable;
   (b) $\tilde{F}(P_{k+1}) = \frac{1}{\gamma^2} E^T Z_k DD^T Z_k E$ (see (5.3.1));
   (c) $(E, A + \frac{1}{\gamma^2} DD^T P_k E - BB^T P_k E)$ is Hurwitz;
   (d) $P \geq P_{k+1} \geq P_k \geq 0$.

3. the limit

$$P := \lim_{k\to\infty} P_k$$

exists with $P \geq 0$. Furthermore, P is the unique stabilizing solution of $\mathcal{H}_\infty$-ARE (5.1.3).

Proof. The proof is similar to the proof of Theorem 3 in [82] for descriptor systems (5.1.1)-(5.1.2). □

A useful condition to terminate the recursive iteration is given below.

Corollary 5.3.3. Assume that the matrix triple (E, A, B) is stabilizable and the matrix triple (E, A, C) has no unobservable modes on the imaginary axis and let $\{P_k\}$ and $\tilde{F} : \mathbb{R}^{n\times n} \mapsto \mathbb{R}^{n\times n}$ be defined as in Theorem 5.3.2. If there exists a $k \geq 0$ such that $(E, A + \frac{1}{\gamma^2}DD^TP_kE, B)$ is not stabilizable, then there does not exist a stabilizing solution $P \geq 0$ to $\tilde{F}(P) = 0$.

Proof. This is a direct consequence of 2.a in Theorem 5.3.2. □

The algorithm given in [82, Section IV] is extended to descriptor systems (5.1.1)-(5.1.2) below (Algorithm 1). The algorithm in [82] is recovered by substituting $E = I$ and $\gamma = 1$.

Algorithm 1 Algorithm to calculate the solution to $\mathcal{H}_\infty$-ARE (5.1.3).

Input : E, A, B, C, D, D_{12} as in (5.1.1)-(5.1.2), $\epsilon > 0, \gamma > 0$.

Assumptions : The system (E, A, B) is stabilizable; (E, A, C) has no unobservable modes on the imaginary axis.

Output : Solution $P \geq 0$ of (5.1.3), if it exists. Feedback $K = B^TPE$, if P exists.

Step 1: Let $P_0 = 0$ and $k = 0$.

Step 2: Set $A_k = A + \frac{1}{\gamma^2}DD^TP_kE - BB^TP_kE$.

Step 3: Construct the unique real symmetric stabilizing solution $Z_k \geq 0$ which satisfies

$$0 = E^TZ_kA_k + A_k^TZ_kE - E^TZ_kBB^TZ_kE + \tilde{F}(P_k). \tag{5.3.10}$$

Step 4: Set $P_{k+1} = P_k + Z_k$.

Step 5: If $\sigma_{\max}(\frac{1}{\gamma}D^TZ_kE)^2 < \epsilon$, then set $P = P_{k+1}$ and stop. Otherwise, go to step 6.

Step 6: If $(E, A + \frac{1}{\gamma^2}DD^TP_{k+1}E, B)$ is stabilizable, then let $k = k + 1$ and go to step 2. Otherwise, solution of (5.1.3) $P \geq 0$ does not exist.

The rate of convergence proved in [82, Section V] for standard systems extends to large-scale descriptor systems. The local rate of convergence for Algorithm 1 is quadratic for descriptor systems and is formally stated below.

Theorem 5.3.4. Assume that the matrix triple (E, A, B) is stabilizable and the matrix triple (E, A, C) has no unobservable modes on the imaginary axis and let $\{P_k\}$ and $\tilde{F} : \mathbb{R}^{n\times n} \mapsto \mathbb{R}^{n\times n}$ be defined as in Theorem 5.3.2. Suppose there exists a stabilizing solution $P \geq 0$ for (5.1.3). Then there exists a $\epsilon > 0$ such that the rate of convergence of the series P_k is quadratic in the region $\|P_k - P\| < \epsilon$.

Proof. This follows from the proof of Theorem 5 in [82, Section V]. □

Properties such as uniqueness and monotonicity of solutions to $\mathcal{H}_\infty$-AREs for standard systems are preserved for descriptor systems using this algorithm.

Algorithm 1 can be used for large-scale systems. The two main issues are solution of the intermediate LQ-AREs (step 3) and checking stabilizability (step 6). A special algorithm to calculate the solutions to intermediate descriptor LQ-AREs in step 3 is described next.

5.3.1 Solution of Large Descriptor LQ-Riccati Equations

Several numerical methods to calculate solutions to large LQ-AREs have been discussed in Section 3.5. The Newton-Kleinman method (3.5.5) suggested in [78] is very popular among researchers, for *e.g.,* [55, 110], since the rate of convergence of this method is quadratic. Here, the LQ-ARE (5.3.10) is solved using a variant of Newton-Kleinman method which is implemented in [110]. The toolbox [110] employs the low-rank Cholesky factor Newton method to calculate the solution of large LQ-AREs for generalized systems without re-writing in the standard form.

At each step, a generalized low-rank Cholesky ADI solver (see [110, Section 3.1]) is used to compute the solution of large Lyapunov equations. An efficient implementation that uses the Sherman-Morrison-Woodbury (SMW) formula for iteratively solving shifted systems of linear equations is employed here. The stopping criteria for solving the Lyapunov equations is chosen as the smallness of the ADI iterate solution. The stopping criteria for the Kleinman method is the smallness of the relative change in the feedback matrix.

Kleinman iterative schemes require a stabilizing feedback to initiate the algorithm. A stabilizing feedback for the system $(E, A + \frac{1}{\gamma^2}DD^TP_kE - BB^TP_kE, B)$ is required.

Note that $(E, A + \frac{1}{\gamma^2} DD^T P_k E, B)$ is stabilizable, if and only if $(E, A + \frac{1}{\gamma^2} DD^T P_k E - BB^T P_k E, B)$ is stabilizable. A numerical method to calculate the stabilizing feedback F for $(E, A+\frac{1}{\gamma^2} DD^T P_k E, B)$ will be discussed below. The formula employed here to calculate the stabilizing feedback $\tilde{F}$ for $(E, A + \frac{1}{\gamma^2} DD^T P_k E - BB^T P_k E, B)$ is

$$\tilde{F} = F - B^T P_k E. \tag{5.3.11}$$

Thus, Step 3 of Algorithm 1 has now been extended to handle descriptor systems of large model order.

5.3.2 Stabilizability of descriptor systems

Another critical step of Algorithm 1 in handling large systems is the verification of stabilizability of $(E, A + \frac{1}{\gamma^2} DD^T P_k E, B)$ in step 6. Explicit inversion of E should be avoided in order to prevent a possible loss of accuracy when the condition number of E is large. In our implementation, stabilizability is verified using Algorithm 2 which is a minor change of the algorithm in [129]. The algorithm presented in [129, Algorithm RSDS] is recovered if Steps 6.1 and 6.3 are omitted.

This algorithm separates the stable and unstable parts of the spectrum using orthogonal similarity transformations. The orthogonal factors in Step 6.2 of Algorithm 2 are calculated by a QZ algorithm [54], which is a generalization of the QR algorithm. In particular, the orthogonal matrices Q and Z are obtained by first reducing the matrix pencil $A - \lambda E$ to the generalised Schur form and then reordering the diagonal blocks.

Systems obtained by approximating partial differential equations typically have a few unstable modes. A stabilizing feedback for the unstable part is calculated by solving a low-order Lyapunov equation [35]. Stabilizability of the system is verified by checking the controllability of the low-order anti-stable part. Furthermore, a stabilizing feedback F for the complete system $(E, A + \frac{1}{\gamma^2} DD^T P_k E, B)$ is constructed using the feedback calculated for the anti-stable modes in Step 6.5 of Algorithm 2. Thus, Algorithm 1 has now been extended to handle descriptor systems of large model order. In our implementation of this extended algorithm, inverting the mass matrix E is avoided.

Algorithm 2 Algorithm to verify the stabilizability in step 6 of Algorithm 1.

Input : $A, E \in R^{n\times n}$ and $B \in R^{n\times m}$.

Output : if (E, A, B) is stabilizable then $F \in R^{m\times n}$ such that $(E, A + BF)$ is stable, otherwise, no solution.

Step 6.1 : If (E, A) is stable, $F = 0$. stop else go to Step 6.2.

Step 6.2 : Reduce the pair (E, A) by an orthogonal similarity transformation, to the ordered generalized real Schur form (GRSF)

$$QEZ = \begin{bmatrix} E_{11} & E_{12} \\ 0 & E_{22} \end{bmatrix}, QAZ = \begin{bmatrix} A_{11} & A_{12} \\ 0 & A_{22} \end{bmatrix},$$

where Q and Z are orthogonal matrices such that (E_{11}, A_{11}) corresponds to the stable spectrum and (E_{22}, A_{22}) corresponds to the unstable spectrum. Compute $QB = [B_1^T, B_2^T]^T$ partitioned conformally with the above matrices.

Step 6.3: If (E_{22}, A_{22}, B_2) is controllable, then (A, B) is stabilizable, go to Step 6.4, else, no solution. STOP.

Step 6.4: Solve the Lyapunov equation

$$A_{22}YE_{22}^T + E_{22}YA_{22}^T - 2B_2B_2^T = 0$$

Step 6.5 : Compute $F_2 = -B_2^T(YE_{22}^T)^{-1}$; then, $F = [0, F_2]Z^T$.

Complexity of the algorithm

The complexity of all the existing methods described in Section 5.2 is $\mathcal{O}(n^3)$ flops except the convex method which requires $\mathcal{O}(n^6)$ flops. The overall complexity of our extended algorithm is $\mathcal{O}(n^3)$. Solving the generalized Lyapunov equations in our implementation of the N-K method for solving the LQ-AREs is cheaper than $32n^3$ flops as discussed below. In this implementation [110], a low-rank Cholesky factor-ADI iteration is used to solve the generalised Lyapunov equations with 20 shift parameters. The calculation of LU factors of systems shifted by these parameters require $\frac{40}{3}n^3$ flops. These factors are stored and used cyclically to solve the Lyapunov equation which involves $\mathcal{O}(40n^2)$ flops at every LRCF-ADI iteration. Additionally, only $\frac{4}{3}n^3$ and $8n^3$ flops are required for the calculation of LU factors of the system in Step 2 and maximum singular value in Step 5 of Algorithm 1.

5.4 Calculation of optimal $\mathcal{H}_\infty$-attenuation

Optimal attenuation is calculated using a bisection method. An improved bisection algorithm (Algorithm 3) is used to calculate optimal $\mathcal{H}_\infty$ attenuation, where the upper and lower bounds are first estimated. This improvement is based on the observation that the actual attenuation of (5.1.1)-(5.1.2) achieved with the controller calculated for some fixed attenuation is very close to the optimal $\mathcal{H}_\infty$-attenuation. The upper bound is updated with the achieved closed-loop attenuation. Then, the solvability of a $\mathcal{H}_\infty$-ARE with 95% of this updated upper bound is used as a criterion to estimate the lower bound on optimal attenuation. If a solution to this $\mathcal{H}_\infty$-ARE exists then the upper bound is re-assigned, else this is set as the lower bound. This fine-tuning is repeated if necessary to obtain a lower bound. A standard bisection algorithm is then applied with these tight bounds and optimal attenuation is calculated up to the specified accuracy ($\delta_{\hat{\gamma}}$). This modified algorithm converged within a few iterations.

In the case of large-scale descriptor systems, optimal attenuation is calculated using Algorithm 3, where Algorithm 1 is used to solve the fixed attenuation problem in Steps 1, 4 and 6. A significant amount of time and computational resources are consumed in Steps 4 and 6 of Algorithm 3, particularly when γ is close to the optimal value. In the case

Algorithm 3 An improved bisection algorithm

Input : A, B, C, D, D_{12}, E, γ_H, $\delta_{\hat{\gamma}}$

Assumption : The system (E, A, B) is stabilizable and (E, A, C) is detectable.

Output : K, $\hat{\gamma}$

Step 1: Calculate the controller K_{γ_H} for the $\mathcal{H}_\infty$-attenuation problem with γ_H.

Step 2: Update γ_H with the closed-loop attenuation of (5.1.1)-(5.1.2) achieved with K_{γ_H}.

Step 3: Define $\gamma := 0.95 \times \gamma_H$.

Step 4: If the solution to the $\mathcal{H}_\infty$-attenuation problem for γ exists then update $\gamma_H = \gamma$ and go to Step 3, else $\gamma_L := \gamma$.

Step 5: Calculate $\gamma := \frac{1}{2}(\gamma_H + \gamma_L)$.

Step 6: Solve the $\mathcal{H}_\infty$-attenuation problem for γ calculated in Step 5. If there exists a controller K, that achieves γ-attenuation then, $\gamma_H = \gamma$, else $\gamma_L = \gamma$.

Step 7: If $\|\gamma_H - \gamma_L\| < \delta_{\hat{\gamma}}$ then $\hat{\gamma} = \gamma$ and STOP, else go to Step 5.

where $\gamma < \hat{\gamma}$, a significantly longer time is generally required for Algorithm 1 to determine that a solution does not exist compared to the case where it does ($\gamma > \hat{\gamma}$). This is because when $\gamma < \hat{\gamma}$, several outer iterations are performed in Algorithm 1 before reaching the terminating condition, that is the failure of the stabilizability condition in Step 6. Such a situation happens only when the controllability condition in Step 6.3 of Algorithm 2 fails. This condition is met only when the corresponding controllability matrix (of order 1) loses its numerical rank. However, the solution series $\{P_k\}$ begins to diverge much before the uncontrollability condition is reached. It is recommended to keep a check on the growth of the residual,

$$\sigma_{\max}(\tilde{F}(P_k)) \not> 1/\epsilon, \tag{5.4.1}$$

and terminate Algorithm 1 when (5.4.1) fails. Implementing this change speeds up the computation of optimal attenuation for large-scale descriptor systems.

5.5 Parallel Implementation

A parallel implementation of Algorithm 1 which is used in the calculation of $\mathcal{H}_\infty$ optimal attenuation in Chapter 6 is discussed here for the sake of completeness. The numerical algorithms required to solve large $\mathcal{H}_\infty$-AREs are decomposed into basic matrix computations, such as solving linear systems, matrix products, LU factorization and eigenvalue computation. Efficient implementations of these operations exist in modern linear-algebra libraries for parallel distributed-memory computers. The underlying computational libraries, communication routines, and the target architecture determine the performance. The form of parallelization used here is called data parallelization. Data parallelization consists of three basic steps: first, break the set of input data into smaller sets; then, perform computation on each of the smaller sets in parallel and lastly, combine computation results from previous step to get the final solution.

A ScaLAPACK parallel library [24] is used here, which is a freely available package that implements parallel extensions of many of the kernels in [4] using a message passing paradigm. ScaLAPACK is based on BLACS for communication and can be ported to any (serial and) parallel architecture with an implementation of the MPI or PVM libraries [56]. The sub-library PBLAS (Parallelized Basic Linear Algebra Subprograms) performs basic vector and matrix operations in parallel.

Most of the computations are performed using ScaLAPACK routines. A standard Newton-Kleinman method is used to solve (5.3.10) using [24]. As each iteration step of the Newton procedure requires the solution of a linear matrix equation, solvers for Lyapunov equations are also included. A generalization to the low-rank Cholesky factor ADI iteration method [104] is used without converting the descriptor form into the standard form. Optimal set of ADI parameters are calculated using [44], which is implemented using [45] since this step is not time-consuming. A set of generalized eigenvalues was computed using [4], since the accurate computation of eigenvalues closer to imaginary axis becomes an issue in [24]. The ScaLAPACK routines used in solving $\mathcal{H}_\infty$-AREs and some basic matrix operations performed using PBLAS routines are listed in Table 5.1. The calculation of orthogonal similarity transformations in Algorithm 2 is implemented using [4]. A stabilizing feedback is calculated (Algorithm 2) by solving a low-order generalized

Table 5.1: ScaLAPACK routines used in the parallel implementation of Algorithm 1 are listed below.

Routine name	**Description**
pdgeadd	General matrix addition $C = \beta C + \alpha A$, where α and β are scaling factors. Matrix A is transposed before addition
pdgemm	General matrix multiplication $C = \beta C + \alpha AB$, where α and β are scaling factors. Matrices A, B or both can be transposed before multiplication
pdgehrd and *pdlahqr*	Hessenberg reduction an computation of eigenvalues
pdgesvd	Computation of singular values
pdgetrf	LU factorization
pdgetrs	Solution of system of equations using the LU factorization obtained from *pdgetrf*
pdgesv	Solution of system of equations
pdlange	Frobenius norm of a matrix

Lyapunov equation using *SG03AD* from SLICOT[20].

A logical grid of $n_p = p_r \times p_c$ processors is used to compute the solution of a $\mathcal{H}_\infty$-ARE. This set of n_p processors form a process grid. All matrices are partitioned into $n_b \times n_b$ blocks and these blocks are distributed among the n_p processors cyclically. Distributing matrices on the process grid is the programmer's responsibility. There are ScaLAPACK kernels that perform this data distribution, starting with a matrix contained in the memory of a single process. Once matrices are distributed on the process grid, a program that implements Algorithm 1 using ScaLAPACK routines are run on this grid. All processes in this grid run through each step of the same program, but on different data. But since matrices are distributed across these processes, whenever a matrix operation (say, for instance, LU factorization) is encountered, the processes synchronize with each other at that point in order to perform the matrix operation. This is where parallelization using the single program multiple data paradigm comes into effect. During this operation, the processors communicate among each other, if required. In the end, the different blocks of the solution

to a $\mathcal{H}_\infty$-ARE resides in different processors and is retrieved from all the processors via communication. Thus, all n_p processors in one process grid work together to solve a $\mathcal{H}_\infty$-ARE.

Furthermore, for the calculation of optimal $\mathcal{H}_\infty$-attenuation, multiple (n_g) process grids work together by solving multiple (n_g) $\mathcal{H}_\infty$-AREs simultaneously. That is, instead of the regular sequential bisection-type algorithm, optimal attenuation is calculated by dividing (γ_L, γ_H) into (n_g+1) sub-intervals. This speeds up the convergence of optimal attenuation; see [131] for details.

5.6 Examples

In this section, some problems that were used to compare the solvers are described. Systems motivated by partial differential equation models: vibrations on a simply supported beam, cantilevered plate and diffusion on an irregular 2D geometry are used. The performance of all solvers are compared based on the following criteria: (a) achieved closed-loop attenuation, (b) time taken to calculate the $\mathcal{H}_\infty$ controller and (c) normalized residual norm of the calculated Riccati solution that indicates the accuracy of the computed solution. All simulations are performed using Matlab 7.11 (R2010b) on a Sun x4600 with 8 opteron 8218 CPU's (2.6 GHz) and 32 GB RAM.

Example 5.6.1 (Series of integrators)**.** The first test problem has appeared in [82] as example 3. Consider a system of n integrators connected in series given in the standard state space form. A feedback controller has to be applied at the nth system. This problem has earlier appeared in [84] as example 6. Choose the matrices $E = I_{21}, A \in \mathbb{R}^{21\times 21}, B \in \mathbb{R}^{21\times 1}, D \in \mathbb{R}^{21\times 1}, C \in \mathbb{R}^{22\times 21}$ as follows:

$$A = \begin{bmatrix} 0 & 1 & 0 & \dots & 0 \\ & \ddots & \ddots & \bigcirc & \vdots \\ \vdots & & \ddots & \ddots & 0 \\ & \bigcirc & & \ddots & 1 \\ 0 & & \dots & & 0 \end{bmatrix}, B = \begin{bmatrix} 0 \\ \vdots \\ 0 \\ 0 \\ 1 \end{bmatrix}, D = \begin{bmatrix} 0 \\ \vdots \\ 0 \\ 0.01 \\ 0 \end{bmatrix}, C = \begin{bmatrix} 1 & 0 & 0 & \dots & 0 \\ 0 & 0 & \ddots & \bigcirc & \vdots \\ \vdots & & \ddots & \ddots & 0 \\ & \bigcirc & & \ddots & 0 \\ 0 & & \dots & & 0 \\ 0 & & \dots & & 0 \end{bmatrix}.$$

The difficulty in this example lies in the fact that the norm of the solution to LQ-ARE calculated using Schur method (2.4×10^9) is very large, when the condition number of the corresponding Hamiltonian is 1.

Example 5.6.2 (Simply supported beam)**.** Consider a simply supported Euler-Bernoulli beam with viscous damping presented in Example 4.4.2. By choosing moment and velocity as state components, the system (4.4.5)-(4.4.6) re-written as an abstract Cauchy problem is well-posed on the state space $\mathcal{Z} = L_2(0,1) \times L_2(0,1)$ [37]. The state space formulation of (4.4.5)-(4.4.6) is

$$\frac{d}{dt} z(t) = Az(t) + Bu(t) + Dv(t), \tag{5.6.1}$$

where

$$A = \begin{bmatrix} 0 & \frac{d^2}{dx^2} \\ -\frac{d^2}{dx^2} & -\xi I \end{bmatrix}, B = \begin{bmatrix} 0 \\ b_{0.5}(\cdot) \end{bmatrix}, D = \begin{bmatrix} 0 \\ d(\cdot) \end{bmatrix}, \tag{5.6.2}$$

with domain

$$\mathbf{D}(A) = \{(\phi, \psi) \in H_s(0,1) \times H_s(0,1) \mid \psi'' \in H_s(0,1)\},$$

where $H_s(0,1)$ is defined in Example 4.4.2. Since a closed form solution to the partial differential equation problem is not available, $\mathcal{H}_\infty$-controllers must be calculated using an approximation. Let $\phi_i(x)$ indicate the eigenfunctions of $\frac{\partial^4 w}{\partial x^4}$ with boundary conditions (4.4.6). For any positive integer N, define Z^N to be the span of $\phi_i, i = 1...N$. Choose $\mathcal{Z}^N = Z^N \times Z^N$ and define P^N to be the projection onto $\mathcal{Z}^N$. Conditioning of the matrices arising in the approximations to this PDE are better with this realization than with the standard first-order realization of position and velocity as shown in Figure 5.3. The original

Figure 5.3: Conditioning of the beam problem with the first-order standard state space realization of position and velocity is compared against the energy-based realization of moment and velocity

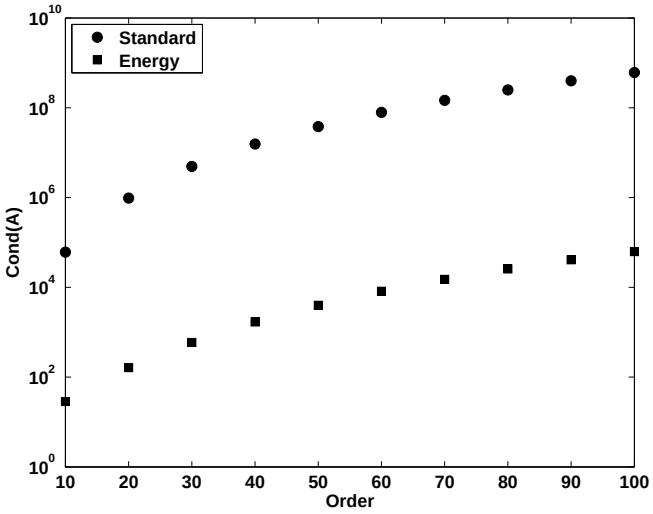

problem is exponentially stable; see [96, 99] for details. Approximating problems that correspond to the first 50 eigenmodes are used in comparing the performance of $\mathcal{H}_\infty$ solvers, where the finite-dimensional matrices are

$$[A] = \begin{bmatrix} 0 & \Lambda^N \\ -\Lambda^N & -\xi I \end{bmatrix}, [B] = \begin{bmatrix} 0 \\ b^N \end{bmatrix}, [D] = \begin{bmatrix} 0 \\ d^N \end{bmatrix}, [C] = I^N, \text{ where}$$

$$[b^N]_i = \sqrt{2} \int_0^1 b_{0.5}(x)\phi^i(x)dx, \quad i = 1, \ldots, N,$$

$$[d^N]_i = 10\ \sqrt{2} \int_0^1 b_{0.5}(x)\phi^i(x)dx, \quad i = 1, \ldots, N,$$

and Λ^N is the diagonal matrix with i^{th} entry $(i\pi)^2$. The order of the systems is twice the number of eigenmodes.

Example 5.6.3 (Diffusion on an irregular plate)**.** Consider the heat diffusion problem on a two-dimensional plane with the irregular geometry Ω in Figure 5.4. Assume Dirichlet

Figure 5.4: Irregular geometry : With origin referenced at bottom left corner, a 4×4 units square where a circle of radius 0.4 units centered at $(3, 1)$ removed is considered as the domain Ω

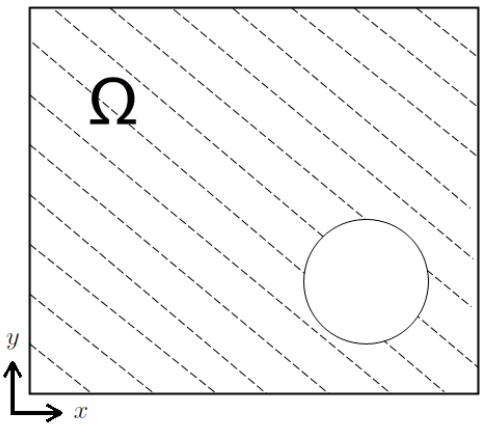

boundary conditions at the edges of the geometry $\partial\Omega$. Let $z(x, y, t)$ denote the heat distribution at the point $(x, y) \in \Omega$ at time t. The heat distribution is controlled by applying a heat source (square-sized actuator patch) $u(t)$. The exogenous disturbance $v(t)$ induces a distributed load $d(x, y)v(t)$ where $d(x, y) \in \mathbf{C}(\Omega)$. If the variables are normalized, then the equations obtained are

$$\begin{aligned} \frac{\partial z}{\partial t}(x, y, t) &= \frac{\partial^2 z}{\partial x^2} + \frac{\partial^2 z}{\partial y^2} + b(x, y)u(t) + d(x, y)v(t), \quad \text{on } \Omega \\ z(x, y, \cdot) &= 0 \text{ on } \partial\Omega, \\ y(t) &= \int_\Omega b(x, y)z(x, y, t)\ d\Omega, \end{aligned} \tag{5.6.3}$$

where b is a function in $\mathbf{C}(\Omega)$. Here

$$b(x, y) = \begin{cases} \frac{1}{2\epsilon}, & |x - r_x| < \epsilon \text{ and } |y - r_y| < \epsilon \\ 0, & \text{otherwise,} \end{cases}.$$

It is assumed that $d(x,y) = 100b(x,y)$. A square-shaped actuator with half-width $\epsilon = 0.2$ is placed at the center of the square, that is $(r_x, r_y) = (2,2)$. Average temperature is measured at the same spot where the actuator is placed. A state space formulation of (5.6.3) on $\mathcal{Z} = L_2(\Omega)$ is

$$\begin{aligned} \frac{dz}{dt} &= Az(t) + Bu(t) + Dv(t), \\ y(t) &= Cz(t) + D_{12}u(t) \end{aligned} \tag{5.6.4}$$

where

$$Ah := \nabla \cdot (\nabla h), \quad Bu := b(x,y)u, \quad Dv := 100\ b(x,y)v, \quad Cz := \int_\Omega b(x,y)z(t)\ d\Omega,$$

with domain

$$\mathbf{D}(A) = \{h \in \mathcal{H}^2(\Omega) \mid h = 0 \ \text{ on } \partial\Omega\},$$

where $z(\cdot)$ is the temperature profile $w(x,y,\cdot)$. Since there is only one control, choose control weight $D_{12} = 1$. A finite element method [2] with linear splines $\{\phi_i\}$ as the basis for the finite-dimensional subspace $\mathcal{H}_0^{1^N}$ is used for approximating (5.6.3). This yields a finite-dimensional system in descriptor form (5.1.1)-(5.1.2) with the system matrices are given by

$$[E]_{ij} = \int_\Omega \phi_i\phi_j\ d\Omega, \qquad [A]_{ij} = \int_\Omega \nabla\phi_i\nabla\phi_j\ d\Omega,$$
$$[B]_j = \int_\Omega b(x,y)\phi_j\ d\Omega, \qquad \text{where } i,j = 1,\ldots,N,$$

Here, $C = B^T, D = 100B$ are used. The original problem is both stabilizable and detectable and so are the approximating problems; see e.g. [96] for details. Eigenvalues of this system lie on the negative real line as shown in Figure 5.5.

Example 5.6.4 (Cantilever plate)**.** Consider a Euler-Bernoulli cantilever plate with Kelvin-Voigt damping of dimensions $0.5m \times 0.5m \times 2mm$ clamped at one end and free to vibrate at the other end. The partial differential equation model that describes the transverse

Figure 5.5: Spectrum of cantilever plate (order - 1100) and diffusion problem (order - 1077)

(a) Spectrum (b) Spectrum near imaginary axis

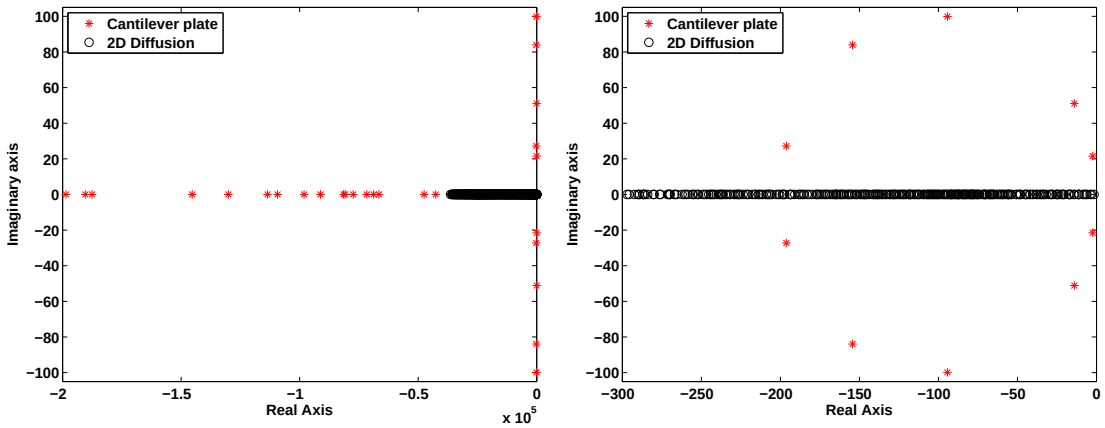

displacement of the plate may be found in [13]. The disturbance is located at the same spot as the collocated actuator/sensor pair. Since there is only one control, choose control weight $D_{12} = 1$. Three different approximations generated using ANSYS with 64, 100 and 225 elements, where an actuator/sensor pair is placed on 25th, 50th and 105th elements respectively, are considered. The order of these 3 approximations are $720, 1100$ and 2400 respectively. The dimensions of the actuator/sensor pair used is identical to the dimensions of a single element. The standard cubic B-spline approximation [106] of this second-order model leads to

$$M\ddot{w} + (C_v I + C_d K)\dot{w} + Kw = Bu + Dv,$$
$$y = Cx$$

where Kelvin-Voigt damping with $C_v = 1 \times 10^{-6}$, $C_d = 1 \times 10^{-2}$ is considered. Here, M is the mass matrix, and K is the stiffness matrix. Also, $C = B^T, D = 1000B$ are used. This is re-formulated in the descriptor state space form (5.1.1)-(5.1.2)

$$E = \begin{bmatrix} I & 0 \\ 0 & M \end{bmatrix}, \text{ and } A = \begin{bmatrix} 0 & K^{\frac{1}{2}} \\ -K^{\frac{1}{2}} & -C_v I - C_d K \end{bmatrix}.$$

Table 5.2: Spectral radius of residue of the solution to (5.1.3), $\sigma_{\max}(\tilde{F}(P))$, calculated using different methods

Name of the $\mathcal{H}_\infty$ solver	**Spectral radius of residue**
Schur method	1.69×10^3
Matrix sign function method	3.16×10^2
Iterative method with Schur method to solve (5.3.10)	2.0×10^3
Iterative method with Kleinman algorithm to solve (5.3.10)	1.4×10^{-4}

Eigenvalues of the cantilever plate problem lie on a sector in the negative-half of the complex plane (see Figure 5.5). The condition number of these approximated systems vary in the range of $8.5 \times 10^{13} - 3 \times 10^{14}$, which is much larger than the diffusion problem.

5.6.1 $\mathcal{H}_\infty$-Attenuation

Performance of different solvers for the calculation of $\mathcal{H}_\infty$-disturbance attenuation on both medium-scale standard systems and large-scale descriptor systems are compared in this section.

Medium-scale systems

Consider the system of n integrators (Example 5.6.1). Let $\tilde{F}$ be defined as in (5.3.1). The $\mathcal{H}_\infty$-disturbance attenuation problem on this problem with $\gamma = 1$ is solved using Schur method [35] and matrix sign function method [31, 39]. The accuracy of any solution to (5.1.3) is determined by the size of the spectral radius of its residue. As shown in Table 5.2, the spectral radius is much larger than 0 for both Schur and matrix sign function methods. A pair of conjugate eigenvalues are on the imaginary axis for this problem. Thus, both Schur and matrix sign function methods suffer accuracy issues in calculating the stable invariant subspace of the corresponding Hamiltonian.

Game theoretic iterative method [82] is used on this example, where the sequence of intermediate LQ-AREs is solved using both a Schur method and a Kleinman method. The corresponding spectral radius of the residue of the solution obtained using these 2 methods are shown in Table 5.2. Clearly, the Schur method does not work well on this example, likely because the LQ-ARE obtained in the first iteration of game theoretic iterative method was not solved accurately using a Schur method. Since the game theoretic iterative method is analogous to the modified Newton-Kleinman method [11], the residuals add up cumulatively at the end of each outer iteration ($\sigma_{\max}(\tilde{F}(P_4)) = 2.0 \times 10^3$); see [47, Section 7] for details. However, when a Newton-Kleinman method is used to solve the LQ-AREs that appear in step 3 of algorithm presented in [82] then this method remains stable ($\sigma_{\max}(\tilde{F}(P_3)) = 1.4 \times 10^{-4}$). With this implementation, an accurate solution was achieved within 3 iterations on this example. The convex method cannot be used here, since the hypothesis of [112, Thm. 3.4] does not hold. The non-linear optimization based HIFOO method does not find a stabilizing controller even when it was invoked with an initial controller calculated using the game theoretic iterative method. This example illustrates that the game theoretic iterative method with Kleinman method to solve the intermediate LQ-ARE produces an accurate solution when the standard methods fail.

Consider the finite-dimensional approximations of simply supported beam (Example 5.6.2). The game theoretic iterative method presented in [82] is implemented using Schur method to solve the intermediate series of LQ-AREs on this problem. The sequence of LQ-AREs obtained in this problem is solved accurately by Schur method, and thus, this implementation works. The stabilizability condition is verified using a Hautus criterion (*e.g.* [134, Page 50]). All solvers performed well on this problem for calculating the fixed attenuation $\mathcal{H}_\infty$-controller for $\gamma = 10$, which is close to the optimal attenuation $\hat{\gamma} = 9.95$. The closed-loop plant with controllers calculated by all methods are stable and achieved the specified attenuation. However, the convex method is extremely slow when compared to the other methods even for systems of order as small as $n \leq 20$; see Figure 5.6. Therefore, the convex method was not used for systems with $n > 20$. The HIFOO method is slower than the game theoretic iterative method. Since HIFOO is invoked with random initial controller, the computation time is different for different runs.

As shown in Figure 5.7, both Schur and iterative methods are highly accurate in solving

Figure 5.6: Computation time of all solvers on different approximations of the simply supported beam (Example 5.6.2) for the fixed attenuation problem $\gamma = 10$. ITERATIVE denotes the game-theoretic iterative method.

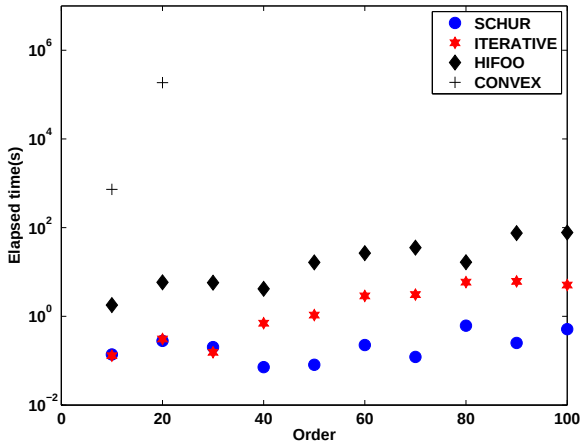

Figure 5.7: Numerical accuracy of Schur, game-theoretic iterative and convex methods on different approximations of the simply supported beam (Example 5.6.2) for the fixed-attenuation problem $\gamma = 10$

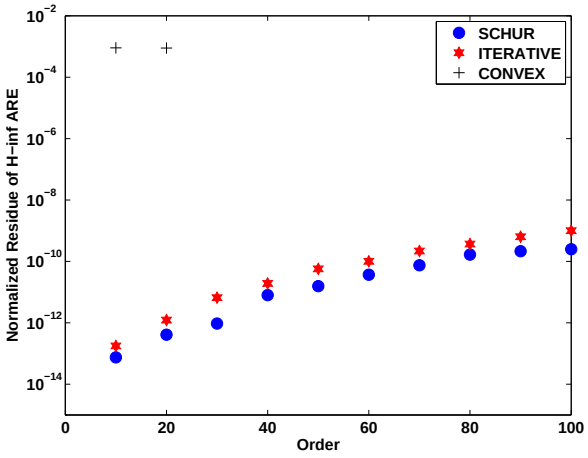

$\mathcal{H}_\infty$-ARE. Although the convex method is less accurate than other methods because it solves the Riccati inequality instead of the Riccati equation, it is still consistent. Since the HIFOO method does not rely on solving Riccati equations, the numerical accuracy of this method cannot be assessed. Thus, all methods can be used for calculating $\mathcal{H}_\infty$-control for fixed attenuation problems for the beam with $n \leq 100$, although the Schur and game-theoretic methods are the fastest.

Large-scale descriptor systems

Figure 5.8: Numerical accuracy of Schur and iterative methods on different approximations of the 2D diffusion problem (Example 5.6.3) for the fixed attenuation $\gamma = 7$. ITERATIVE denotes the extended game-theoretic iterative method.

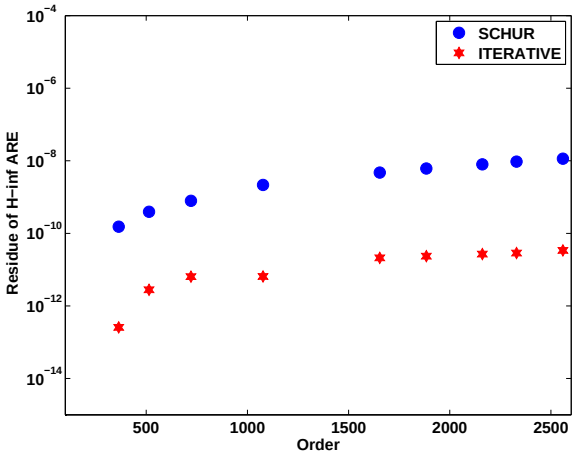

Consider the finite-dimensional approximations of diffusion systems (Example 5.6.3). The $\mathcal{H}_\infty$- controllers for the fixed attenuation $\gamma = 7$ obtained from Schur, extended game-theoretic iterative (Algorithm 1) and HIFOO methods stabilized the closed loop system and achieved the specified attenuation. The HIFOO method is very slow for large systems. Beyond $n > 2000$, HIFOO method did not produce a result after running for 12 days. Hence, HIFOO method is not used for $n > 2000$. Both Schur and our extended iterative methods are numerically accurate in solving $\mathcal{H}_\infty$-AREs for fixed attenuation as seen in

Figure 5.9: Computation time of Schur, extended iterative and HIFOO methods on different approximations of the 2D diffusion problem (Example 5.6.3) for the fixed attenuation $\gamma = 7$

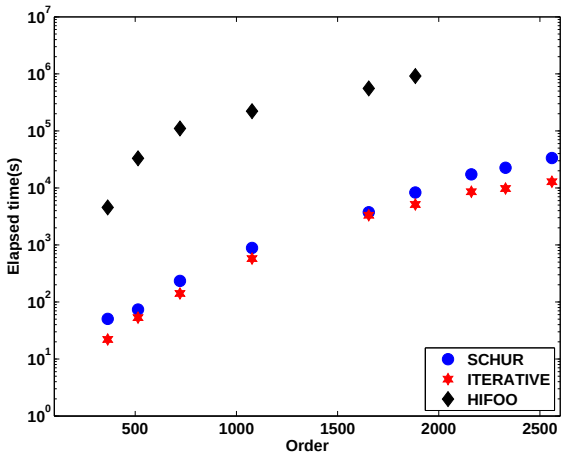

Figure 5.8. Performance of the Schur method on this problem is good. However, as shown in Figure 5.9, our implementation of the iterative method is slightly faster than the Schur method.

The Schur method failed to accurately isolate the stable invariant subspace of the corresponding Hamiltonian on the approximated cantilever plate model described in Example 5.6.4. This is likely because, even with the reformulation of the state space, this second-order model is not as well-conditioned as the diffusion model. However, our proposed implementation of the iterative method calculated the solution of $\mathcal{H}_\infty$-ARE reaching a limiting accuracy of $\epsilon = 1 \times 10^{-12}$ for the fixed attenuation problem. Table 5.3 illustrates that the iterative method is much faster than the HIFOO method on the first 2 approximated systems. For the third system, HIFOO method didn't produce a result even after 12 days. The controllers calculated by both methods stabilize the closed-loop system and the $\mathcal{H}_\infty$-norm achieves the specified attenuation.

Table 5.3: Elapsed time of Iterative method and HIFOO method for the calculation of $\mathcal{H}_\infty$ controller on cantilever plate described in Example 5.6.4

System order	**Fixed attn.**	**Iterative Time**	**HIFOO Time**
720	4	40 mins	6hrs 12 mins
1100	2.5	1 hr 42 mins	11 hrs 22 mins
2400	1.5	11 hrs 58 mins	>12 days

5.6.2 Optimal Attenuation

Optimal $\mathcal{H}_\infty$-attenuation was calculated using the improved bisection algorithm (Algorithm 3) where each fixed attenuation problem is solved using both Schur and iterative method in [82] on medium-scale systems. Schur, HIFOO and the modified game-theoretic algorithm are compared.

Medium-scale systems

Both Schur and matrix sign function methods failed to calculate the optimal $\mathcal{H}_\infty$-attenuation ($\hat{\gamma} = 0.5594$) accurately on Example 5.6.1. The game theoretic iterative method using Kleinman iteration to solve the intermediate LQ-ARE worked on this problem and the optimal $\mathcal{H}_\infty$-attenuation was calculated accurately up to 4 decimal digits and the resulting residue had the spectral radius 1.51×10^{-4}. The convex method cannot be used here, since the perturbation richness assumption does not hold. The non-linear optimization based HIFOO method failed to calculate the optimal attenuation even when it was invoked with the initial controller calculated using game theoretic iterative method.

The optimal $\mathcal{H}_\infty$-attenuation $\hat{\gamma} = 9.95$ computed using all methods was accurate up to 2 decimal digits on different approximations of the beam (Example 5.6.2). The closed-loop plant with optimal $\mathcal{H}_\infty$-controllers are stable for all methods. The optimal $\mathcal{H}_\infty$-control calculated by both Schur and iterative methods achieved the optimal $\mathcal{H}_\infty$-attenuation. The $\mathcal{H}_\infty$-controllers calculated by non-linear optimization and convex methods achieved a performance close to optimal. However, as seen in Figure 5.10, the Schur method is

Figure 5.10: Numerical accuracy of Schur and iterative methods on different approximations of simply supported beam (Example 5.6.2) for calculating optimal attenuation ($\delta_{\hat{\gamma}} = 0.001$)

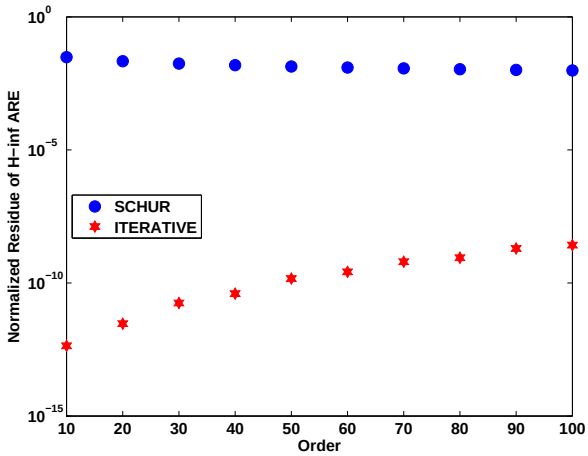

numerically less accurate in solving $\mathcal{H}_\infty$-AREs for calculating optimal attenuation, while the iterative method is highly accurate even for a lower tolerance($\delta_{\hat{\gamma}} = 1 \times 10^{-3}$).

Large-scale descriptor systems

In the case of diffusion (Example 5.6.3), with $\gamma_H = 10, \delta = 0.01$, the optimal $\mathcal{H}_\infty$-attenuation, $\hat{\gamma} = 5.77$, calculated using all methods was accurate up to 2 decimal digits. The optimal attenuation converged for different approximations. The $\mathcal{H}_\infty$-controllers obtained from all methods stabilize the closed loop system and achieved an attenuation close to the optimal. It is clear from Figure 5.11 that both the extended game theoretic algorithm and Schur method are numerically accurate in solving $\mathcal{H}_\infty$-AREs in the calculation of optimal attenuation. Numerical accuracy of the HIFOO solver cannot be determined, since it does not calculate the solution to the $\mathcal{H}_\infty$-ARE. Figure 5.12 shows that the extended iterative method is quicker than the Schur method for large systems. The HIFOO method is slow for large-scale systems and therefore, it is not used beyond $n > 2000$.

Results for calculating optimal attentuation with the plate are shown in Table 5.4. The

Figure 5.11: Numerical accuracy of Schur and iterative methods on different approximations of the 2D diffusion problem (Example 5.6.3) for calculating optimal attenuation

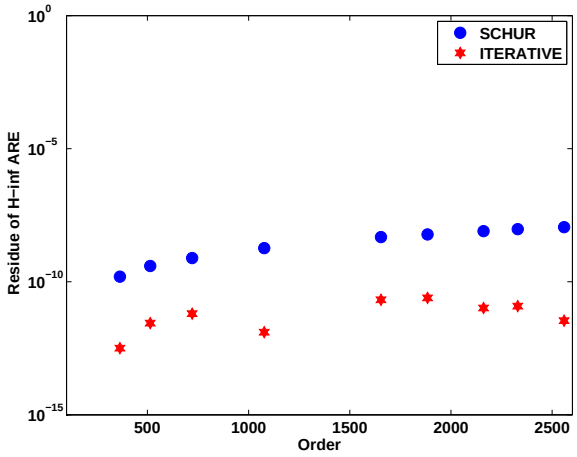

Figure 5.12: Computation time for calculating optimal attenuation of Schur and iterative method on very large approximations of diffusion problem (Example 5.6.3)

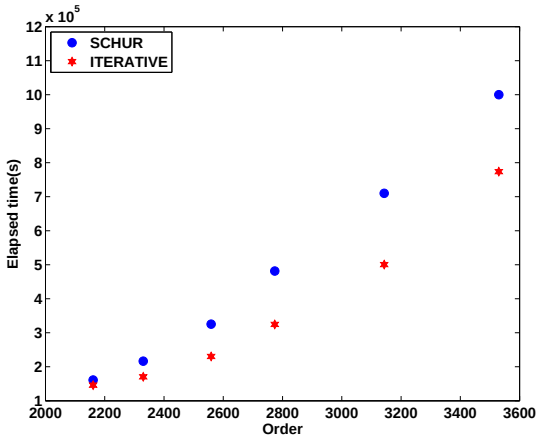

HIFOO method did not produce a result on the system $n = 2400$ even after 12 days. The Schur method failed to compute optimal attenuation on the approximated plate model. It cannot accurately isolate the stable invariant subspace of the corresponding Hamiltonian pencil even for $\gamma > \hat{\gamma}$. This is likely because the conditioning of the matrices, even when the

Table 5.4: Computation time of Iterative method and HIFOO method for the calculation of optimal attenuation on cantilever plate (Example 5.6.4)

Order system	**Optimal attn.**	**Iterative Time**	**HIFOO Time**
720	3.712	8 hrs 21 mins	9 hrs 30 mins
1100	2.3757	11 hrs 53 mins	14 hrs 5 mins
2400	1.0558	1 day 19 hrs	>12 days

energy realization is used, is not as good as the diffusion problem. However, our proposed method calculated the optimal attenuation within a tolerance of $\delta_{\hat{\gamma}} = 0.01$ and a limiting accuracy of $\epsilon = 1 \times 10^{-12}$ for solving the $\mathcal{H}_\infty$-AREs.

5.7 Conclusion

In this chapter, the game-theoretic iterative algorithm is extended to calculate solutions to large $\mathcal{H}_\infty$-AREs for descriptor systems. This algorithm is compared to a number of other algorithms for the calculation of fixed and optimal $\mathcal{H}_\infty$ attenuation using examples arising in control of partial differential equations. All methods were satisfactory for the beam and diffusion problems, although the speed of the Schur and iterative algorithms was better than the others. The extended game-theoretic iterative method was faster than all the other methods for large problems. Also, in the beam example, the residuals in the Riccati equation when using the Schur method for optimal attenuation indicate that this method is less accurate for this type of problem. The Schur method did not work well for the plate for even fixed attenuation. Both problems are likely due to the fact that the eigenvalues of the plate and beam models contain significant imaginary components. This leads to a Hamiltonian with eigenvalues close to the imaginary axis, particularly for attenuation close to optimal.

Although either the Schur or the game-theoretic iterative algorithm can be used for many problems, the iterative algorithm is a better choice for problems where the Hamiltonian may have eigenvalues near the imaginary axis. This difficulty typically arises in

optimal attenuation and in second-order systems such as plate vibrations.

Chapter 6

Calculation of $\mathcal{H}_\infty$-Optimal Actuator Locations

Several numerical issues are key to the calculation of $\mathcal{H}_\infty$-optimal actuator locations: the computation of optimal attenuation for the full partial differential equation model at a location, and the issue of minimizing the optimal attenuation over all possible locations for the original model. The issue of calculating optimal attenuation at a point was discussed in Chapter 5. A derivative-free optimization algorithm for calculating $\mathcal{H}_\infty$-optimal actuator locations is described in this chapter. One difficulty with $\mathcal{H}_\infty$-optimal actuator location problem is the lack of gradient information. The use of a derivative-free method will be justified. The directional direct-search method, which is a well-known derivative-free optimization algorithm, is used in an algorithm to optimize the actuator locations based on $\mathcal{H}_\infty$-cost. Several advantages of the directional-direct search method are exploited. A multi-level parallel implementation of calculating $\mathcal{H}_\infty$ optimal actuator locations for large-scale systems is described. The effectiveness of our proposed algorithm is illustrated using several examples motivated by partial differential equation models.

6.1 Derivative-Free Optimization

Even with use of an improved bisection algorithm (Algorithm 3) calculation of optimal attenuation at a point requires multiple solutions of a fixed attenuation problem and solving each $\mathcal{H}_\infty$-ARE requires $\mathcal{O}(n^3)$ flops. The computation of $\mathcal{H}_\infty$-optimal actuator locations, defined by (4.2.1)-(4.2.2), is an additional layer of optimization over the calculation of optimal attenuation, defined by (2.4.13). It is therefore important to find an efficient method for calculating optimal actuator location.

Figure 6.1: Variation of $\mathcal{H}_\infty$-cost function with respect to actuator location over the length of a viscously damped beam (Example 4.4.2) with $d = b_{0.7}, C = I$ approximated with 5 eigenmodes

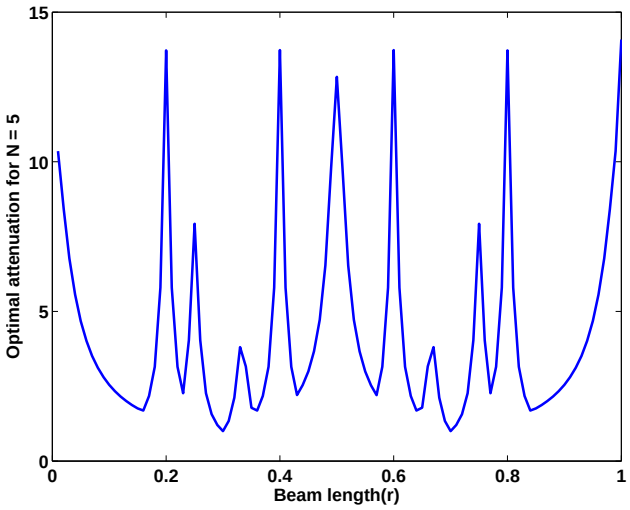

Consider the problem of calculating optimal actuator location for $\mathcal{H}_\infty$-cost on a simply supported beam with viscous damping (Example 4.4.2). Figure 6.1 indicates that $\mathcal{H}_\infty$-cost function with respect to actuator location on this problem is non-convex and non-differentiable. Even if the cost could be shown to be differentiable for a sub-class of problems, the derivative calculation would likely be time-consuming. We therefore used a derivative-free method [34].

Among many derivative-free methods a few of the popular ones include Nelder-Mead method [105], derivative-free trust-region method [115], line-search methods based on simplex derivatives [74]. Global convergence to stationary points of such methods involved restrictive conditions on the objective function; see [34, Theorems 8.4, 9.3, 10.13] for details. Such assumptions may not be satisfied for the objective function of our interest, $\hat{\gamma}(r)$.

Directional direct-search method is a derivative-free method that samples the objective function at finite number of points and searches for a better function value at each iteration. The decisions are made based on function values without any explicit or implicit derivative approximation. There are several advantages to this method for the calculation of $\mathcal{H}_\infty$-optimal actuator location. One is that the function evaluations may be done in parallel, which speeds up convergence in a multi-processor architecture. Another advantage is that a simpler, so-called *surrogate model* (discussed below) may be used, which considerably improves performance for this problem. A detailed description of directional direct-search algorithm may be found in [34, Chapter 7]. Here we only describe briefly the main points and the use of the surrogate model. Some basic properties of positive spanning sets and bases are reviewed first.

6.1.1 Positive Spanning Sets and Positive Bases

Definition 6.1.1. [34] The *positive span* of a set of vectors $[e_1, \ldots, e_r]$ in $\mathbb{R}^n$ is the convex cone

$$\{e \in \mathbb{R}^n : e = \alpha_1 e_1 + \ldots + \alpha_r e_r, \quad \alpha_i \geq 0, i = 1, \ldots r\}.$$

Definition 6.1.2. [34] A set of vectors in $\mathbb{R}^n$ whose positive span is $\mathbb{R}^n$ is a *positive spanning set*.

Definition 6.1.3. [34] The set $[e_1, \ldots, e_r]$ is said to be *positively dependant* if one of the vectors is in the convex cone positively spanned by the remaining vectors, that is, if one of the vectors is a positive combination of the others; otherwise, the set is *positively independent*.

Definition 6.1.4. [34] A *positive basis* in $\mathbb{R}^n$ is a positively independent set whose positive span is $\mathbb{R}^n$.

The following result indicates that a positive spanning set for $\mathbb{R}^n$ contains at least $n+1$ vectors.

Theorem 6.1.5. [34, Thm 2.2] If $[e_1, \ldots, e_r]$ spans $\mathbb{R}^n$ positively, then it contains a subset with $r-1$ elements that spans $\mathbb{R}^n$.

Definition 6.1.6. [34] The direction d is said to be a *descent direction* for f at the point $x \in \mathbb{R}^n$ if there exists an $\tilde{\alpha}$ such that for all $\alpha \in (0, \tilde{\alpha}]$,

$$f(x + \alpha d) < f(x).$$

The following result is important in derivative-free optimization techniques based on direct-search methods.

Theorem 6.1.7. [34, Thm 2.3] Let $[e_1, \ldots, e_r]$, with $e_i \neq 0$ for all $i \in \{1, \ldots, r\}$, span $\mathbb{R}^n$. Then $[e_1, \ldots, e_r]$ spans $\mathbb{R}^n$ positively if and only if for every non-zero vector $w \in \mathbb{R}^n$, there exists an index i in $\{1, \ldots, r\}$ for which $w^T e_i > 0$.

Thus, there must always exist a direction of descent in a positive basis. That is, there is at least one direction in a positive basis that makes an acute angle with the negative gradient. The idea of a positive basis is key for this derivative-free method.

6.1.2 Directional Direct-Search Method

Consider any current iterate r_k and a current value for the step size parameter α_k. The goal of the iteration k is to determine a new point r_{k+1} such that $\hat{\gamma}(r_{k+1}) < \hat{\gamma}(r_k)$. The process of finding a new iterate is described in two phases (search step and poll step). The search step consists of evaluating the objective function at a finite number of points. The search step and the current iteration are declared successful if a new point r_{k+1} is found such that $\hat{\gamma}(r_{k+1}) < \hat{\gamma}(r_k)$. If the iteration is successful, then the poll step is skipped and

the algorithm proceeds with the next iteration. The poll step is a local search around the current iterate, exploring a set of points

$$P_k = \{r_k + \alpha_k d : d \in D_k\},$$

defined by the step size α_k and a positive basis D_k. The points $r_k + \alpha_k d \in P_k$ are called the poll points. The poll step and the current iteration is declared successful if a new point $r_k + \alpha_k d_k$ is found such that $\hat{\gamma}(r_k + \alpha_k d_k) < \hat{\gamma}(r_k)$ for some $d_k \in D_k$. In this case, $r_{k+1} := r_k + \alpha_k d_k$. If the poll step fails to produce a point in P_k where the objective function is lower than $\hat{\gamma}(r_k)$, then both the poll step and the iteration are declared unsuccessful. The step size parameter α_k is decreased if the iteration is unsuccessful, and unchanged if the iteration is successful. The algorithm continues with the next iteration untill α_k reaches the limiting tolerance ϵ.

Convergence of this method to first-order stationary points is obtained under various assumptions [34, Sections 7.3 - 7.7]. For minimizing the $\mathcal{H}_\infty$-cost function $\hat{\gamma}(r)$ with respect to actuator location, a sufficient decrease condition

$$\hat{\gamma}(r_{k+1}) < \hat{\gamma}(r_k) - g(\alpha_k) \tag{6.1.1}$$

is imposed on the acceptance of new points, both in the search step and the poll step, where $g : \mathbb{R}_+ \mapsto \mathbb{R}_+$ is a *forcing function*, and this guarantees convergence to a first-order stationary point; see [34, Thm. 7.12] for details.

A significant advantage of directional direct-search method is that this algorithm is parallelizable. Function evaluations at different points are independant of each other and can be done simultaneously on parallel machines. Alternatively, when individual function evaluations are expensive, the speed of direct-search method can easily be improved many-fold by suitably ordering the points chosen in search and poll steps before starting to evaluate the function. This strategy reduces the number of function evaluations.

6.1.3 Surrogate Model

Optimal attenuation $\hat{\gamma}$ at each point r_k is calculated using a bisection-type algorithm. Even with use of an improved bisection algorithm (Algorithm 3) multiple solutions of a

Algorithm 4 Calculation of $\mathcal{H}_\infty$-optimal actuator locations

Input : Choose a starting point $r_0 \in \Omega^m$. Calculate the optimal attenuation at r_0, $\hat{\gamma}(r_0)$.

Parameters : Choose $\alpha_0 > 0, 0 < \beta_1 \leq \beta_2 < 1, p_k \in \mathbb{Z}_+$ and $\epsilon > 0$. Choose a forcing function $g : \mathbb{R}_+ \mapsto \mathbb{R}_+$; for example $g(\alpha) = \alpha^2$. Let $\mathcal{D}$ be a set of positive bases.

Surrogate model : At a new location r, use $\gamma(r) := \hat{\gamma}(r_k)$ and solve the fixed attenuation $\mathcal{H}_\infty$ control problem. Then, define the surrogate model

$$sm_k(r) := \begin{cases} \|G_{yv}(K, r)\|_\infty & \text{if solution exists,} \\ \infty, & \text{otherwise.} \end{cases}$$

For $k = 0, 1, 2, \ldots$ until $\alpha_k < \epsilon$

Step 1(Search step) : (a) Evaluate $sm_k(.)$ at points $R_k = \{r_k^1, \ldots, r_k^{p_k}\}$.

(b) Order R_k: $sm_k(r_k^1) \leq \ldots \leq sm_k(r_k^{p_k})$. If $sm_k(r) = \infty$ for some $r \in R_k$, then r is removed from R_k.

(c) If R_k is not empty, then start evaluating $\hat{\gamma}(r)$, $r \in R_k$, in this order until a point r is found such that $\hat{\gamma}(r) < \hat{\gamma}(r_k) - g(\alpha_k)$.

(d) If such a point r is found, then set $r_{k+1} := r$, declare the iteration and search step succesful, and go to Step 3. If such a point r is not found or R_k is empty, then declare search step as unsuccessful and go to Step 2.

Step 2(Poll step) : (a) Choose a positive basis $D_k \in \mathcal{D}$.

(b) Order the poll set $P_k = \{r_k + \alpha_k d : d \in D_k\}$ by evaluating $sm_k(\cdot)$ at points in P_k.

(c) Evaluate $\hat{\gamma}(\cdot)$ at the poll points in this order.

(d) If a poll point $r_k + \alpha_k d_k$ is found such that $\hat{\gamma}(r_k + \alpha_k d_k) < \hat{\gamma}(r_k) - g(\alpha_k)$, then stop. Set $r_{k+1} := r_k + \alpha_k d_k$, and declare the iteration and poll step to be successful. Otherwise, declare the iteration (and the poll step) unsuccessful. Set $r_{k+1} := r_k$.

Step 3(Model calibration) :- Set $\gamma(r) := \hat{\gamma}(r_{k+1})$ and update the definition of $sm_{k+1}(\cdot)$ accordingly.

Step 4(Step size update) :- If the iteration was successful, then maintain the step size parameter: $\alpha_{k+1} = \alpha_k$. Otherwise decrease the step size parameter: $\alpha_{k+1} \in [\beta_1 \alpha_k, \beta_2 \alpha_k]$.

fixed attenuation problem are required. Since each solution requires solution of a Riccati equation, this is very time-consuming. However, the actual attenuation achieved by a given controller (for some attenuation γ) is generally quite close to the optimal attenuation. (See Table 6.1). Furthermore, the optimal attenuation is a continuous function of the actuator location (Theorem 4.2.4).

Table 6.1: Comparison of optimal attenuation and actual attenuation achieved at different actuator locations on the 2D diffusion problem (Example 6.2.5) with a coarse mesh (size = 0.625)

Location (r)	$\gamma(r)$	$\|G_{yv}(K,r)\|_\infty$	$\hat{\gamma}(r)$
$(3.24, 2.14)$	18.8483	14.3323	12.1604
$(2.92, 3.30)$	10.7992	10.7535	10.3666
$(3.13, 2.94)$	10.277	10.2726	10.1585
$(3.15, 2.98)$	10.1219	10.1216	10.1153

We therefore define a surrogate model, sm as follows. Let $G_{yv}(K,r)$ indicate the closed loop transfer function with K a given state feedback controller and r an actuator location. For any r, the fixed attenuation $\gamma(r) := \hat{\gamma}(r_k)$ is used and

$$sm(r) := \|G_{yv}(K,r)\|_\infty. \tag{6.1.2}$$

If the attenuation $\gamma(r)$ is not achieved at r then $sm(r) := \infty$. Since the optimal attenuation is a continuous function of r, the optimal attenuation at points near r_k will be close to $\hat{\gamma}(r_k)$. This strategy works efficiently at points further away from the neighborhood of r_k as well since if the attenuation $\hat{\gamma}(r_k)$ is not achieved at r, the optimal cost cannot be achieved at r. Evaluation of the surrogate model requires the solution of one $\mathcal{H}_\infty$-ARE and the closed-loop $\mathcal{H}_\infty$-norm, if the γ-attenuation is achievable. This requires much less computation time than evaluating optimal attenuation $\hat{\gamma}(r)$.

6.1.4 Parallel Implementation

Approximation of partial differential equations yield systems of large model order. Even with the use of the surrogate model in Algorithm 4, function evaluation at a point (that is, calculating $\mathcal{H}_\infty$-optimal attenuation at a particular actuator location) is time-consuming.

The bottleneck is solving multiple large $\mathcal{H}_\infty$-AREs. In Section 5.5, a parallel implementation of Algorithm 1 to solve large $\mathcal{H}_\infty$-AREs is briefly discussed. This involves partitioning matrices into several blocks and distributing the matrices cyclically among n_p processes. This set of n_p processors form a process grid and work together to solve a $\mathcal{H}_\infty$-ARE. For the calculation of optimal $\mathcal{H}_\infty$-attenuation at a fixed actuator location, multiple (n_g) process grids work together by solving multiple (n_g) $\mathcal{H}_\infty$-AREs simultaneously.

In the implementation of Algorithm 4, calculation of the surrogate model on different locations is performed simultaneously on the same set of multiple n_g subgrids. In both search and poll steps, surrogate model evaluations at different locations are performed in parallel.

6.2 Examples

Several examples motivated by partial differential equation models, vibrations on a simply supported beam (Example 4.4.2) and diffusion on an irregular geometry in 2D (Example 5.6.3), are examined to illustrate the algorithm.

In the implementation of Algorithm 4, evaluation of the surrogate model at different locations is carried out simultaneously on parallel processors which speeds up the calculations. The percentage savings in CPU time with the inclusion of the surrogate model to directional direct-search method is calculated as

$$\frac{\#\hat{\gamma}(\cdot) \text{ without } sm(\cdot) - \#\hat{\gamma}(\cdot) \text{ with } sm(\cdot)}{\#\hat{\gamma}(\cdot) \text{ with } sm(\cdot)} \times 100. \tag{6.2.1}$$

Also, the choice of our surrogate model is close to the true function (see Table 6.1), and therefore, at most only one function evaluation is carried out in the search and poll steps in each iteration. Thus, several expensive function evaluations are avoided because of the inclusion of a surrogate model.

The beam problem (Section 6.2.1) was simulated using Matlab 7.11 (R2010b) on a Sun x4600 with 8 opteron 8218 CPU's (2.6 GHz) and 32 GB RAM. An improved bisection algorithm (Algorithm 3) is used to calculate the $\mathcal{H}_\infty$-optimal attenuation for fixed actuator

locations. For systems of moderate size (Section 6.2.1), the iterative method proposed in [82] is used to solve the fixed attenuation $\mathcal{H}_\infty$-control problem. A Schur method [84] is used to solve the intermediate sequence of linear quadratic control problems. A Hautus test (for *eg.* [134, pg. 50]) is used to verify stabilizability in step 6 of algorithm presented in [82]. A set of 4 search points and 2 poll points are chosen in each iteration of Algorithm 4. The surrogate model is evaluated simultaneously on 4 parallel threads at these points. The forcing function $g(\alpha) = \alpha^2$ is used for these systems.

The diffusion problem was simulated using GSL libraries in C with SCALAPACK routines on a HP Proliant SL165z G7 server with 320 nodes, where each node contains 12-core AMD opteron 6174 CPU's(2.2 Ghz) and 32 GB RAM. On the diffusion problem (Section 6.2.2), an extended iterative method (Algorithm 1) that is suitable for large-scale descriptor systems such as this was used to solve $\mathcal{H}_\infty$ Riccati equations. A 2×2 processor grid is used and the matrices are distributed among different processors to solve large $\mathcal{H}_\infty$ Riccati equations in parallel using ScaLAPACK routines. Here, 8 points are chosen in both search and poll steps in each iteration of Algorithm 4. The surrogate model on 8 locations are evaluated simultaneously on 8 such processor grids. Thus, in all, 32 processors were used for the calculation of optimal actuator location for large-scale systems. The forcing function $g(\alpha) = 0.01 \times \alpha^3$ and the tolerance $\epsilon = 0.05$ are used in the directional direct-search algorithm.

6.2.1 Simply supported beam with Kelvin-Voigt damping

Example 6.2.1. Consider a simply supported Euler-Bernoulli beam presented in Example 4.4.2 with Kelvin-Voigt damping:

$$\frac{\partial^2 w}{\partial t^2} + C_v \frac{\partial w}{\partial t} + C_d \frac{\partial^5 w}{\partial x^4 \partial t} + \frac{\partial^4 w}{\partial x^4} = b_r(x)u(t) + d(x)v(t), \quad t \geq 0, 0 < x < 1, \tag{6.2.2}$$

In computer simulations, the parameters were set to $C_v = 0.1, C_d = 0.0001$. By choosing moment and velocity as state components ($z(t) = (\frac{\partial^2}{\partial x^2} w(\cdot, t), \frac{\partial}{\partial t} w(\cdot, t))$), the system (6.2.2)-(4.4.6) is well-posed on the state space $\mathcal{Z} = L_2(0,1) \times L_2(0,1)$ [37]; see Example 5.6.2 for details. An obvious choice of measurement is equal weights on all states $C = I$. The

approximation scheme in Example 4.4.2 is used here, since it satisfies all the assumptions of Theorem 4.2.4 and Theorem 4.4.1; see [99] for details.

Figure 6.2: Variation of $\mathcal{H}_\infty$-cost with respect to actuator location on the length of the beam (6.2.2) with $d = b_{0.7}, C = I$ approximated with 15 eigenmodes

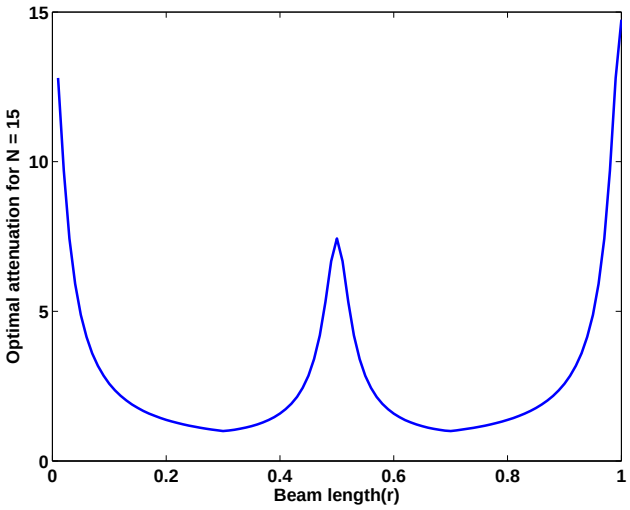

Consider the problem of finding the optimal location of an actuator on (6.2.2) with a disturbance $d = b_{0.7}$ centered at $x = 0.7$ of width $\epsilon = 0.001$. Since there is only one control, choose control weight $R = 1$. Figure 6.2 shows that the $\mathcal{H}_\infty$-cost is not convex over the length of the beam with $N = 15$ eigenmodes. As shown in Figure 6.3, the optimal cost and the corresponding actuator location for different approximations ($N = 1, \ldots 15$ eigenmodes) converge to $\mu = 0.9976$ and the corresponding optimal actuator location is $\hat{r} = 0.7$. If the actuator was placed instead at $r = 0.65$, then the $\mathcal{H}_\infty$-cost increases to $\hat{\gamma}(r) = 1.1613$; a degradation of 16.4%.

Example 6.2.2. Consider the problem of finding an optimal location of an actuator for (6.2.2) now with 2 disturbances $d_1 = 10 \times b_{0.25}$, $d_2 = 10 \times b_{0.75}$, centered at $x = 0.25$ and $x = 0.75$ respectively with width $\epsilon = 0.001$. Since there is only one control, choose control weight $R = 1$. It is natural to think that the optimal actuator location might fall at the

Figure 6.3: Convergence of optimal performance and corresponding $\mathcal{H}_\infty$-optimal actuator location on a simply supported beam with $d = b_{0.7}$ (Example 6.2.1)

(a) Optimal cost

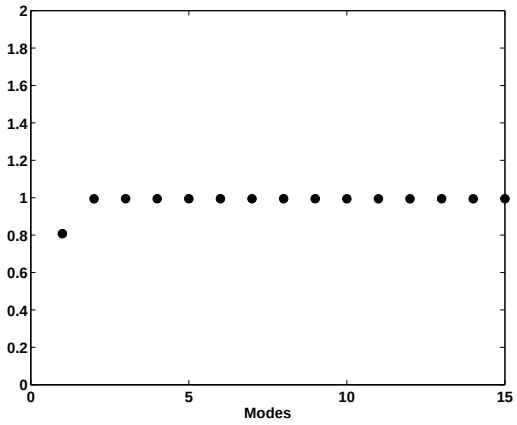

(b) Optimal actuator location

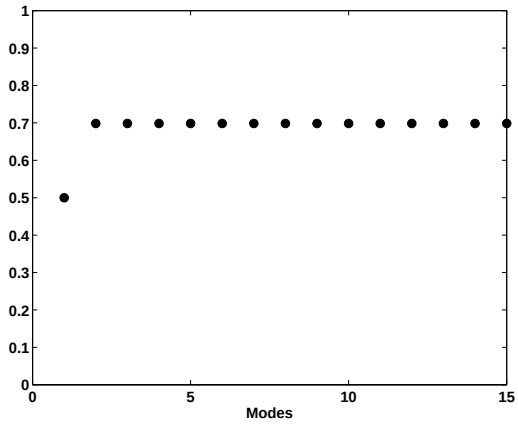

Figure 6.4: Variation of $\mathcal{H}_\infty$-cost with respect to actuator location on (6.2.2) with 2 disturbances placed at $x = 0.25$ and $x = 0.75$ (Example 6.2.2)

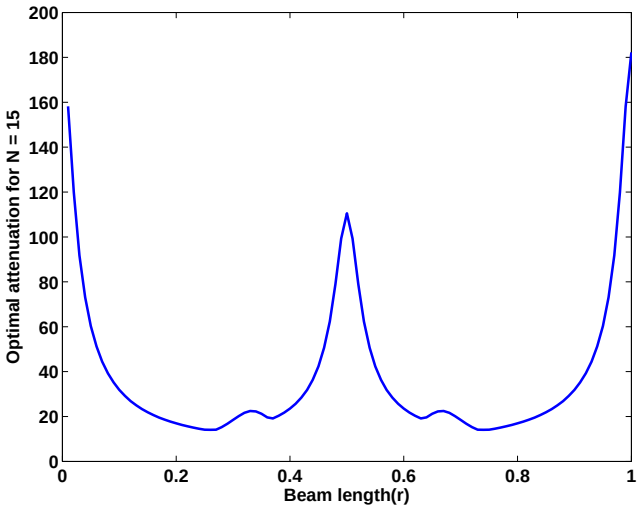

Figure 6.5: Convergence of optimal performance and corresponding $\mathcal{H}_\infty$-optimal actuator location on a simply supported beam with 2 disturbances located at $x = 0.25$ and $x = 0.75$ (Example 6.2.2)

(a) Optimal cost

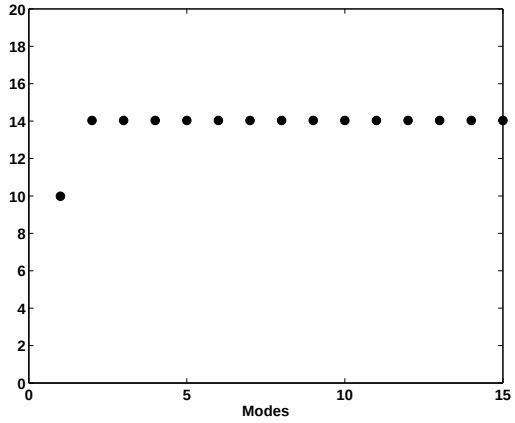

(b) Optimal actuator location

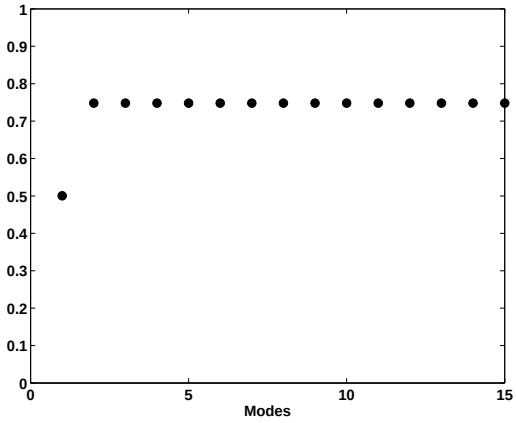

center $x = 0.5$ since the 2 disturbances are symmetrical with respect to the center of the beam. Figure 6.4 shows the $\mathcal{H}_\infty$ cost function for $N = 15$ eigenmodes over the length of the beam. As shown in Figure 6.5, the $\mathcal{H}_\infty$-optimal cost and the corresponding actuator location calculated for different approximations converge to $\mu = 14.0$ and the optimal actuator location $\hat{r} = 0.75$. The $\mathcal{H}_\infty$-optimal actuator location for this problem falls on either of the two disturbance locations. The optimal attenuation at $r = 0.5$ is $\hat{\gamma}(r) = 110$ and the percentage error in performance at this location is 686%. This indicates that center of the beam is a poor choice to place the actuator.

Example 6.2.3. Now consider placing two actuators on the simply supported beam: $d_1 = 10 \times b_{0.25}$, $d_2 = 10 \times b_{0.75}$, centered at $x = 0.25$ and $x = 0.75$ respectively, each with width $\epsilon = 0.001$. Since there are two controls, choose control weight $R = I_{2\times 2}$. The parameters used for this problem are same as the above examples except here the number of poll points used is 4 instead of 2. Figure 6.6 shows the $\mathcal{H}_\infty$ cost function for $N = 5$ eigenmodes when the locations of both actuators are varied over the length of the beam. As shown

Figure 6.6: Variation of $\mathcal{H}_\infty$-cost with respect to the locations of two actuators on the beam with 2 disturbances placed at $x = 0.25$ and $x = 0.75$ approximated with 5 eigenmodes (Example 6.2.3)

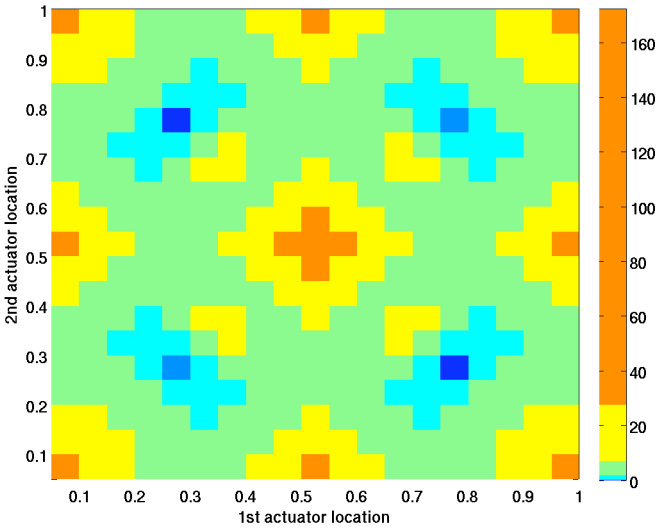

in Figure 6.7, the $\mathcal{H}_\infty$-optimal cost and the corresponding actuator locations for different approximations $N = 1, \ldots 15$ calculated using our Algorithm 4 converge to $\mu = 9.9$ and the optimal actuator locations are $\hat{r}_1 = 0.25, \hat{r}_2 = 0.75$. As expected, the $\mathcal{H}_\infty$-optimal actuator locations for this problem falls on the two disturbance locations. Instead, if the actuators are placed at $r_1 = 0.3, r_2 = 0.6$, then the $\mathcal{H}_\infty$-performance is $\hat{\gamma}(r_1, r_2) = 16$. The degradation in performance is 61.6%.

Example 6.2.4. Now consider placing two actuators on the simply supported beam where the 2 disturbances are not symmetric, that is, $d_1 = 10 \times b_{0.4}$, $d_2 = 10 \times b_{0.9}$, centered at $x = 0.4$ and $x = 0.9$ respectively, each with width $\epsilon = 0.001$. Since there are two controls, choose control weight $R = I$. The $\mathcal{H}_\infty$-optimal cost for different approximations converged to $\mu = 8.5$ (Figure 6.9a). As shown in Example 6.2.3, one might expect that the optimal locations would be the same spots as that of the disturbances. Figure 6.8 shows that there are multiple local minima on this problem. However, they are not at disturbance locations. As shown in Figure 6.9b, the optimal actuator locations are $\hat{r}_1 = 0.58$ and $\hat{r}_2 = 0.23$ which

Figure 6.7: Convergence of optimal cost and corresponding $\mathcal{H}_\infty$-optimal actuator locations of 2 actuators on a simply supported beam with 2 disturbances (Example 6.2.3)

(a) Optimal cost (b) Optimal actuator locations

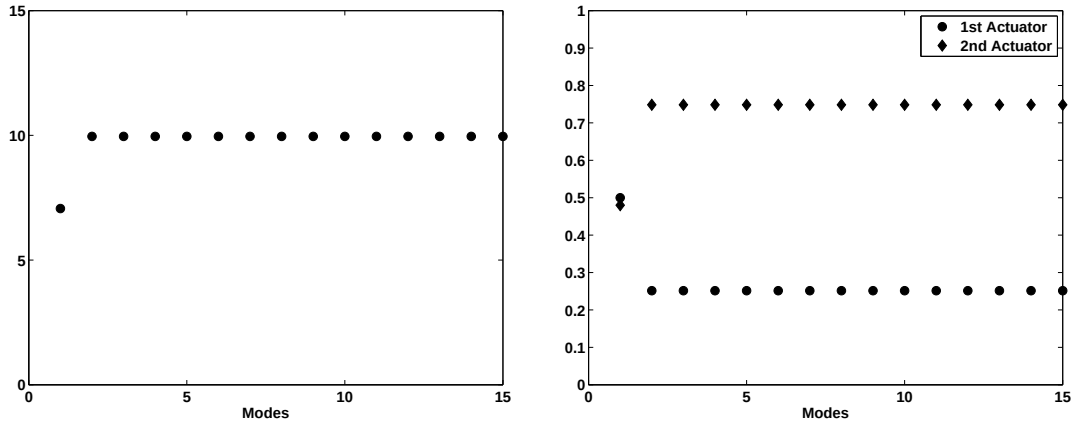

Figure 6.8: Variation of $\mathcal{H}_\infty$-cost with respect to the locations of two actuators (on X and Y axes) on the beam with $d_1 = 10\ b_{0.4}, d_2 = 10\ b_{0.9}, C = I$, approximated with 5 eigenmodes (Example 6.2.4)

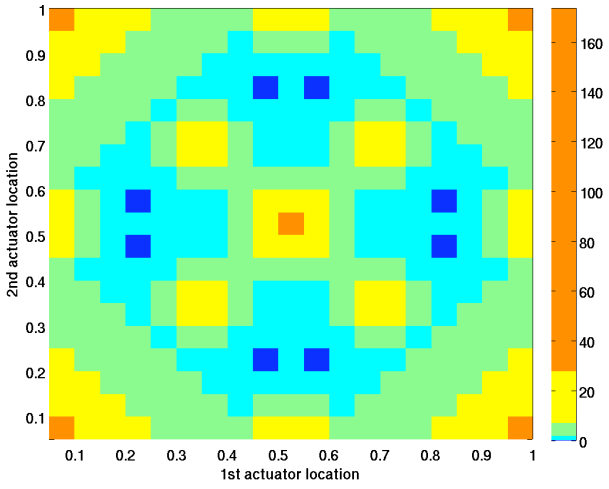

Figure 6.9: Convergence of $\mathcal{H}_\infty$-performance and corresponding optimal actuator location for different approximations of the K-V damped beam with $d_1 = 10\, b_{0.4}, d_2 = 10\, b_{0.9}, C = I$ (Example 6.2.4)

(a) Optimal $\mathcal{H}_\infty$-cost (b) Optimal actuator location

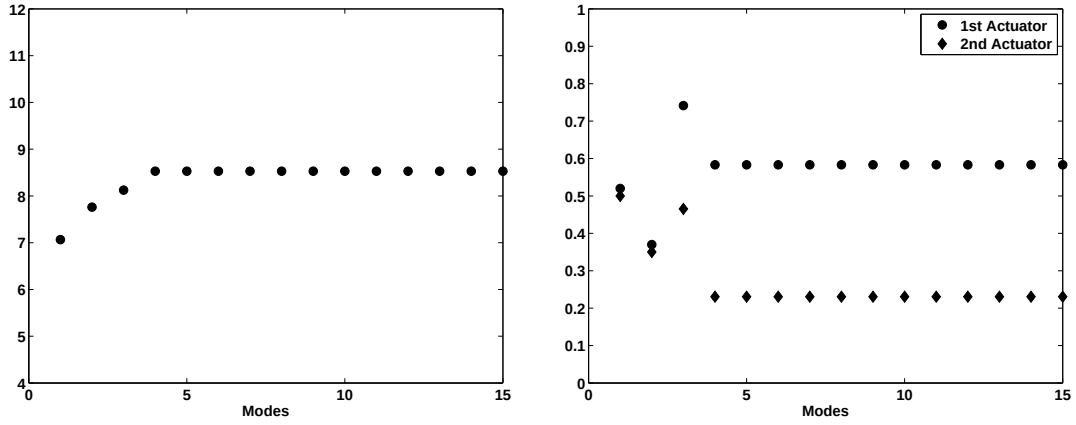

are not near the disturbances. If, instead of placing the actuators at the optimal location, the actuators are collocated with the disturbances, that is $r_1 = 0.4$ and $r_2 = 0.9$, then the $\mathcal{H}_\infty$-performance is $\hat{\gamma}(r_1, r_2) = 10$. The degradation in performance is 17.5%.

Table 6.2 shows the improvement in computation time caused by use of the surrogate model in Algorithm 4.

6.2.2 Diffusion on 2D

Example 6.2.5. Consider the heat diffusion problem in Example 5.6.3. Now, consider variable diffusivity coefficient $\kappa(x, y)$ (Figure 6.10) on the irregular geometry Ω (Figure 5.4). Let the exogenous disturbance $v(t)$ induce a uniform load on the geometry. The average temperature of the whole domain is measured. The approximation method used in Example 5.6.3 is used for the calculation of optimal actuator location. The original problem is both stabilizable and detectable and so are the approximating problems; see [96]. This

Table 6.2: Performance of Algorithm 4 on simply supported beam (Example 6.2.1) for 2 different approximations. The savings in computation time over an algorithm that doesn't use the surrogate model is shown.

Property	$N = 1$	$N = 15$
Order	2	30
# iterations in Algorithm 4	26	8
Overall time taken by Algorithm 4	141.7 secs	41.63 secs
# $\hat{\gamma}(\cdot)$ evaluations	26	1
# $sm(\cdot)$ evaluations	153	48
% savings in CPU time	192%	2300%

Figure 6.10: Diffusivity coefficient $\kappa(x, y) = 3(3 - x)^2 e^{-(2-x)^2-(2-y)^2} + 0.01$

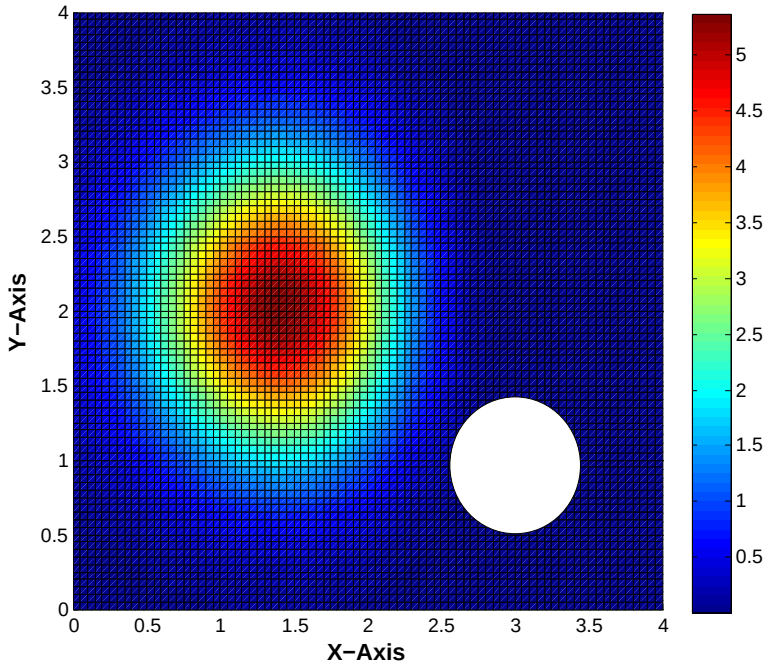

Figure 6.11: Optimal $\mathcal{H}_\infty$-cost of diffusion problem (Example 6.2.5) over different approximations

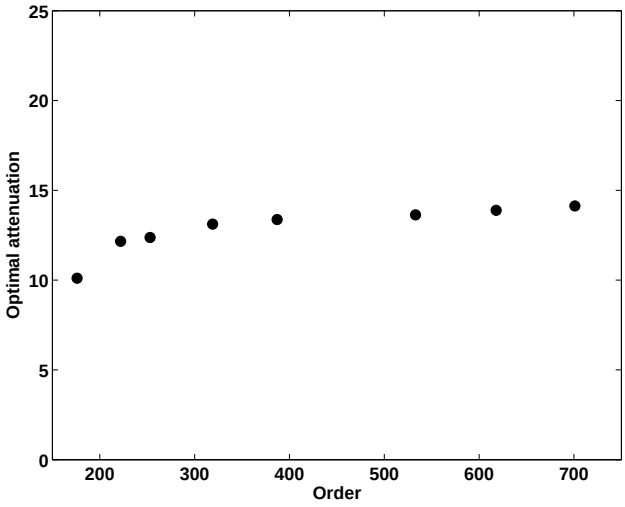

approximation scheme satisfies all the assumptions of Theorem 4.2.4 and Theorem 4.4.1; see [99] for details. The optimal $\mathcal{H}_\infty$-cost calculated over Ω using Algorithm 4 on different approximation sizes converged $\mu = 15$ as shown in Figure 6.11. The corresponding $\mathcal{H}_\infty$-optimal actuator location converged to $\hat{r} = (3.1, 3.35)$. If the actuator was placed instead at $r = (1.5, 3)$, then the $\mathcal{H}_\infty$-cost increases to $\hat{\gamma}(r) = 28$ which is almost twice the optimal $\mathcal{H}_\infty$ cost. In this problem, optimal actuator location is not the center of the geometry due to the irregularity in the domain and the variable diffusivity coefficient.

Evaluation of $\hat{\gamma}(\cdot)$ is highly expensive since the order of the approximating system can be high. Table 6.3 shows that the use of a surrogate model considerably improves the speed of the algorithm.

Example 6.2.6. Now consider a different disturbance. Let the effect of disturbance be concentrated in a region of high diffusivity (a square patch centered at $(2, 1.5)$ with half-width 0.2). The optimal actuator location is $(2.2, 3.1)$, which is in a region of low-diffusivity. If instead, the disturbance is in a low-diffusivity region, a square patch centered at $(3, 3)$

Table 6.3: Performance of Algorithm 4 on Example 6.2.5 for different approximations. The savings in computation time over an algorithm that doesn't use the surrogate model is shown.

Property	**Coarse**	**Fine**
Order	200	700
# iterations in Algorithm 4	15	4
Overall time taken by Algorithm 4	1 hr 10 mins	5 hrs 50 mins
# $\hat{\gamma}(\cdot)$ evaluations	10	1
# $sm(\cdot)$ evaluations	208	64
% savings in CPU time	940%	3100%

with half-width 0.2, then the optimal actuator location falls close to the same location as the disturbance as shown in Figure 6.12. This suggests that in diffusion problems, the actuator should be placed in a region of low diffusivity, but further investigation is needed.

Example 6.2.7. Suppose now there are 2 disturbances contained within square patches centered at $(0.5, 0.5)$ and $(0.5, 3)$, each with half-width 0.2. Consider the problem of placing 2 actuators. The control weight $R = I$ is chosen. Since 2 actuators are to be placed 16 combinations of poll directions are considered. Our algorithm calculated the optimal locations as $\hat{r}_1 = (0.52, 0.48)$ and $\hat{r}_2 = (1.8, 3.13)$ and the optimal cost converged to $\mu = 9.22$. One of the actuators is close to the disturbance that is in a region of low diffusivity. The optimal location for the other actuator is far from the other disturbance as shown in Figure 6.13. If the actuators are placed at the same location as the disturbances $r_1 = (0.5, 0.5), r_2 = (0.5, 3)$ then the $\mathcal{H}_\infty$-cost increases to $\hat{\gamma}(r_1, r_2) = 10.02$; a degradation of 8.6%. Thus, optimal actuator placement depends on the shape of the domain, location of the disturbance(s) and diffusivity.

An algorithm for calculating $\mathcal{H}_\infty$-optimal actuator locations has been described and illustrated with several examples arising from partial differential equation models. Use of a surrogate model considerably improves the speed of the algorithm. Examples indicate that performance is strongly dependent on actuator location, and the optimal locations

Figure 6.12: When disturbance is concentrated in a region of high diffusivity ($D1$ in figure), optimal actuator location falls at a region of low diffusivity ($A1$ in figure). When disturbance is concentrated in a region of low diffusivity, optimal actuator location collocates ($D\&A$ in figure).

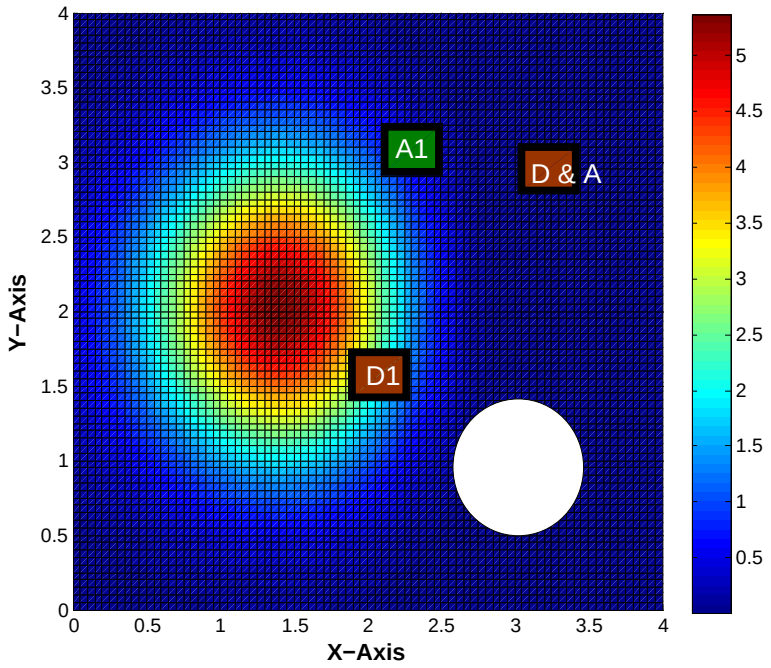

do not always agree with intuition, which supports the use of an algorithm for optimal actuator location.

Figure 6.13: When 2 disturbances are concentrated at $(0.5, 0.5)$ ($D1$ in figure) and $(0.5, 3)$ ($D2$ in figure) respectively, then one actuator collocates ($A1$ in figure) but the other doesnt ($A2$ in figure)

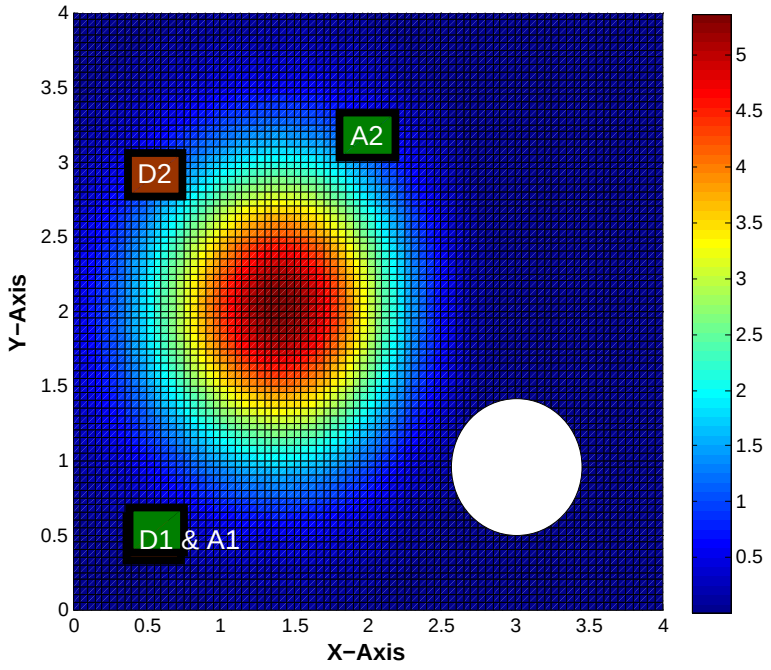

Chapter 7

Conclusion and Future Research

The central focus of this thesis has been the development of a mathematical framework for calculating optimal actuator locations in the context of $\mathcal{H}_\infty$ control with state feedback. The $\mathcal{H}_\infty$-cost at a particular actuator location is the optimal $\mathcal{H}_\infty$-disturbance attenuation at that location. This cost is the best attenuation of the worst-case disturbance [117]. In Section 4.2, it was shown that under certain weak conditions the $\mathcal{H}_\infty$-cost function is continuous with respect to actuator location, and thus, the $\mathcal{H}_\infty$-optimal actuator location problem is well-posed. Both the control operator B and the disturbance operator D must be compact. In contrast to the LQ-optimal actuator location problem, there is no restriction on the measurement operator C. In many control systems modeled by partial differential equations, approximations are used in $\mathcal{H}_\infty$ controller design and thus in selection of the actuator location. It was established that the assumptions on the approximation scheme required for $\mathcal{H}_\infty$ controller design also lead to a convergent sequence of $\mathcal{H}_\infty$-optimal actuator locations. In Section 4.4, examples have been provided to illustrate that convergence may fail when the assumptions are not satisfied.

Several numerical issues are associated with the calculation of $\mathcal{H}_\infty$-optimal actuator locations. Consider the standard problem of calculation of optimal attenuation, with a fixed actuator location. Some existing numerical methods (for instance [31, 57, 84, 82, 112]) to calculate optimal attenuation were reviewed in Section 5.2. An extension of the game theoretic iterative method to large-scale descriptor systems that arise in approximation of

partial differential equations has been developed (Section 5.3). An improved bisection algorithm to calculate optimal attenuation has been suggested in Section 5.4. A distributed parallel implementation of solving large $\mathcal{H}_\infty$-Riccati equations on a multi-processor architecture was described in Section 5.5. Using several examples motivated by partial differential equations, it was showed that the performance of our extended algorithm is similar to Schur method [84] in many cases. However, on several examples, the extended iterative method was both faster and more accurate than the Schur method and other methods (Section 5.6).

The calculation of $\mathcal{H}_\infty$-optimal actuator locations is difficult due to the lack of gradient information. Directional direct-search, which is a popular derivative-free method, is used for minimizing optimal attenuation over all actuator locations. Several advantages of this method for calculating $\mathcal{H}_\infty$-optimal actuator locations have been exploited to speed up the convergence. An algorithm for calculating $\mathcal{H}_\infty$-optimal actuator locations is described in Section 6.1.

The $\mathcal{H}_\infty$ optimal actuator location algorithm was used on several examples arising from partial differential equation models in Section 6.2. It was shown that the use of a surrogate model considerably improves the speed of the algorithm. Performance is strongly dependent on actuator location, and the optimal locations do not always agree with intuition, which supports the use of an algorithm for optimal actuator location.

This thesis has only been concerned with the optimal actuator location problem. Optimal sensor location problem is dual to this problem, since the design of an estimator is dual to the design of a state-feedback controller [102]. If the actuator and sensor location problems are treated separately, then all the results in this thesis extend immediately to $\mathcal{H}_\infty$ optimal sensor location problem, which would involve calculating the solution of a dual $\mathcal{H}_\infty$-algebraic Riccati equation.

The control operators for a class of boundary control systems are often unbounded. In the case of linear quadratic optimal actuator location problem, it was shown that the compactness assumption on control operators can often be weakened if the underlying semigroup is analytic [83]. This suggests that the results in this thesis might possibly extend to the case when B is not compact by considering analytic semigroups.

An interesting extension would be to consider output feedback. In many practical applications, all the states are not available for measurement. In the case of linear-quadratic criterion, an estimator is designed first by solving the dual Riccati operator equation and then, a state-feedback controller is designed [37]. Several challenges are involved in the calculation of LQ optimal actuator location using output feedback.

In the case of $\mathcal{H}_\infty$ control with output feedback, the two $\mathcal{H}_\infty$ Riccati operator equations are coupled. This coupling makes the problem complicated and challenging. For fixed actuator locations, conditions under which approximations yield reliable results are given in [101]. The problem of using approximations to determine optimal actuator locations for $\mathcal{H}_\infty$-control with output feedback is open.

The problem of calculating the optimal number of actuators and sensors for the full partial differential equation model is open.

Future research includes considering the effect of modelling errors, uncertain spatial location of the disturbance and comparing the effect of different cost functions, such as $\mathcal{H}_2$ and $\mathcal{H}_\infty$, on optimal actuator location.

Bibliography

[1] M.M. Abdullah, A. Richardson, and J. Hanif. Placement of sensors/actuators on civil structures using genetic algorithms. *Earthquake Engineering and Structural Dynamics*, 30:1167–1184, 2001.

[2] J. Alberty, C. Carstensen, and S.A. Funken. Remarks around 50 lines of Matlab: short finite element implementation. *Numerical Algorithms*, 20:117–137, 1999.

[3] L. Amodei and J.-M. Buchot. An invariant subspace method for large-scale algebraic Riccati equation. *Applied Numerical Mathematics*, 60(11):1067–1082, 2010.

[4] E. Anderson, Z. Bai, C. Bischof, S. Blackford, J. Demmel, J. Dongarra, J. Du Croz, A. Greenbaum, S. Hammarling, A. McKenney, and D. Sorensen. *LAPACK Users' Guide*. Society for Industrial and Applied Mathematics, Philadelphia, PA, third edition, 1999.

[5] C. Antoniades and P.D. Christofides. Integrated optimal actuator/sensor placement and robust control of uncertain transport-reaction processes. *Computers and Chemical Engineering*, 26:187–203, 2002.

[6] A. Arbel. Controllability measures and actuator placement in oscillatory systems. *International Journal of Control*, 33(3):565–574, 1981.

[7] A. Armaou and M.A. Demetriou. Optimal actuator/sensor placement for linear parabolic pdes using spatial $\mathcal{H}_2$ norm. *Chemical Engineering Science.*, 61:7351–7367, 2006.

[8] W.F. Arnold, III, and A.J. Laub. Generalized eigenproblem algorithms and software for algebraic Riccati equations. *Proceedings of the IEEE*, 72(12):1746–1754, 1984.

[9] D. Arzelier, G. Deaconu, S. Gumussoy, and D. Henrion. $\mathcal{H}_2$ for hifoo. In *3rd International Conference on Control and Optimization with Industrial Applications*, 2011.

[10] J.M. Badia, P. Benner, R. Mayo, and E.S. Quintana-Orti. Parallel solution of large-scale and sparse generalized algebraic Riccati equations. In *Lecture Notes in Computer Science 4128 LNCS*, pages 710–719, 2006.

[11] H.T. Banks and K. Ito. A numerical algorithm for optimal feedback gains in high dimensional linear quadratic regulator problems. *SIAM Journal on Control and Optimization*, 29(3):499–515, 1991.

[12] H.T. Banks and K. Kunisch. The linear regulator problem for parabolic systems. *SIAM Journal on Control and Optimization*, 22(5):684–698, 1984.

[13] H.T. Banks, R.C. Smith, and Y. Wang. *Smart Material Structures: Modeling, Estimation and Control*. Wiley-Masson, New York, 1996.

[14] P. Benner and R. Byers. An exact line search method for solving generalized continuous time algebraic Riccati equations. *IEEE Transactions on Automatic Control*, 43(1):101–107, 1998.

[15] P. Benner, R. Byers, P. Losse, V. Mehrmann, and H. Xu. Robust formulas for optimal $\mathcal{H}_\infty$ controllers. *Automatica*, 47(12):2639–2646, 2011.

[16] P. Benner, R. Byers, V. Mehrmann, and H. Xu. Numerical computation of deflating subspaces of skew-Hamiltonian/Hamiltonian pencils. *SIAM Journal on Matrix Analysis and Applications*, 24(1):165–190, 2002.

[17] P. Benner, R. Byers, V. Mehrmann, and H. Xu. A robust numerical method for the γ-iteration in $\mathcal{H}_\infty$ control. *Linear algebra and its applications*, 425:548–570, 2007.

[18] P. Benner, R. Byers, E.S. Quintana-Orti, and G. Quintana-Orti. Solving algebraic Riccati equations on parallel computers using Newton's method with exact line search. *Parallel computing*, 26:1345–1368, 2000.

[19] P. Benner, M. Castillo, R. Mayo, E. S. Quintana-Orti, and G. Quintana-Orti. Stabilizing large-scale generalized systems on parallel computers using multithreading and message-passing. *Concurrency and Computation : Practice and Experience*, 19:531–542, 2007.

[20] P. Benner, V. Mehrmann, V. Sima, S. Van Huffel, and A. Varga. Slicot - a subroutine library in systems and control theory. In *Applied and Computational Control, Signal and Circuits, (B.N. Datta, Ed.), ch. 10*, volume 1, pages 499–539. Birkauser, 1999.

[21] P. Benner, E. S. Quintana-Orti, and G. Quintana-Orti. Solving linear-quadratic optimal control problems on parallel computers. *Optimization methods and software*, 23(6):879–909, 2008.

[22] P. Benner and V. Sima. Solving algebraic Riccati equations with slicot. In *CD-ROM Proc. of The 11th Mediterranean Conference on Control and Automation*, 2003.

[23] A. Bensoussan and P. Bernhard. On the standard problem of $\mathcal{H}_\infty$-optimal control for infinite dimensional systems. *In Identification and Control in Systems Governed by Partial Differential Equations, H.T. Banks, R.H. Fabiano and K.Ito eds., SIAM, Philadelhpia*, pages 117–140, 1993.

[24] L. S. Blackford, J. Choi, A. Cleary, E. D'Azevedo, J. Demmel, I. Dhillon, J. Dongarra, S. Hammarling, G. Henry, A. Petitet, K. Stanley, D. Walker, and R. C. Whaley. *ScaLAPACK Users' Guide*. Society for Industrial and Applied Mathematics, Philadelphia, PA, 1997.

[25] J. Borggaard and M. Stoyanov. An efficient long-time integrator for Chandrasekhar equations. In *Proceedings of the 47th IEEE Conference on Decision and Control*, 2008.

[26] J. Borggaard, M. Stoyanov, and L. Zietsmann. Linear feedback control of a von Karman street by cylinder rotation. In *Proceedings of the 2010 American Control Conference*, pages 5674–5681, 2010.

[27] J.V. Burke, D. Henrion, A.S. Lewis, and M.L. Overton. Hifoo - a Matlab package for fixed-order controller design and $\mathcal{H}_\infty$ optimization. In *5th IFAC Symposium on Robust Control Design*, 2006.

[28] J.A. Burns, K. Ito, and R.K. Powers. Chandrasekhar equations and computational algorithms for distributed parameter systems. In *Proceedings of the 23rd IEEE Conference on Decision and Control*, 1984.

[29] J.A. Burns, K. Ito, and G. Propst. On non-convergence of adjoint semigroups for control systems with delays. *SIAM Journal on Control and Optimization*, 26(6):1442–1454, 1988.

[30] J.A. Burns, E.W. Sachs, and L. Zietsman. Mesh independence of Kleinman-Newton iterations for Riccati equations in Hilbert space. *SIAM Journal on Control and Optimization*, 47(5):2663–2692, 2008.

[31] R. Byers. Solving the algebraic Riccati equation with the matrix sign function method. *Linear algebra and its applications*, 85:267–279, 1987.

[32] J. Casti. *Dynamical Systems and Their Applications: Linear Theory.* Academic Press, New York, 1997.

[33] B.M. Chen. Non-iterative computation of optimal value in $\mathcal{H}_\infty$ control. *In V.D. Blondel, A. Megretski (Eds.), Unsolved Problems in Mathematical Systems and Control Theory, Princeton University Press*, pages 271–275, 2004.

[34] Conn, Scheinberg, and Vicente. *Introduction to Derivative-Free Optimization.* MPS-SIAM series on optimization, Philadelphia, 2009.

[35] Matlab control toolbox. `http://www.mathworks.com/`.

[36] R. Curtain, K. Mikkola, and A. Sasane. The Hilbert-Schmidt property of feedback operators. *Journal of Mathematical Analysis and Applications*, 329:1145–1160, 2007.

[37] R.F. Curtain and H. Zwart. *An Introduction to Infinite-Dimensional Linear Systems Theory*. Springer Verlag, Berlin, 1995.

[38] N. Darivandi, K.A. Morris, and A. Khajepour. LQ-optimal actuator location in structures. In *Proceedings of the 2012 American Control Conference*, 2012.

[39] B.N. Datta. *Numerical Methods for Linear Control Systems*. Elsevier Academic Press, New York, 2004.

[40] M.A. Demetriou. Integrated actuator−sensor placement and hybrid controller design of flexible structures under worst case spatiotemporal disturbance variations. *Journal of Intelligent Material Systems and Structures*, 15(12):901–921, 2004.

[41] M.A. Demetriou and K.M. Grigoriadist. Collocated actuator placement in structural systems using an analytical bound approach. In *Proceeding of the 2004 American Control Conference*, pages 1604–1609, 2004.

[42] M.A. Demetriou and K.M. Grigoriadist. Utilizing spatial robustness measures for the optimization of a pzt-actuated flexible beam. In *Proc. of SPIE Vol. 6523, 65230N, Modeling, Signal Processing, and Control for Smart Structures 2007, edited by Douglas K. Lindner*, 2007.

[43] J.C. Doyle, K. Glover, P. Khargonekar, and B.A. Francis. State-space solutions to standard $\mathcal{H}_2$ and $\mathcal{H}_\infty$ control problems. *IEEE Transactions on Automatic Control*, 34(8):831–847, 1989.

[44] N. Ellner and E.L. Wachspress. Alternating direction implicit iteration for systems with complex spectra. *SIAM Journal on Numerical Analysis*, 28(3):859–870, 1991.

[45] M. Galassi et al. GNU Scientific Library Reference Manual (3rd Ed.).

[46] F. Fahroo and M.A. Demetriou. Optimal actuator/sensor location for active noise regulator and tracking control problems. *Journal of Computational and Applied Mathematics*, 114:137–158, 2000.

[47] F. Feitzinger, T. Hylla, and E.W. Sachs. Inexact Kleinman-Newton method for Riccati equations. *SIAM Journal on Matrix Analysis and Application*, 31(2):272–288, 2009.

[48] B.A. Francis. *A Course in $\mathcal{H}_\infty$ Control Theory, Lecture Notes in Control and Information Science, vol. 88*. Springer Verlag, Berlin, 1987.

[49] M.I. Frecker. Recent advances in optimization of smart structures and actuators. *Journal of Intelligent Material Systems and Structures*, 14:207–216, 2003.

[50] W. Gawronski. *Dynamics and Control of Structures : A Modal Approach*. Springer-Verlag, New York, 1998.

[51] J.C. Geromel. Convex analysis and global optimization of joint actuator location and control problems. *IEEE Transactions on Automatic Control*, 34(7):711–720, 1989.

[52] J.S. Gibson. The Riccati integral equations for optimal control problems on Hilbert spaces. *SIAM Journal on Control and Optimization*, 17(4):637–665, 1979.

[53] K. Glover and J.C. Doyle. State-space formulae for all stabilizing controllers that satisfy an $\mathcal{H}_\infty$ norm bound and relations to risk sensitivity. *Systems and Control Letters*, 11:167–172, 1988.

[54] G.H. Golub and C.F. Van Loan. *Matrix Computations, third ed.* John Hopkins University Press, Baltimore, 1996.

[55] J.R. Grad and K.A. Morris. Solving the linear quadratic optimal control problem for infinite-dimensional systems. *Computers and Mathematics with Applications*, 32(9):99–119, 1996.

[56] W. Gropp, E. Lusk, and A. Skjellum. *Using MPI: Portable Parallel Programming with Message Passing Interface*. MIT Press, Cambridge, M.A., second edition, 1999.

[57] S. Gumussoy, D. Henrion, M. Millstone, and M.L. Overton. Multiobjective robust control with hifoo 2.0. In *Proceedings of the 6th IFAC Symposium on Robust Control Design*, 2009.

[58] S. Gumussoy, M. Millstone, and M.L. Overton. $\mathcal{H}^\infty$ strong stabilization via hifoo, a package for fixed-order controller design. *Proceedings of 47th IEEE Conference on Decision and Control*, pages 4135–4140, 2008.

[59] S. Gumussoy and M.L. Overton. Fixed-order $\mathcal{H}^\infty$ controller design via hifoo, a specialized nonsmooth optimization package. In *Proceedings of the 2008 American Control Conference*, pages 2750–2754, 2008.

[60] A. Hac and L. Liu. Sensor and actuator location in motion control of flexible structures. *Journal of Sound and Vibration*, 167(2):239–261, 1993.

[61] L. M. Hanagan, E. C. Kulasekere, K. S. Walgama, and K. Premaratne. Optimal placement of acutators and sensors for floor vibration control. *Journal of Structural Engineering*, 126(12):1380–1387, 2000.

[62] P. Hebrard and A. Henrot. A spillover phenomenon in the optimal location of actuators. *SIAM Journal on Control and Optimization*, 44(1):349–366, 2005.

[63] K. Hiramoto, H. Doki, and G. Obinata. Optimal sensor/actuator placement for active vibration control using explicit solution of algebraic Riccati equation. *Journal of Sound and Vibration*, 229(5):1057–1075, 2000.

[64] K. Ito. Strong convergence and convergence rates of approximating solutions for algebraic Riccati equations in Hilbert spaces. *In W.Schappacher, F.Kappel, K.Kunisch, editor, Distributed Parameter Systems, Springer-Verlag*, 1987.

[65] K. Ito and K.A. Morris. An approximation theory of solutions to operator Riccati equations for $\mathcal{H}_\infty$ control. *SIAM Journal on Control and Optimization*, 36(1):82–99, 1998.

[66] K. Jbilou. Block Krylov subspace methods for large algebraic Riccati equations. *Numerical algorithms*, 34:339–353, 2003.

[67] K. Jbilou. An Arnoldi based algorithm for large algebraic Riccati equations. *Applied Mathematics letters*, 19:437–444, 2006.

[68] F.A.K. Jha and D.J. Inman. Optimal sizes and placements of piezoelectric actuators and sensors for an inflated torus. *Journal of Intelligent Material Systems and Structures*, 14:563–576, 2003.

[69] T. Kailath. Some Chandrasekhar-type algorithms for quadratic regulators. In *Proceedings of IEEE Conference and Decision and Control*, pages 219–223, 1972.

[70] D. Kasinathan and K. Morris. $\mathcal{H}_\infty$-optimal actuator location. Submitted to IEEE Transactions on Automatic Control.

[71] D. Kasinathan and K. Morris. An iterative method for solving $\mathcal{H}_\infty$-control problems for large-scale regular descriptor system. Submitted to 51st IEEE CDC-ECC 2012.

[72] D. Kasinathan and K. Morris. A numerical method for the calculation of $\mathcal{H}_\infty$-optimal actuator locations. Submitted to 51st IEEE CDC-ECC 2012.

[73] D. Kasinathan and K. Morris. Convergence of $\mathcal{H}_\infty$-Optimal Actuator Locations. In *Proceedings of the 50th IEEE Conference on Decision and Control*, pages 627–632, 2011.

[74] C.T. Kelley. *Iterative Methods for Optimization*. SIAM, Philadelphia, 1999.

[75] C.S. Kenney, A.J. Laub, and M. Wette. A stability-enhancing scaling procedure for Schur-Riccati solvers. *Systems and Control Letters*, 12:241–250, 1989.

[76] B. Van Keulen. $\mathcal{H}_\infty$ *Control for Distributed Parameter Systems : A State-Space Approach*. Birkhauser, Boston, 1993.

[77] R.K. Kincaid and S. L. Padula. D-optimal designs for sensor and actuator locations. *Computers and Operations Research*, 29:701–713, 2002.

[78] D.L. Kleinman. On an iterative techniqe for Riccati equation computations. *IEEE Transactions on Automatic Control*, 13:114–115, 1968.

[79] C.S. Kubrusly and H. Malebranche. Sensors and controllers location in distributed systems - a survey. *Automatica*, 21(2):117–128, 1985.

[80] K.R. Kumar and S. Narayanan. The optimal location of piezoelectric actuators and sensors for vibration control of plates. *Smart Materials and Structures*, 16:2680–2691, 2007.

[81] P. Lancaster and L. Rodman. *Algebraic Riccati Equations*. Oxford University Press, 1995.

[82] A. Lanzon and B.D.O. Anderson. Computing the positive stabilizing solution to algebraic Riccati equations with an indefinite quadratic term via a recursive method. *IEEE Transactions on Automatic Control*, 53(10):2280–2291, 2008.

[83] I. Lasiecka and R. Triggiani. *Control Theory for Partial Differential Equations: Continuous and Approximation theories, Volume I,II.* Cambridge Univeristy Press, Cambridge, U.K., 2000.

[84] A.J. Laub. A Schur method for solving algebraic Riccati equations. *IEEE Transactions on Automatic Control*, 24(6):913–921, 1979.

[85] F. Leibfritz. *Compleib: constraint matrix optimization problem library. A collection of test examples for nonlinear semidefinite programs, control system design and related problems*. Univ. Trier, Germany, `www.compleib.de`, 2005.

[86] S. Leleu, H. Abou-Kandil, and Y. Bonnassieux. Piezoelectric actuators and sensors location for active control of flexible structures. *IEEE Transactions on Instrumentation and Measurement*, 50(6):1577–1582, 2001.

[87] W.S. Levine and M. Athans. On the determination of the optimal constant output feedback gains for linear multivariable systems. *IEEE Transactions on Automatic Control*, 15(1):44–48, 1970.

[88] J.-R. Li and J. White. Low rank solution of Lyapunov equations. *SIAM Journal on Matrix Analysis and Applications*, 24(1):260–280, 2003.

[89] Y. Li, J. Onido, and K. Minesugi. Simultaneous optimization of piezoelectric actuator placement and feedback for vibration suppression. *Acta Astronautica*, 50(6):335–341, 2002.

[90] C.C. Lin. An impedance approach to the design of optimal actuator location for acoustic response synthesis. *Smart Materials and Structures*, 19(5):1–10, 2010. art. no. 055021.

[91] P. Losse, V. Mehrmann, L.K. Poppe, and T. Reis. The modified optimal $\mathcal{H}_\infty$ control problem for descriptor systems. *SIAM Journal on Control and Optimization*, 47(6):2795–2811, 2008.

[92] D.G. Luenberger and Y. Ye. *Linear and Nonlinear Programming*. Springer, Newyork, 2008.

[93] A.R. Mehrabian and A. Yousefi-Koma. Optimal positioning of piezoelectric actuators on a smart fin using bio-inspired algorithms. *Aerospace Science and Technology*, 11:174–182, 2007.

[94] V. Mehrmann. *The Autonomous Linear Quadratic Control Problem, Theory ad Numerical Solution, Lecture notes in Control and Information Sciences*. Springer-Verlag, Heidelberg, Germany, 1991.

[95] M. Millstone. Hifoo 1.5: structured control of linear systems with non-trivial feedthrough. Master's thesis, Newyork University, 2006.

[96] K. Morris. Control of systems governed by partial differential equations. In *ed. W.S. Levine, The Control Handbook, Second Edition, Control System Advanced Methods*. CRC Press, 2010.

[97] K. Morris. Linear-quadratic optimal actuator location. *IEEE Transactions on Automatic Control*, 56(1):113–124, 2011.

[98] K. Morris and M. Demetriou. Using $\mathcal{H}_2$ control metrics for the optimal actuator location of infinite-dimensional systems. In *Proceeding of the 2010 American Control Conference*, pages 4899–4904, 2010.

[99] K.A. Morris. Design of finite-dimensional controllers for infinite-dimensional systems by approximation. *Journal of Mathematical systems, Estimation and Control*, 4:1–30, 1994.

[100] K.A. Morris. Noise reduction achievable by point control. *ASME Journal on Dynamic Systems, Measurement and Control*, 120(2):216–223, 1998.

[101] K.A. Morris. $\mathcal{H}_\infty$-output feedback of infinite-dimensional systems via approximation. *Systems and Control Letters*, 44:211–217, 2001.

[102] K.A. Morris. *Introduction to Feedback Control*. Harcourt-Brace, San Diego, 2001.

[103] K.A. Morris and C. Navasca. Solution of algebraic Riccati equations arising in control of partial differential equations. In J. Cagnola and J-P Zolesio, editors, *Control and boundary analysis, Lect. Notes Pure Appl. Math.*, volume 240, chapter 20, pages 257–280. Chapman & Hall/CRC, 2005.

[104] K.A. Morris and C. Navasca. Approximation of low rank solutions for linear quadratic control of partial differential equations. *Computational Optimization and Applications*, 46(1):93–111, 2010.

[105] J.A. Nelder and R. Mead. A simplex method for function minimization. *Computer Journal*, 7:308–313, 1965.

[106] N. Ottosen and H. Petersson. *Introduction to the Finite Element Method*. Prentice-Hall, Engelwood Cliffs, NJ, 1992.

[107] S. L. Padula and R.K. Kincaid. Optimization strategies for sensor and actuator placement. *Technical Report NASA/TM-1999-209126*, 1999.

[108] A. Pazy. *Semigroups of Linear Operators and Appplications to Partial Differential Equations*. Springer-Verlag, 1983.

[109] F. Peng, A. Ng, and Y-R Hu. Actuator placement optimization and adaptive vibration control of plate smart structures. *Journal of Intelligent Material Systems and Structures*, 16:263–271, 2005.

[110] T. Penzl. *Lyapack - a Matlab toolbox for large Lyapunov and Riccati equations, model reduction problems, and linear-quadratic optimal control problems, Users's guide (Version 1.0)*, 1999.

[111] T. Penzl. A cyclic low-rank Smith method for large sparse Lyapunov equations. *SIAM Journal on Scientific Computing*, 21(4):1401–1418, 2000.

[112] P.L.D. Peres, J.C. Geromel, and S.R. Souza. Optimal $\mathcal{H}_\infty$-state feedback control for continuous-time linear systems. *Journal of Optimization theory and Applications*, 82(2):343–359, 1994.

[113] I.R. Peterson. Disturbance attenuation and $\mathcal{H}_\infty$ optimization: A design method based on the algebraic Riccati equation. *IEEE Transactions on Automatic Control*, AC-32(5):427–429, 1987.

[114] J.E. Potter. Matrix quadratic solutions. *SIAM Journal on Applied Mathematics*, 14:496–501, 1966.

[115] M.J.D. Powell. On trust region methods for unconstrained optimization without derivatives. *Mathematical Programming, Series B*, 97(3):605–623, 2003.

[116] S. Pulthasthan and H.R. Pota. The optimal placement of actuator and sensor for active noise control of sound-structure interaction systems. *Smart Materials and Structures*, 17(3), 2008. art. no. 037001.

[117] M.G. Raja and S. Narayanan. Simultaneous optimization of structure and control of smart tensegrity structures. *Journal of Intelligent Material Systems and Structures*, 20(1):109–117, 2009.

[118] A.R.M. Rao and K. Sivasubramanian. Optimal placement of actuators for active vibration control of seismic excited tall buildings using a multiple start guided neighbourhood search (msgns) algorithm. *Journal of Sound and Vibration*, 311:133–159, 2008.

[119] J.D. Roberts. Linear model reduction and solution of the algebraic Riccati equation by use of the sign function. *International Journal of Control*, 32(4):677–687, 1980.

[120] D.L. Russell. *Mathematics of Finite Dimensional Control Systems: Theory and Design, Lecture Notes in Pure and Applied Math., vol. 43*. Marcel Dekker, New York, second edition, 1979.

[121] C. Scherer. $\mathcal{H}_\infty$-control by state feedback: An iterative algorithm and characterization of high-gain occurence. *Systems and Control Letters*, 12:383–391, 1989.

[122] C. Scherer. $\mathcal{H}_\infty$-control by state feedback and fast algorithms for the computation of optimal $\mathcal{H}_\infty$-norms. *IEEE Transactions on Automatic Control*, 35:1090–1099, 1990.

[123] S.D. Silva, V. Lopes, and M.J. Brennan. Design of a control system using linear matrix inequalities for the active vibration control of a plate. *Journal of Intelligent Material Systems and Structures*, 17(1):81–93, 2006.

[124] Y.G. Sung. Modelling and control with piezo actuators for a simply supported beam under a moving mass. *Journal of Sound and Vibration*, 250(4):617–626, 2002.

[125] R. Sweeney, M.A. Demetriou, and K.M. Grigoriadist. $\mathcal{H}_\infty$ control of a piezo-actuated flexible beam using an analytical bound approach. In *Proceeding of the 2005 American Control Conference*, pages 2505–2509, 2005.

[126] D.M. Topkis. A cutting-plane algorithm with linear and geometric rates of convergence. *Journal of Optimization theory and applications*, 36(1):1–22, 1982.

[127] P. Tseng. Fortified-descent simplicial search method: A general aproach. *SIAM Journal on Optimization*, 10:269–288, 1999.

[128] M. van de Wal and B. de Jager. A review of methods for input/output selection. *Automatica*, 37:487–510, 2001.

[129] A. Varga. On stabilization methods of descriptor systems. *Systems and Control Letters*, 24:133–138, 1995.

[130] J. Wiedmann. *Linear Operators in Hilbert Spaces*. Springer-Verlag, 1980.

[131] S. Yang. Parallelized iterative solver for $\mathcal{H}_\infty$ control of large descriptor systems. preprint, 2011.

[132] H.H. Yue, Z.Q. Deng, and H.S. Tzou. Optimal actuator locations and precision micro-control actions on free paraboloidal membrane shells. *Communications in Nonlinear Science and Numerical Simulation*, 13:2298–2307, 2008.

[133] K. Zhou and J. C. Doyle. *Essentials of Robust Control*. Prentice Hall, New Jersey, 1996.

[134] K. Zhou, J. C. Doyle, and Keith Glover. *Robust and Optimal Control*. Prentice Hall, New Jersey, 1997.